Università degli Studi di Cagliari

Ph.D Course in

Mathematics and Computer Science

Curriculum: Mathematics

Cycle XXIX

Title

Statistical Physics of Evolutionary Game Theory and its Applications

SSD: MAT/07 (Mathematical Physics)

Doctoral Dissertation of Marco Alberto Javarone
PhD Coordinator Prof. Giuseppe Rodriguez
Tutor Prof. Salvatore Mignemi
Co-Tutor Dr. Adriano Barra

Academic Year 2015 - 2016
Thesis presented during the session March-April 2017

To my family, for their continuous support and encouragement.

Acknowledgements

During these three years, I had the opportunity to meet and to work with a number of very nice people. First of all, I wish to thank my supervisor Prof. Salvatore Mignemi who granted me a lot of scientific freedom, and always provided a great support. I am deep grateful to my co-turor Dr. Adriano Barra that, beyond to be a extraordinary scientific mentor, always behaves as a friend. So, I wish to thank him for all the time he spent in giving priceless advises, suggestions and continuous support. Here, I am happy to have the opportunity to thank Prof. Serge Galam, who invited me in his laboratory when I was at the beginning of this path, moving the first steps in the area of social dynamics and of statistical physics. I strongly appreciate his wise suggestions, and his continuous friendly support. It is a pleasure to thank also Dr. Elena Agliari and Prof. Daniele Marinazzo. Now, they are like friends, and they deserve a big thank for their time and a support. I want to thank here Prof. Giuseppe Rodriguez, the Director of the PhD School, since from the beginning of this path, in a number of occasions, has always been very willing and helpful. In addition, many more people deserve a big thank, among them I wish to mention Prof. Mirko Degli Esposti, Prof. Giuliano Armano, Prof. Christian Beck, Prof. Hendrik Jensen, Prof. Andrea Tagarelli, Prof. Monasson, and Prof. Fiorenzo Toso. Last but not least, among my colleagues and friends deserve a special mention Francesco Caravelli, Alberto Antonioni, Roberto Interdonato, Federico Battiston, Daniele Tantari, Andrea Galluzzi, and Andrea Pizzoferrato. We had the opportunity to work together, and often attended same conferences. So I hope that we will have soon the opportunity of further collaborations. Finally, I take the opportunity to thank my first student, now successfully graduated in Theoretical Physics, Antonio Emanuele Atzeni who collaborated with me in the early works on Evolutionary Game Theory. Therefore, I thank Prof. Piero Olla that made possible this collaboration. To conclude, I wish to thank also the National Group of Mathematical Physics (GNFM-INdAM) for support received during this year.

Preface

In this dissertation, I present some of the results obtained in the period between January 2014 and December 2016, during my phd school in Mathematics. Although most of the work was carried out at University of Cagliari, I had the opportunity to visit some external laboratories. In particular, the Ecole Polytecnique de Paris and the CNRS (Paris), the University of Ghent, the University of Rome - La Sapienza, the Queen Mary University of London, the Ecole Normale Superiere de Paris, and the Invenia Lab - Cambridge. Therefore, I wish to acknowledge all these institutions for their support and kind hospitality.

List of Papers in the dissertation

- Chapter 1 provides an overview on Evolutionary Game Theory (EGT), and briefly describes results presented in:

  Javarone, M.A., Atzeni, A.E.: The role of competitiveness in the Prisoners Dilemma. *Computational Social Networks* **2-15** (2015)

- Chapter 2, in part, is based on the following paper:

  Galam, S., Javarone, M.A.: Modeling Radicalization Phenomena in Heterogeneous Populations. *PloS One* **11-5** e0155407 (2016)

- Chapter 3 is based on the following paper:

  Javarone, M.A.: Statistical Physics of the Spatial Prisoner's Dilemma with Memory-Aware Agents *EPJ-B* 89 (2016)

- Chapter 4 is based on the following paper:

  Javarone, M.A., Battiston, F.: The Role of Noise in the Spatial Public Goods Game. *JSTAT* 073404(2016)

- Chapter 5 is based mainly based on a letter and, in part, on a previous paper:

Javarone, M.A., Antonioni, A., Caravelli, F.: Conformity-Driven Agents Support Ordered Phases in the Spatial Public Goods Game. *EPL* **114** (2016) 38001

Javarone, M.A., Atzeni, A.E., Galam, S.: Emergence of Cooperation in the Prisoner's Dilemma Driven by Conformity. *European Conference on the Applications of Evolutionary Computation* 155–163 (2014)

- Chapter 6 is based on two main papers:

  Javarone, M.A.: Solving Optimization Problems by the Public Goods Game. *arxiv:1604.02929* (2016)

  Javarone, M.A.: An Evolutionary Strategy based on Partial Imitation for Solving Optimization Problems. *Physica A* **463** 262269 (2016)

- Chapter 7 is based on the following papers:

  Javarone, M.A.: Modeling Poker Challenges by Evolutionary Game Theory. *Games* **7-4** 39 (2016)

  Javarone, M.A.: Is Poker a Skill Game? New Insights from Statistical Physics. *EPL* **110-5** (2015)

  Javarone, M.A.: Poker as a Skill Game: Rational versus Irrational Behaviors. *Journal of Statistical Mechanics: Theory and Experiment* P03018 (2015)

- Chapter 8 is based on the following paper:

  Javarone, M.A., Marinazzo, D.: Evolutionary Dynamics of Group Formation. *arxiv:1612.03834* (2016)

- Eventually, the Appendix A is based on the following papers:

  Javarone, M.A., Squartini, T.: Conformism-driven phases of opinion formation on heterogeneous networks: the q-voter model case *J. Stat. Mech.* (2015) P10002 (2015)

  Javarone, M.A.: Social Influence in Opinion Dynamics: The Role of Conformity. *Physica A* **414** 19–30 (2014)

Abstract

Evolutionary Game Theory represents a vibrant and interdisciplinary research field, that is attracting the interest of scientists belonging to different communities, spanning from physicists to biologists, and from mathematicians to sociologists. In few words, it represents the attempt to study the evolutionary dynamics of a population by the framework of Game Theory, taking into account the Darwinian theory of natural evolution. As result, Evolutionary Game Theory allows to model a number of scenarios, as social and biological systems, with a high level of abstraction. On one hand, the contribution of the classical Game Theory can be identified at a local level, i.e. in the interactions among the agents. For instance, when agents play games like the Prisoner's Dilemma, according to the Nash Equilibrium, they should defect. On the other hand, in some conditions, it is possible to observe final equilibria far from the expected one. Notably, here we identify the contribution of the Darwinian theory, since the agents can change their behavior according to adaptive mechanisms. Remarkably, often populations reaching non-expected equilibria show emergent behaviors, resulting from their interaction pattern, or from specific local behaviors. For this reason, evolutionary games must be considered as complex systems. Accordingly, we believe that statistical physics constitutes one of the most suitable approaches for studying and understanding their underlying dynamics. In this scenario, one of the aims of this dissertation is to illustrate some models that let emerge a direct link between Evolutionary Game Theory and statistical physics. In addition, we show that the link between the two fields allows to envision new applications beyond the current horizon of Evolutionary Game Theory, as defining optimization strategies. So, at the beginning, we focus on a statistical physics model devised for understanding 'why' random motion, in continuous spaces (and within a particular speed range), is able to trigger cooperation in the Prisoner's Dilemma. Then, we study the role of the temperature in the spatial Public Goods Game, defining a link between this game and the classical Voter Model. Eventually, mapping strategies to spins, we study the spatial Public Goods Game in presence of agents susceptible to local fields, i.e. fields generated by their nearest-neighbors. It is worth to note that, from a social point of view, an agent susceptible to a local field can be considered as a conformist, since it imitates the strat-

egy (or behavior) of majority in its neighborhood. Later, we propose three applications of Evolutionary Game Theory. In particular, the first one is a new method for solving combinatorial optimization problems. The second application is focused on the definition of a game for studying the dynamics of Poker challenges. Finally, the third application aims to represent a phenomenon of social evolution, named group formation. To conclude, we deem that the achieved results shed new light on the relation between Evolutionary Game Theory and Statistical Physics, and allow to get insights useful to devise new applications in different domains.

Contents

List of figures

fitted by power-law functions. After the final green plateau, temperatures are too high to play the spatial PD.

9. Figure 3.4. Maximum value of T_s to achieve full cooperation at equilibrium in function of N, i.e., the size of the population. The fitting function (dotted line) is a power-law characterized by a scaling parameter equal to 2.

10. Figure 3.5. Order-disorder phase transitions in the population. For $T_s < T_c$, the population is in a ferromagnetic phase: **a.** Applying an external negative field, the system converges to the Nash equilibrium, corresponding to $m = -1$ (as $\sigma = -1$ represents defection); **b.** Applying an external positive field, the population converges to cooperation ($\sigma = +1$), corresponding to $m = +1$. **c.** For temperatures higher than T_c, a disordered paramagnetic phase emerges.

11. Figure 4.1. Pictorial representation of the PGG on the considered topology. Agents are arranged in bidimensional square lattice with continuous boundary conditions, forming a toroid as shown in **(a)**. Each agent belongs to five groups of size $G = 5$: one where he is the central player, in red, and four as a peripheral node, in black **(b)**. At each time step, two agents x and y are randomly selected and they play the PGG with all the players in their groups for all groups of belonging. In **(c)**, we show the group where x and y are central: the green nodes are neighbors of node x, and this group has a orange shadow; while neighbors of agent y are cyan and this group has a violet shadow. The dotted lines in the area between x and y indicate the intersection between the groups formed by x and y. Notably, y belongs to the group formed by x and vice versa. In **(d)** we show for both x and y one of the possible groups where they are peripheral.

12. Figure 4.2. Strategy distribution diagram showing the average density of cooperators $\langle\rho\rangle$ at the steady state (a), time to reach the absorbing state T (b) and standard deviation of the density of cooperators $\langle\rho\rangle$ at the steady state (c) as a function of the synergy factor r and the rationality K. Different regions are highlighted. In region (1) the system is stuck in a metastable active phase, macroscopically at the equilibrium, with coexistence of cooperators and defectors due to network reciprocity (the simulations have been stopped after $T = 10^6$ updates per agent). In region (2) the system always reaches the absorbing state predicted by the well-mixed population approximation, i.e. full defection for $r < r_{\mathrm{wm}} = 5$ and full cooperation for $r > r_{\mathrm{wm}}$. In region (3) both steady states become accessible with different probability, as in a biased voter model. Results are averaged over 100 simulation runs.

List of tables

Summary

In this work, we present some models and applications of Evolutionary Game Theory. In particular, the general approach adopted in all investigations is based on the framework of Statistical Physics. In particular, as discussed in the first part, Evolutionary Games can be considered as Complex Systems, therefore Statistical Physics becomes one of the most suitable tool for investigating their behavior. In addition, combining the two fields (i.e. Evolutionary Game Theory and Statistical Physics), some interesting applications can be envisioned. As result the work is organized in four different parts: **I)** a general introduction to Evolutionary Game Theory, and to the main mathematical and physical models used in the presented models and applications; **II)** three chapters focused on the studying of the relations between Evolutionary Game Theory and Statistical Physics; **III)** three chapters focused on some applications arising from a combined view of Evolutionary Game Theory and Statistical Physics; **IV)** a conclusion and an appendix. Then, the content of each chapter can be summarized as follows:

Part I.
Chapter 1. Here, we provide a brief presentation of Evolutionary Game Theory. From the main concepts, to the description of some mechanisms for triggering Cooperation.
Chapter 2. This chapter is devised for describing the main mathematical and physical models used in this dissertation. In particular, we provide a brief overview of statistical physics models for studying the phase transitions. Then, we present some models of population dynamics. The latter is suported by a special case focused on a problem of sociophysics.

Part II
Chapter 3. The first analysis here presented is focused on a model, based on the kinetic theory of gases, for investigating the motivations that lead random motion to support (in a finite range of speeds) cooperative behaviors.
Chapter 4. Here, we analyze the dynamics of the spatial Public Goods Game, and provide a link with the famous Voter Model. In particular, we study the effects of noise in the dynamics of the population.
Chapter 5. In this chapter, we study the outcomes of the Public Goods

Game when the population contains agents susceptible to a local field. In particular, since strategies are mapped to spins, a set of agents generate a field that can, in principle, affects the process of 'strategy selection' of close agents. From a social point of view, this phenomenon can be described as conformity. Appendix *A* provides further details with investigations performed on a more classical model (i.e. the q-Voter model).

Part III

Chapter 6. Here, we present an application of Evolutionary Game Theory to a combinatorial optimization problem. In particular, we focus on the Travelling Salesman Problem.

Chapter 7. Poker games are investigated by defining a simple evolutionary game inspired by the rule of Texas Hold'em. In particular, we present an investigation whose aim is to evaluate wether, and under which conditions, Poker can be considered as a skill game. *Chapter* 8. In this chapter, we propose an investigation on the phenomenon of group formation, by defining a simple game. In particular, we focus on the emergence of homogeneous groups, that we can observe in different animal species.

Part IV

Chapter 9. Here, we briefly summarize the main results presented in this dissertation, and discuss potential future works.

Appendix A. Eventually, we present results of an investigation on the q-voter model in particular conditions. Notably, we study the dynamics in presence of conformist agents, in order to show the role of this 'social behavior' investigated in Chapter 5 (in relation to an evolutionary game).

Part I

General Introduction

Chapter 1

Evolutionary Game Theory

Evolutionary Game Theory represents a vibrant and interdisciplinary research field, that is attracting the interest of scientists belonging to different communities, spanning from physicists to biologists, and from mathematicians to sociologists [1, 2, 3, 4, 5, 6, 7, 8, 9, 10, 11, 12, 13, 14, 15, 16, 17, 18, 19]. In particular, it represents the attempt to study the dynamics of a population, combining the principles of Game Theory [20], and the Darwinian theory of evolution [21]. On one hand, the classical Game theory, proposed by John von Neumann and Oskar Morgenstern, was devised for modeling the human behavior mainly in economic contexts [22]. This field was strongly influenced by the mathematician, and Nobel laureate, John Nash who defined the so-called Nash Equilibrium. The latter can be viewed as a particular state of equilibrium of a game, involving a number of 'rational' agents that have to take an action without prior communications. On the other hand, the Darwinian theory that can be considered as one of the most important breakthrough in Biology and, after more than a century, still constitutes a living theory and one of the major references in the modern science. His father, Charles Darwin, yielded this theory after a long journey around the world, then after direct of observations of nature was able to envision a general theory for explaining natural evolution. Remarkably, Evolutionary Game Theory (EGT hereinafter) allows to model a wide number of scenarios, spanning from social systems to biological processes. In particular, it allows to study the dynamics of a population and its equilibria, considering specific mechanisms, interaction patterns, and behaviors. It is worth to emphasize that, even if EGT models consider 'rational' agents, i.e. agents that aim to increase their gain, interesting emergent phenomena not predicted by the classical Game Theory, can be observed. The previous observation deserves a particular attention since emergent phenomena are one of the topics studied in the modern area of complex systems. The latter has a number of definitions, however in our view it can be summarized by the title of the famous Anderson's work 'More is different' [23]. In particular, the

complexity of many systems often cannot be observed locally, but only at a macroscopic level, being the result of different mechanisms, as for instance non-trivial interaction patterns. From this point of view, EGT models can be framed in the area of complex system. In particular, they implement agent populations whose local interactions are simple, and based on a specific game, like the Prisoner's Dilemma later described. Then, during their evolution, these populations show critical phase transitions and behaviors that, as stated before, cannot be directly related to the local interactions. For instance, considering a population playing the Prisoner's Dilemma, EGT models allow to investigate the emergence of an ordered state of cooperation. The latter corresponds to an equilibrium characterized by all agents playing as cooperators, despite the Nash Equilibrium of this game is 'defection'. In particular, in absence of a prior communication, 'cooperation' is a risky strategy and the 'rational' action is to defect. However, even if Game Theory is a solid mathematical description of a scenario, a number of observations both in nature and in the real societies show that cooperation is quite common. Therefore, one of the task of EGT is trying to understand, with the support of the Darwinian theory, why and how the Nash Equilibrium is not always reached. One of the key points of an evolutionary approach is providing a population with an adaptive mechanism. Remarkably, as Darwin stated, the best (i.e. the fittest) individual is not the strongest one, but that who is more able to adapt herself/himself to new environments/scenarios. Accordingly, EGT models study populations whose agents can change their strategy by a process named 'strategy revision phase', later explained with more details. In particular, agents can modify their strategy observing the payoff of their opponents after an iteration. As result, the final equilibrium of a population strongly depends on the interactions among the agents, and to the mechanisms they adopt to modify their strategy over time. In general, a game can have many strategies, and the resulting payoff function maps all the possible combinations among strategies to a specific gain. In most of the works here presented, we consider only 2-strategy games. Therefore, in these cases, we might observe only two ordered phases, and a disordered one. In particular, the ordered phases correspond to the two possible strategies, while the disordered phase corresponds to an equilibrium (or a steady-state), characterized by the co-existence of agents adopting the two strategies in the population.

Nash Equilibrium

As previously stated, from the point of view of the classical Game Theory, local interactions between two (or more) agents can be solved according to the Nash Equilibrium of the considered game. The Nash Equilibrium [20] corresponds to the solution of a game such that no player has anything to gain whether she/he is the only one that changes her/his own strategy. Here,

it is worth to recall that before an interaction, agents are not allowed to communicate, therefore for a rational agent the payoff function is a fundamental reference to take an action (i.e. to select a strategy). The mathematical definition of the Nash Equilibrium requires a more formal description of a game. In general, the latter is described by a set S of strategy profiles, and a payoff function f, i.e. by (S, f). A game might involve n players, so that each one adopts a strategy. Then, a strategy profile S is defined as $S = S_1 \times S_2 \times ... \times S_n$, and the payoff function computes that gain for a specific $x \in S$ as $f(x) = (f_1(x), f_2(x), ..., f_n(x))$.

Now, a set of strategies $x^* \in S$ is a Nash Equilibrium if $\forall_i, x_i \in S_i$: $f_i(x_i^*, x_{-i}^*) \geq f_i(x_i, x_{-i}^*)$. Accordingly, the expected equilibrium of a population corresponds to the Nash Equilibrium of the game used to define the agent interactions.

1.1 2-Strategy Games

In this section, we describe 2-strategy games, i.e. games with only two possible actions/strategies. In particular, we focus on the Prisoner's Dilemma [20] and on the Public Goods Game (also defined as n-person Prisoner's Dilemma), whose strategies are 'Cooperation' and 'Defection'. Eventually, we remind that in the third part of this work, we propose some applications of EGT (combined with a statistical physics approach) where the number of strategies can be higher than 2 and, in the case of 2-strategy games, the meaning of each strategy can be different from those here defined (i.e. Cooperation and Defection).

1.1.1 Prisoner's Dilemma

The Prisoner's Dilemma (PD hereinafter) is a very simple game where agents may behave as cooperators or as defectors, then set of strategies is $\Sigma = \{C, D\}$. In this game, the payoff function takes the form of a matrix, that describes the gain each agent receives according to its strategy. In particular, the payoff matrix reads

$$\begin{array}{c} \\ C \\ D \end{array} \begin{array}{c} \begin{array}{cc} C & D \end{array} \\ \begin{pmatrix} 1 & S \\ T & 0 \end{pmatrix} \end{array} \tag{1.1}$$

with T representing the *Temptation*, i.e. the payoff an agent gains if it defects while its opponent cooperates, while S representing the *Sucker's payoff*, i.e. the gain obtained by a cooperator while the opponent defects. In principle, the matrix 3.1 can correspond also to other games, so it is important to define the range of T and S. Notably, in the PD the values of the two parameters T and S are in the following ranges: $1 \leq T \leq 2$ and

$-1 \leq S \leq 0$. Therefore, the dynamics of a population can be studied in the TS-plane, in order to observe the final equilibria on varying the two parameters within their range. For instance, for low values of T defectors have a small increasing of their payoff when they play against cooperators, whereas for high value of S cooperators have small losses (i.e. small risks) when face defectors.

1.1.2 Public Goods Game

The Public Goods Game (PGG hereinafter) considers a population of N agents that, as for the PD, can behave as cooperators or as defectors. In this game, cooperators provide a unitary contribution to a common pool, whereas defectors do the opposite, i.e. do not contribute. The summation of all contribution is then enhanced by a numerical factor, named synergy factor, and the final value is equally divided among all agents. According to this set of rules, the payoff of a cooperator (i.e., π^c) and that of a defector (i.e., π^d) read

$$\begin{cases} \pi^c = r\frac{N^c}{G} - c \\ \pi^d = r\frac{N^c}{G} \end{cases} \tag{1.2}$$

where N^c is the number of cooperators among the G agents involved in the game (it can be smaller than N in one iteration), r synergy factor, and c agents' contribution (we set to 1 for all cooperators, without the loss of generality). The value of G depends on the considered topology, for instance when agents are arranged in a square lattice, $G = 5$. Finally, we recall that as for the PD, the Nash Equilibrium of the PGG is defection.

1.2 Modeling Evolutionary Games

Agent populations playing evolutionary games show critical behaviors, well known in statistical physics, as order-disorder phase transitions [24, 25]. The main physical phenomena of interest in EGT are briefly presented in the chapter 2. Here, we remind that early studies, in this direction, have been proposed by Hauert and Szabo. For instance, in [26] authors refer to the PD for illustrating several connections between Physics and EGT. It is worth also to recall that other authors tried to link the classical Game Theory with Physics, as reported in [27]. Therefore, it is important to understand why Evolutionary Games have different points of contact with physical phenomena. In particular, it is of interest to understand the mechanism underlying the evolution of a population, usually defined as 'strategy revision phase'. Before going through the details, we show some methods that can be adopted for modeling the dynamics of evolutionary games (see [22] for further details). Although analytical approaches can be often quite difficult, mainly for problems related to the complexity of a specific scenario or to

the number of features that characterize the agents, there are some models as the 'replicator dynamics'. The latter uses differential equations, and has been proposed by Taylor and Jonker ([28]), and later by many others (e.g. [29, 30, 31]). One of the assumptions of this approach (i.e. replicator dynamics) is that the payoff can be considered as a fitness. Notably, given a strategy i, used with a frequency x_i in a population, the frequency rate reads

$$\dot{x}_i = x_i(f_i - \phi) \tag{1.3}$$

with f_i expected payoff associated to the strategy i, and ϕ average payoff. In more recent years, different scientists focused their attention towards structured populations, i.e. populations whose agent interactions depend on a particular topology. Here, both simple structures, as regular lattices, and more complex ones, as scale-free networks, have been widely investigated in order to understand the relation between the interaction topology and the equilibrium of a population. We start mentioning results obtained with regular lattices [2, 4, 5, 6, 32, 33, 34], usually implemented with periodic boundary conditions. For instance, in the case of the PGG, Perc and Szolnoki computed a critical threshold of the synergy factor. In particular, they found the minimum value of the synergy factor to allow cooperators to survive (and even to succeed) [34]. Later on, different authors investigated the influence of more complex topologies in many games. Just to cite few, authors of [35] showed that heterogeneous networks do not promote cooperation when humans play the PD. In [36] authors studied the evolution of cooperation in heterogeneous structured populations, demonstrating that cooperation increases as the heterogeneity, of the network structure, increases. In [37], authors studied an EGT model in growing and network-structured populations, finding that as the network increases the level of cooperation is smaller than that obtained in a static network; in [38] the effects of social punishment have been studied in complex networks, achieving as result that different equilibria can be observed. Remarkably, Santos and Pacheco [39, 40] found that scale-free networks support the emergence of cooperation. Eventually, the fundamental role of the network topology in evolutionary games was investigated in [41], where the role of hubs (i.e. nodes with a high number of connections) as elements for sustain cooperation has been clarified. Finally further works focused on EGT models using interdependent networks (e.g. [42, 3]) and multiplex networks [43, 44, 45, 46, 47, 48] as [49, 50]. It is worth to highlight that both in simple lattice structures and in more complex ones, the analytical tractability of evolutionary games is easily lost. As result, investigations must be performed by means of numerical simulations. Then, let us present the mechanism defined as 'strategy revision phase'. The latter can be implemented according to different methods, related to the analysis of the payoff of the involved agent. In addition, further methods can consider different behaviors, as conformity (see chapter

5, and pure imitation (see chapter 4). In general, those methods based on the payoff analysis can be divided in the following categories:

- Comparison
- Self-evaluation
- Imitation

Notably, the first one, i.e. the payoff comparison, is often implemented as a stochastic rule by a Fermi-like function. The latter allows to compute the probability an agent y takes the strategy of an agent x, and reads

$$W(s_y \leftarrow s_x) = \left(1 + \exp\left[\frac{\pi_y - \pi_x}{K_y}\right]\right)^{-1} \tag{1.4}$$

where π_x and π_y correspond to the payoffs of two agents, and s_x and s_y indicate their strategy. $K_y > 0$ is an agent-dependent parameter whose role will be described in the chapter 4. The self-evaluation method entails an agent decides to modify its strategy if the current payoff is smaller than the previous one, thus it entails agents have some memory of the past events (in many EGT models, the agent payoff is reset after each iteration). Eventually, imitative mechanisms based on the payoff, usually lead an agent to imitate a richer agent.

1.2.1 Emergence of Cooperation

Before to conclude this chapter, we briefly summarize some of the previous works in EGT, devised for identifying and describing mechanisms and principles responsible for the emergence of cooperation in games characterized by a Nash equilibrium of defection. Let us begin with the famous 5 rules of cooperation, related to the concept of natural selection, presented by Nowak [51]: kin selection, direct reciprocity, indirect reciprocity, network reciprocity, and group selection. The kin selection is a simple principle based on the similarity between the donor and the recipient of an altruistic act. In particular, if a parental relation exists between the two individuals, cooperation can be observed. The direct reciprocity comes from the observation that if a game involves many times always the same individuals, cooperation might become a promising option. The indirect reciprocity is a mechanism that explains why an individual acts as a donor, even if knows that the one receiving the benefit is not in the condition to exchange the favor. Notably, especially in the human society, forms of cooperation related to indirect reciprocity can be observed because the donor gains the respect of other individuals in the population, so that even in this case an indirect benefit can be obtained. The network reciprocity is similar to the direct reciprocity, and it can be observed in spatially structured populations, where

the individuals interact always with the same neighbors. So, thanks to this mechanism clusters of cooperators emerge. Finally, group selection refers to forms of cooperation observed between people belonging to the same group. Here, groups of cooperators can obtain more benefits than groups of defectors. In the case of complex networks, as previously mentioned, Moreno [35, 37], Pacheco and Santos [39, 40] widely illustrated the relevant role of complex topologies for triggering cooperation in games like the Public Goods Game, Prisoner's Dilemma, and many others. In particular, in [39] authors demonstrated the beneficial role of scale-free networks in supporting the emergence of cooperation. In addition, a further interesting mechanism responsible for the emergence of cooperation is the random motion. Indeed, in this last case, we are considering agent populations in bidimensional continuous spaces. In particular, in [52, 53, 54] authors proposed and studied the role of random motion (considering also Levy-flights [55]) in different evolutionary games. In our view, one of the most interesting results in these works is that cooperation emerges only in a short range of speeds. Therefore, as reported in chapter 3, we propose a model based on the kinetic theory of gases for investigating this behavior[56]. A further work, inspired by the mechanism of random motion, and implemented on complex networks, can be found here [57]. Notably, the latter considers a structured population playing the PD, and a behavior defined 'competitiveness'. In particular, after each iteration, agents with a high payoff generate new links (so that can play with more opponents), while those with a low payoff reduce the number of links. As result a time-varying network constitutes the topology of the agent interactions, and the achieved results indicate that the presence of competitive agents supports the emergence of cooperation, highlighting a potential relation between 'cooperation' and 'competitiveness'.

Chapter 2

Mathematical and Physical Models

In this chapter, we briefly present the main mathematical and physical models used in this work. In particular, we focus on the theory of phase transitions, and on models of population dynamics. In both cases, we introduce only the most relevant concepts, with a particular attention for those methods and phenomena of interest in EGT. Finally, we refer the readers to further books and articles (listed among references) for a more complete description of the following topics.

2.1 Phase Transitions

Phase transitions are one of the most important phenomena studied in Thermodynamics and Statistical Physics [24, 58, 25]. In particular, the latter tries to understand the relation between the macroscopic behavior and the microscopic dynamics of a many-body system, in terms of local rules and interactions. One of the most successful models for studying phase transitions is the Ising model, i.e. a simple and powerful method for studying interactions and processes in many systems. So, we begin providing a brief description of its main characteristics, and then we present the Curie-Weiss model. Eventually, the Landau theory of phase transitions ends the first part of this chapter. The second part presents general models of population dynamics, and also a specific case used in sociophysics [59, 60, 61, 62, 63, 64, 65, 66, 67, 68, 69]. In particular, we report a brief analysis of a population composed of three different species, and study its equilibria and stability.

2.1.1 Ising Model

The Ising Model considers a number of elements N arranged on a lattice (see Figure 2.1). Here, the concept of element is very general, since it may refer to atoms, neurons of a neural network, and so on and so forth. Then,

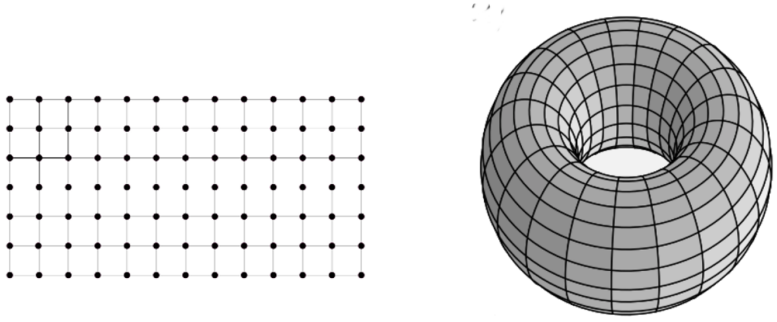

Figure 2.1: On the left, a simple square lattice. On the right, a toroid (i.e. a square lattice with periodic boundary conditions).

each element is placed on a site i of the lattice and has a *spin* with a binary value $\sigma_i = \pm 1$. For instance, in a magnetic system, the value of σ may refer to a magnetic moment, pointing up or down. A pair of sites (e.g. (i, j)) forms a bond (or edge in the jargon of network theory), and a set of bonds is denoted as B. Now, for each bond in B we define an interaction energy of value $-J\sigma_i\sigma_j$, so that it is equal to $-J$ for $\sigma_i = \sigma_j$, and to J in the opposite case. If J is positive, the case $\sigma_i = \sigma_j$ has an energy smaller than the case $\sigma_i = -\sigma_j$, so the former is more stable. Positive interactions (i.e. $J > 0$) are defined as 'ferromagnetic', while negative interactions as 'antiferromagnetic'. In addition, some sites of the lattice can have an own energy of value $-h\sigma_i$ (here h may represent an external field). Thus, the total energy, i.e. the Hamiltonian, of the Ising model reads

$$H = -J \sum_{(i,j)\in B} \sigma_i\sigma_j - h\sum_{i=1}^{N} \sigma_i \tag{2.1}$$

In general, given a Hamiltonian H, we can compute the average value of a physical quantity using the Gibbs-Boltzmann distribution. For instance, in the case of a spin configuration S the distribution reads

$$P(S) = \frac{e^{-\beta H}}{Z} \tag{2.2}$$

with Z partition function. The latter has a fundamental role, since allows to normalize the distribution (i.e. eq. 2.2). However, computing its value is not always trivial, and this task can become even impossible, in a finite

time, due to its computational complexity. In general, it takes the following form

$$Z = \sum_{\sigma} e^{-\beta H} \tag{2.3}$$

It is worth to remind that in some cases, the value of σ_i can be different from ± 1, so other models can be considered (e.g. the XY model). Now, a macroscopic view of the Ising model can be obtained by a parameter called 'magnetization', defined as

$$m = \frac{1}{N} \langle \sum_{i=1}^{N} \sigma_i \rangle \tag{2.4}$$

In the thermodynamic limit (i.e. for $N \to \infty$), m allows to measure the 'order' of a system, and for this reason it is an order parameter. Notably, the magnetization vanishes when the system contains the same amount of positive (i.e. $+1$) and negative (i.e. -1) spins. At low temperatures (i.e. for $\beta \gg 1$), equation 2.2 implies that low-energy states are realized with higher probability than high energy states. In addition, in absence of external fields (i.e. for $h = 0$), low energy states of the Ising model have all spins pointing in the same direction, so that m gets close to 1. Now, increasing the temperature T, states with various energies emerge with equal probabilities. Accordingly, the macroscopic state of the Ising model becomes disordered, and its magnetization goes to zero. As result, it is possible to identify a relation between m and T and, most importantly, a critical temperature T_c such that for $T < T_c$ the magnetization is greater than zero, while for $T > T_c$ the magnetization reduces until its value vanishes (i.e. $m \to 0$). This phenomenon, from a macroscopic point of view, is a phase transition, often defined as 'order-disorder phase transition'. In magnetic systems, states achieved at $T < T_c$ correspond to a ferromagnetic phase, while those achieved at $T > T_c$ result in a paramagnetic phase. Therefore, T_c is a 'critical point'.

Mean Field

At the first glance, the Gibbs-Boltzmann distribution (i.e. equation 2.2) suggests that it is possible to compute the expected value of any physical quantity. However, as previously mentioned, due to the huge amount of sums over 2^N terms in the partition function (i.e. equation 2.3), this task might become even impossible (in a finite time). In this case, methods of approximation become mandatory, as for instance the mean-field approach below described (see also [70, 71, 72, 73]). The underlying idea of the mean-field theory is to neglect fluctuations of variables around the mean values. So that one assumes $m = \frac{\sum_i \langle \sigma_i \rangle}{N} = \sum_i \langle \sigma_i \rangle$, and the deviation $\delta\sigma_i = \sigma_i - m$, in addition the second-order term with respect to the fluctuation $\delta\sigma_i$ is

assumed to be enough small to be neglected. Following this approach the Hamiltonian can be rewritten as

$$H = -J \sum_{(i,j)\in B} (m+\delta\sigma_i)(m+\delta\sigma_j) - h\sum_{i=1}^{N}\sigma_i \sim Jm^2 N_B - Jm\sum\sum_{(i,j)\in B}(\delta\sigma_i+\delta\sigma_j) - h\sum_{i=1}^{N}\sigma_i \tag{2.5}$$

so now $\delta\sigma_i$ and $\delta\sigma_j$, assigned at the ends of each bond, are summed up to z times, with z number of bonds starting from a given site. Thus, the Hamiltonian takes a new simplified form:

$$H = N_B Jm^2 - (Jmz + h)\sum_{i=1}^{N}\sigma_i \tag{2.6}$$

Finally, due to the advent of the modern network science [75, 76, 77, 78, 79], a number of works have been addressed toward the definition of different physical models and processes on complex topologies, as scale-free networks and small-world networks. Therefore, here we briefly report the equation to compute the critical temperature of the Ising model implemented on complex networks. As described in [80], in small-world networks generated according to the Watts-Strogatz (hereinafter WS) model [81], the value of T_c can be approximated as follows

$$T_c \sim \frac{-Jm(m+1)}{log(p)} \tag{2.7}$$

with p rewiring probability of the WS model. In few words, the WS model generates small-world networks by the following simple algorithm: start with a regular ring of nodes; then according to a probability p rewire each edge at random. Therefore a network, from a regular structure (i.e. a ring), increases its disorder by the rewiring process, until becoming a completely random network for $p = 1$.

2.1.2 Curie-Weiss Model

The Ising Model is valid only when the dimension of the system is very small. In particular, in one dimension, the Ising Model has no phase transitions at finite temperature; in two dimensions, according to the Onsager's solution, there is a phase transition (at a finite temperature). Then, in higher dimensions, although there is a phase transition, an analytical solution that describes its behavior is still an open problem. Notably, in three dimensions the problem has been solved only by a numerical approach. Therefore, solving the Ising Model for dimensions D greater than 3 is still an open problem in statistical mechanics. However an interesting toy model, useful for describing the behavior of ferromagnetic transitions with an infinite dimension, is the Curie-Weiss (CW hereinafter) model [82, 83, 84, 138]. The

latter has a great relevance both in statistical mechanics and in information theory [86]. In this model, each spin is connected with all the others, so that the Hamiltonian reads

$$H(\sigma_1, ...\sigma_n) = -\frac{1}{N}\sum_{(i<j)} \sigma_i\sigma_j - h\sum_{i=1}^{N}\sigma_i \tag{2.8}$$

with h external field. As result the CW model defines a complete graph of N nodes, and $N(N-1)/2$ links. Using the magnetization m before introduced, and without to consider the contribution of an external field, the Hamiltonian of the CW model has the following form

$$H(\sigma_1, ...\sigma_n) = -\frac{N}{2}m^2 + O(1) \tag{2.9}$$

eventually, the partition function of the CW model reads

$$Z = \sum_{\{\sigma_i\}} e^{-\beta H(\sigma_1,...,\sigma_N)} \tag{2.10}$$

with H Hamiltonian defined in equation 2.8. Now, further calculations are required to solve the equation, as for instance for computing the summation over the spin variables appearing in eq. 2.10. However, here we recall that the final equation of state of the CW model is the following

$$m = tanh(\beta Jm + \beta h) \tag{2.11}$$

As illustrated in the following chapters, the CW model is very useful as reference for studying the dynamics of EGT models.

2.1.3 Landau Theory of Phase Transitions

The analytical methods before presented for studying the phenomenology of phase transitions by analytical methods (i.e. the Ising Model and the CW model) allow to compute the partition function Z of a system. Therefore, in principle, a number of quantities can be computed according to equation 2.2. In particular, in order to study the final state of equilibrium of a system, the thermodynamical potential named 'free energy' can be analyzed. Notably, the second law of thermodynamics states that a system evolves towards the state that maximizes its entropy. So, since the Helmotz free energy is defined as $F = U - TS$ with U internal energy, T temperature and S entropy, the thermodynamics law can be re-paraphrased as: the state of equilibrium of a system corresponds to one that minimizes its free energy F. In addition, we report the relation between the partition function and the free energy

$$-k_bTlnZ = U - TS \tag{2.12}$$

with k_b Boltzmann constant. Therefore, $Z = e^{-\beta F}$. The mean-field theory allows to get an approximated phase diagram of a system. However, for studying the behavior of a system close the critical point (e.g. the critical temperature), a suitable choice is given by the Landau theory of phase transitions. The latter assumes that a system close to the critical point has a small order parameter (i.e. m), so the free energy can be expressed as the summation of power series as follows

$$F(T;m) = f(T;0) + \frac{1}{2}a(T)m^2 + \frac{1}{4!}b(T)m^4 + ... \tag{2.13}$$

with coefficients $a(T)$ and $b(T)$ that can be computed analytically. Figure 2.2 shows the free energy of the CW model. In particular, for $T > T_c$ there is

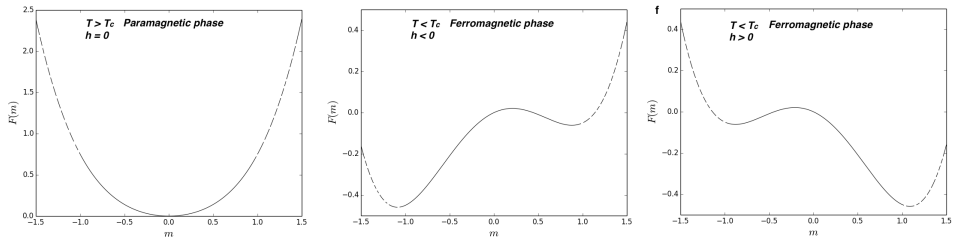

Figure 2.2: Free energy in functions of the order parameter m, in absence of an external field.

only one minimum of free energy (at $m = 0$), corresponding to the state called 'paramagnetic phase'. Instead, for $T < T_c$ there are two possible minima of free energy, and the symmetry $m \to -m$ is spontaneously broken (phenomenon defined as 'symmetry breaking').

2.2 Population Dynamics

In general, population dynamics have been studied in the context of mathematical biology [87], with the aim to represent processes like population growth, competitions among different communities or species living in the same environment, and so on. Evolutionary Game Theory actually constitutes a further framework for studying the behavior of a population. Here, we present some basic approaches to the mathematical formulation of population dynamics, and then focus on a more complete example related to an application in social dynamics [88]. Let us start with the case of a continuous growth of a population composed of N individuals, living in a system without competitors:

$$\frac{dN}{dt} = rN \tag{2.14}$$

with r growth rate (called also Malthusian parameter). The analytical solution of eq. 2.14 is $N(t) = N_0 e^{rt}$, where N_0 indicates the initial population

size. Considering a system with two competing populations, the scenario changes according to the rules of interactiong between the individuals of the two species. For instance the Lotka-Volterra Model, also defined as predator-prey model, describes the dynamics of interactions between two species, i.e. predators (say A) and preys (say B).

$$\begin{cases} \frac{dA}{dt} = \alpha AB - \beta A \\ \frac{dB}{dt} = \gamma A - \delta AB \end{cases} \tag{2.15}$$

with *alpha*, *beta*, γ, *delta* parameters describing the interactions between the two species. These parameters can change meaning depending on the considered scenario. In order to provide a more complete overview of population dynamics, we now report some results applied in a sociophysical model implemented for studying the phenomenon of radicalization [88].

2.2.1 Analytical Solution and Equilibria

In order to study the emergence of radicalization in a heterogeneous population we consider a system with N interacting agents distributed among inflexible (I), peaceful (P) and opponent (O) agents. Each category refers to a different behavior or feeling. Inflexible and opponent agents have behaviors mapped respectively to states $s = \pm 1$. Peaceful agents have a behavior mapped to the state $s = 0$. Inflexible agents never change state (see also [89]) while peaceful and opponent agents may shift state from one to another over time. Opponents may become peaceful and peaceful may become opponents. Hence, neither peaceful nor opponent agents may assume the state of inflexible agents. Inflexible agents interact with sensitive agents both peaceful and opponents. During these pairwise interactions when an inflexible agent meets an opponent it may well turn the opponent to peaceful via different paths. Among those paths most are spontaneous through normal social and friendship practices. But as it will appear latter, exchanges could become intentional as to promote coexistence with sensitive agents via monitored informal exchanges. To account for all interacting pairs a parameter α is introduced to represent on average the rate per unit of time of encounters where opponents become peaceful agents. In parallel and in contrast we introduce the parameter β to account on average for the rate of success of opponents in convincing peaceful agents to turn opponents. Contrary to inflexible agents opponents are acting intentionally to increase the support to their radical view within the sensitive population. The value of β is a function of the power of conviction of opponents. It also takes into account the activeness of opponent agents since opponents are activists. It is not the case of the core inflexible agents who interact spontaneously with sensitive agents without an a priori goal. It is worth to stress that both α and β may in principle vary over time. However, the corresponding time

scale for variation is expected to be much longer than the time scale of the dynamics driven by pairwise interactions. This is why at the present stage of our work α and β are assumed to be fixed and constant. We emphasize that our analytical approach entails to consider the system as if it was continuous, i.e. analyzing the relative densities of agents in the various states. Going to the analytical details of our model we defined the following system of equations

$$\begin{cases} \frac{d\sigma_P(t)}{dt} = \alpha\sigma_I\sigma_O(t) - \beta\sigma_O(t)\sigma_P(t) \\ \frac{d\sigma_O(t)}{dt} = \beta\sigma_O(t)\sigma_P(t) - \alpha\sigma_I\sigma_O(t) \\ \sigma_I + \sigma_P(t) + \sigma_O(t) = 1 \end{cases} \tag{2.16}$$

where σ_I is the constant density of inflexible agents, while $\sigma_O(t)$ and $\sigma_P(t)$ are the respective densities of peaceful and opponent agents at time t. Dealing with densities the third equation of system 2.16 allows to reduce the number of ODEs to one equation. In particular, choosing the peaceful agents density $\sigma_P(t)$ we get

$$\frac{d\sigma_P(t)}{dt} = \alpha\sigma_I(1 - \sigma_I - \sigma_P(t)) - \beta(1 - \sigma_I - \sigma_P(t))\sigma_P(t) \tag{2.17}$$

The equilibrium state of the population can be obtained from $\frac{d\sigma_P(t)}{dt} = 0$, which reads

$$\beta\sigma_P(t)^2 - (\alpha\sigma_I + \beta(1 - \sigma_I))\sigma_P(t) + \alpha\sigma_I(1 - \sigma_I)) = 0 \tag{2.18}$$

The two solutions of equation 2.18 read

$$< \sigma_P >= \frac{\alpha\sigma_I + \beta(1 - \sigma_I) \pm \sqrt{[\alpha\sigma_I + \beta(1 - \sigma_I)]^2 - 4\beta\alpha\sigma_I(1 - \sigma_I)}}{2\beta} \tag{2.19}$$

where $< \sigma_P >$ is the equilibrium value of peaceful agents. Those values simplify to

$$< \sigma_P >= \begin{cases} 1 - \sigma_I \equiv p_1 \\ \frac{\alpha}{\beta}\sigma_I \equiv p_2 \end{cases} \tag{2.20}$$

which implies the two associated equilibrium opponent values

$$< \sigma_O >= \begin{cases} 0 \\ 1 - \frac{\alpha+\beta}{\beta}\sigma_I \end{cases} \tag{2.21}$$

Indeed equation 2.17 can be solved analytically to yield

$$\sigma_P(t) = p_2 + \frac{p_1 - p_2}{1 - \frac{\sigma_P(0) - p_1}{\sigma_P(0) - p_2} e^{\beta(p_1 - p_2)t}} \tag{2.22}$$

Figure 2.3 shows the evolution of the system on varying the initial conditions.

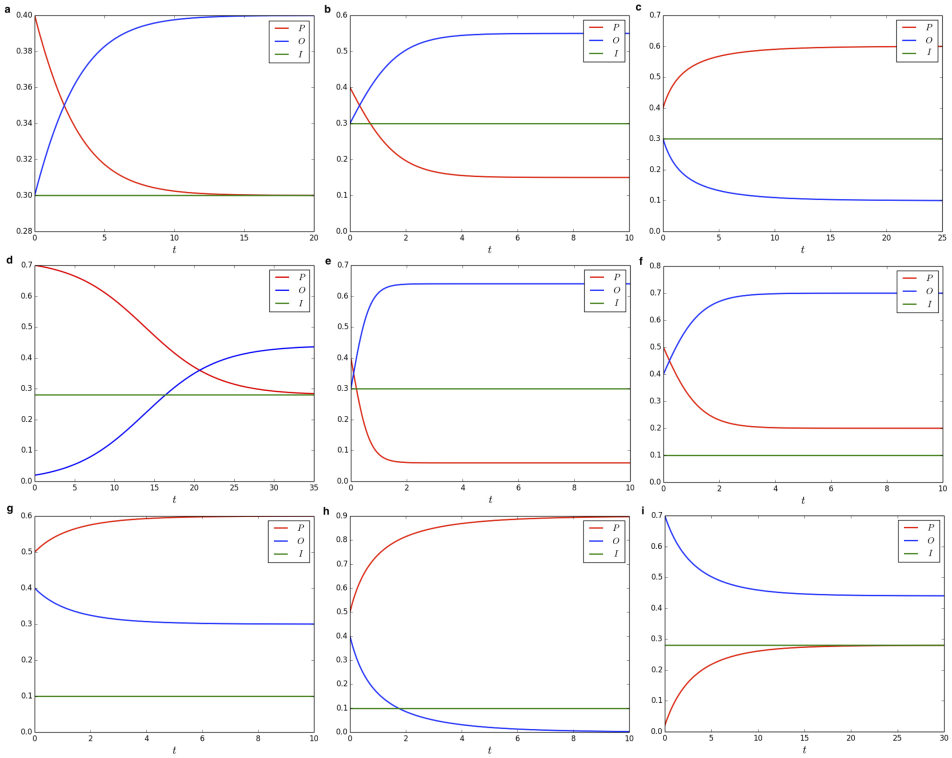

Figure 2.3: Evolution of the system on varying initial conditions: **a** $\sigma_I = 0.3$, and $\sigma_O = 0.3$, $\alpha = 1.0$, $\beta = 1.0$. **b** $\sigma_I = 0.3$, and $\sigma_O = 0.3$, $\alpha = 1.0$, $\beta = 2.0$. **c** $\sigma_I = 0.3$, and $\sigma_O = 0.3$, $\alpha = 4.0$, $\beta = 2.0$. **d** $\sigma_I = 0.28$, and $\sigma_O = 0.02$, $\alpha = 0.5$, $\beta = 0.5$. **e** $\sigma_I = 0.3$, and $\sigma_O = 0.3$, $\alpha = 1.0$, $\beta = 5.0$. **f** $\sigma_I = 0.1$, and $\sigma_O = 0.4$, $\alpha = 4.0$, $\beta = 2.0$. **g** $\sigma_I = 0.1$, and $\sigma_O = 0.4$, $\alpha = 12.0$, $\beta = 2.0$. **h** $\sigma_I = 0.1$, and $\sigma_O = 0.4$, $\alpha = 22.0$, $\beta = 2.0$. **i** $\sigma_I = 0.28$, and $\sigma_O = 0.7$, $\alpha = 0.5$, $\beta = 0.5$.

2.2.2 Analysis of the Stability

We analyze the respective stability ranges for p_1 and p_2:

$$\frac{d\sigma_P}{dt}(\sigma_P) \simeq \frac{d\sigma_P}{dt}(<\sigma_P>) + (\sigma_P - <\sigma_P>)\lambda \tag{2.23}$$

where $\frac{d\sigma_P}{dt}(<\sigma_P>) = 0$ and $\lambda \equiv \frac{d^2\sigma_P}{dtd\sigma_P}|_{<\sigma_P>}$, we obtain

$$\lambda = -[\alpha\sigma_I + \beta(1-\sigma_I)] + 2\beta\sigma_P \tag{2.24}$$

Therefore, for respective values p_1, p_2 we obtain

$$\begin{cases} \lambda_1 = -\alpha\sigma_I + \beta(1-\sigma_I) = \beta(p_1 - p_2) \\ \lambda_2 = \alpha\sigma_I - \beta(1-\sigma_I) = -\beta(p_1 - p_2) \end{cases} \tag{2.25}$$

Stability being achieved for $\lambda < 0$, equation 2.25 shows that $p_1(p_2)$ is stable when $p_1 < p_2 (p_1 > p_2)$. Accordingly we get two stable regimes:

$$\begin{cases} p_1 \leq p_2 \Leftrightarrow \sigma_I \geq I_c \\ p_1 \geq p_2 \Leftrightarrow \sigma_I \leq I_c \end{cases} \tag{2.26}$$

with $I_c \equiv \frac{\beta}{\alpha+\beta}$. These two regimes yield the respective equilibrium values for peaceful and opponent agents as from 2.20 and 2.21

$$\begin{cases} <\sigma_P> = p_1 = 1 - \sigma_I, <\sigma_O> = 0 \\ <\sigma_P> = p_2 = \frac{\alpha}{\beta}\sigma_I, <\sigma_O> = 1 - \frac{\sigma_I}{I_c} = p_1 - p_2 \end{cases} \tag{2.27}$$

The first equation of system 2.27 highlights that in some conditions the amount of opponent agents is equal to zero. Hence, we perform a further investigation to study under which conditions it is possible to avoid the phenomenon of radicalization (i.e. by reaching the equilibrium state $<\sigma_O> = 0$). In terms of opinion dynamics these results indicate that under appropriate conditions it is possible to remove one opinion from the system.

Extinction processes

From the above results radicalization can be totally thwarted if $\sigma_I \geq I_c$. Accordingly, given σ_I and β the individual involvement for the inflexible population in striking up with individual opponents must be at least at a level

$$\alpha > (\frac{1}{\sigma_I} - 1)\beta \tag{2.28}$$

Therefore, as seen from equation 2.28 the larger σ_I the less effort is required from the inflexible population. However, the more active are the opponents (i.e., larger β) the more involvement is required. To visualize the multiplicative factor by which α must overpass β it is worth to draw the curve

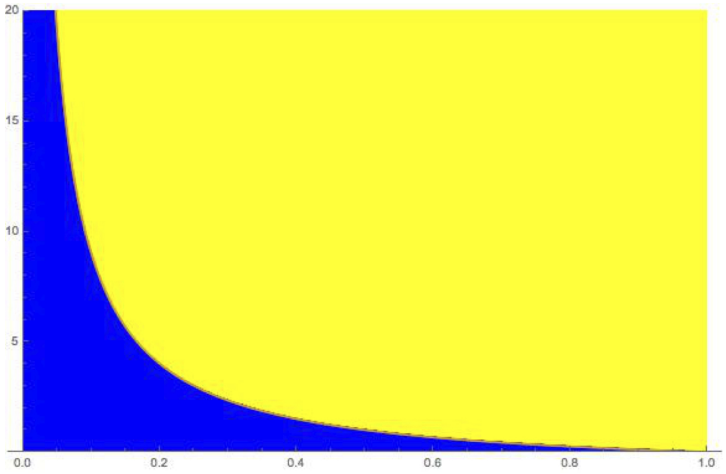

Figure 2.4: The curve $\frac{1}{\sigma_N} - 1$ is shown as a function of σ_N. All cases for which the value of $\frac{\alpha}{\beta}$ is above the curve (yellow, clear) correspond to situations for which radicalization is totally thwarted. When the value of $\frac{\alpha}{\beta}$ is below the curve (blue, dark) radicalization takes place on a permanent basis.

$\frac{1}{\sigma_I} - 1$ as a function of σ_I as shown in fig 2.4. From Equation 2.28 it is seen that to prevent radicalization inflexible agents's involvement must be either lower ($\alpha < \beta$) or larger ($\alpha > \beta$) than that of opponents depending on the magnitude of the multiplicative factor $\frac{1}{\sigma_I} - 1$. When $\frac{1}{\sigma_I} - 1 < 1$, i.e. $\sigma_I > \frac{1}{2}$ core agents do not need to much individual engagement as could be expected in the case of a coexistence of a core majority population with a sensitive minority subpopulation. More precisely, the engagement depends on the opponent activism but the core population benefiting from its majority status. In this case its requirement is always lower than the opponent involvement. However, the situation turns difficult when the initial sensitive minority turns to a majority status as it occurred in some specific urban areas. In that case to avoid a radicalization requires a very high individual engagement from the core agents, which may be rather hard to implement. In particular since no collective information is available about the situation. We thus have three different cases: **1)** $\sigma_I > \frac{1}{2}$, **2)** $\sigma_I = \frac{1}{2}$, and **3)** $\sigma_I < \frac{1}{2}$ to consider to determine the respective level of individual core involvement to avoid the phenomenon of radicalization.

Case 1. For $\sigma_I > \frac{1}{2}$ core agents need little involvement to thwart totally the radicalization of the sensitive subpopulation with values of α much lower than β. Indeed, opponent agents need to produce very high values of β (compared to α) to survive, precisely the condition $\beta \geq \frac{\alpha\sigma_I}{(1-\sigma_I)}$ must be satisfied. However, very large values of β can shrink to zero the amount of peaceful agents yielding a fully radicalized sensitive population, which although in a small minority status may produce substantial violence against inflexible

agents.
Case 2. For $\sigma_I = \frac{1}{2}$ the opponent activism must be counter with an equal core counter activism since $\alpha \geq \beta$ makes opponent agents to extinct. Instead, for $\alpha < \beta$ peaceful and opponent agents coexist and the former disappear for large values of β with again a fully radicalized sensitive population with $< \sigma_O >= \sigma_I$.
Case 3. For values $\sigma_I < \frac{1}{2}$, if $\alpha = \beta$ the equilibrium condition entails that $< \sigma_P >= \sigma_I$ (and $< \sigma_O >= 1 - 2\sigma_I$). If $\alpha > \beta$, we can reach the extinction of opponent agents as $\frac{\sigma_I}{I_c} = 1$. In contrast when $\alpha < \beta$ opponent agents strongly prevail in the population.

Degree of radicalization

In order to asses the degree of radicalization in a population we can introduce two parameters: ζ and η. The former is defined to evaluate the fraction of opponent agents among flexible agents while the latter (i.e. η) evaluates the ratio between opponent and inflexible agents. Therefore, ζ represents the relative ratio of opponents among flexible agents and η gives a measure about the real power of opponents agents in a population. An high value of ζ (i.e. close to 1) in a population with $\sigma_I \gg 0.5$ indicates that strategies to fight radicalization are too weak but at the same time opponents are few. Therefore, in this case governments should take an action even if the situation seems still under control. On the other hand, a low value of ζ (i.e., close to 0) together with a high value of η represent an alarming situation. Indeed, even if there are only a few opponents among flexible agents their amount is bigger than that of inflexible ones [90]. To evaluate these measures, ζ and η have been defined as follows

$$\begin{cases} \zeta = \frac{\sigma_O}{1-\sigma_I} \\ \eta = \frac{\sigma_O}{\sigma_I} \end{cases} \tag{2.29}$$

hence, recalling that $\sigma_O = 1 - \sigma_I - \sigma_P$ and having solved analytically $\sigma_P(t)$ (see 2.22) we are able to compute values of both parameters ζ and η at equilibrium and on varying the initial conditions —see Fig 2.5. It is worth to note that the parameter ζ as defined in 2.29 has a range in $[0, 1]$. At equilibrium $\zeta = 0$ means that there are no opponent agents in the population while $\zeta = 1$ means that all flexible agents became opponents. On the other hand, the parameter η has potentially an unlimited range from 0 to ∞ (in the case σ_I is very close to 0 and σ_O to 1). To conclude, this particular case allows to show the number of applications based on an analytical approach to population dynamics, from biological phenomena to complex social processes.

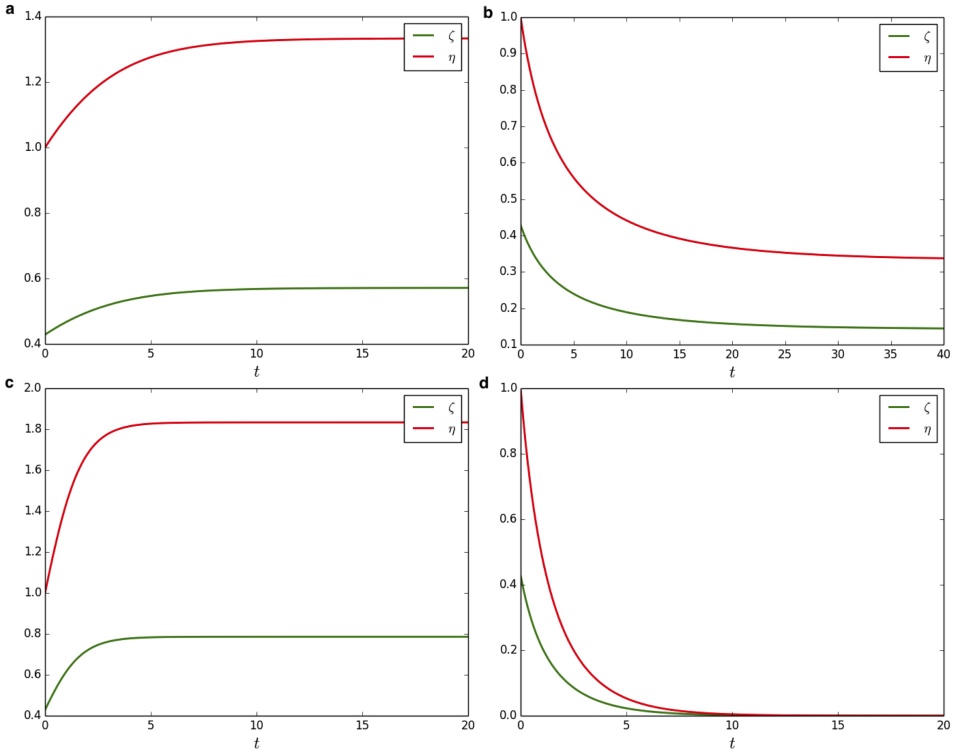

Figure 2.5: Radicalization degree quantified according to the parameters ζ and η, on varying initial conditions: **a** $\sigma_I = 0.3$, and $\sigma_O = 0.3$, $\alpha = 1.0$, $\beta = 1.0$. **b** $\sigma_I = 0.3$, and $\sigma_O = 0.3$, $\alpha = 2.0$, $\beta = 1.0$. **c** $\sigma_I = 0.3$, and $\sigma_O = 0.3$, $\alpha = 1.0$, $\beta = 2.0$. **d** $\sigma_I = 0.3$, and $\sigma_O = 0.3$, $\alpha = 4.0$, $\beta = 1.0$.

Part II

Statistical Physics of Cooperation

Chapter 3

Phase Transitions in the Prisoner's Dilemma

In this chapter, we introduce an analytical model for studying the evolution towards equilibrium in spatial games, with 'memory-aware' agents, i.e. agents that accumulate their payoff over time [56]. In particular, we focus our attention on the spatial Prisoner's Dilemma, as it constitutes an emblematic example of a game whose Nash equilibrium is defection. Previous investigations showed that, under opportune conditions, it is possible to reach, in the evolutionary Prisoner's Dilemma, an equilibrium of cooperation. Notably, it seems that mechanisms like motion may lead a population to become cooperative. In the proposed model, we map agents to particles of a gas so that, on varying the system temperature, they randomly move. In doing so, we are able to identify a relation between the temperature and the final equilibrium of the population, explaining how it is possible to break the classical Nash equilibrium in this game, under the condition that agents are able to increase their payoff over time. Moreover, we introduce a formalism to study order-disorder phase transitions in these dynamics.

3.1 Introduction

Here, we try to provide an analytical description of the spatial PD, in order to explain how a population can become cooperative and to strengthen the link between EGT and statistical physics. It is worth to highlight that we consider 'memory-aware' agents, i.e., agents that accumulate their payoff over time. Remarkably, this last condition represents the major difference with most of the evolutionary game models studied by computational approaches. On the other hand, considering 'memory-aware' agents makes the problem more tractable from an analytical perspective.

3.2 Model

In the proposed model, we are interested in studying the spatial prisoner's dilemma by an analytical approach. Let us start by introducing the general form of a payoff matrix

$$\begin{array}{cc} & \begin{array}{cc} C & D \end{array} \\ \begin{array}{c} C \\ D \end{array} & \begin{pmatrix} R & S \\ T & P \end{pmatrix} \end{array} \tag{3.1}$$

where the set of strategies is $\Sigma = \{C, D\}$: C stands for 'Cooperator' and D for 'Defector'. In the matrix 3.1, R is the gain obtained by two interacting cooperators, T represents the *Temptation*, i.e., the payoff that an agent gains if it defects while its opponent cooperates, S the *Sucker's payoff*, i.e., the gain achieved by a cooperator while the opponent defects, eventually P the payoff of two interacting defectors. In the case of the PD, matrix elements of 3.1 are: $R = 1$, $0 \leq S \leq -1$, $1 \leq T \leq 2$ and $P = 0$. As stated before, during the evolution of the system agents can change their strategy from C to D, and vice versa, following an updating rule, as for instance the one named 'imitation of the best' (see [52]), where agents imitate the strategy of their richest neighbor.

Mean field approach

Now, we consider a mixed population of N agents with, at the beginning, an equal density of cooperators and defectors. Under the hypothesis that all agents interact together, at each time step the payoffs gained by cooperators and defectors are computed as follows

$$\begin{cases} \pi_c = (\rho_c \cdot N - 1) + (\rho_d \cdot N)S \\ \pi_d = (\rho_c \cdot N)T \end{cases} \tag{3.2}$$

with $\rho_c + \rho_d = 1$, ρ_c density of cooperators and ρ_d density of defectors. We recall that defection is the dominant strategy in the PD and, even if we set $S = 0$ and $T = 1$, it corresponds to the final equilibrium because π_d is always greater than π_c. At this point, it is important to highlight that previous investigations [52, 54, 55] have been performed by 'memoryless' agents (i.e., agents that do not accumulate the payoff over time) whose interactions were defined only with their neighbors, and focusing only on one agent (and on its neighbors) at a time. These conditions are fundamental. For instance, if at each time step we randomly select one agent interacting only with its neighbors, there exists the probability to select consecutively a number of close cooperators; thus, in this occurrence, very rich cooperators may emerge and then prevail on defectors, even without introducing mechanisms like motion. It is also worth to observe that as $P = 0$, a homogeneous

population of defectors does not increase its overall payoff. Instead, according to the matrix 3.1, a cooperative population continuously increases its payoff over time.
Now, we consider a population divided into two groups by a wall: a group G^a composed of cooperators, and a mixed group G^b, i.e., composed of cooperators and defectors in equal amount. Agents interact only with members of the same group, then the group G^a never changes and, in addition, it strongly increases its payoff over time. The opposite occurs in the group G^b, as it converges to an ordered phase of defection, limiting its final payoff. Remarkably, in this scenario, we can introduce a strategy to modify the equilibria of the two groups. In particular, we can both change to cooperation the equilibrium of G^b, and to defection that of G^a. In the first case, we have to wait a while, before moving one or few cooperators to G^b, so that defectors increase their payoff, but during the revision phase they change strategy to cooperation as the newcomers are richer than them. In the second case, if we move after few time steps a small group of defectors from G^b to G^a, the latter converges to a final defection phase. These preliminary and theoretical observations let emerge an important property of the 'memory-aware' PD: considering the two different groups, cooperators may succeed when act after a long time and individually. Instead, defectors may succeed acting fast and in group. Notably, rich cooperators have to move individually since otherwise many rich cooperators risk to increase too much the payoff of defectors that, in this case, will not change strategy. The opposite holds for defectors that, acting in group, may strongly reduce the payoff of a community of cooperators (for $S < 0$).

Mapping agents to gas particles

We hypothesize that the spatial PD, with moving agents, can be successfully studied by the framework of kinetic theory [24]. Therefore, in the proposed model, we map agents to particles of a gas. In doing so, the average speed of particles is computed as $< v >= \sqrt{\frac{3T_s k_b}{m_p}}$, with T_s system temperature, k_b Boltzmann constant, and m_p particle mass. Particles are divided into two groups by a permeable wall, so that it can be crossed by particles, but it avoids interactions among particles belonging to different groups. Now, it is worth to emphasize that we can provide a dual description of our system: one in the 'physical' domain of particles, the other in the 'information' domain of agents. Notably, to analyze the system in the 'information' domain we will introduce, as above discussed, the mapping of agents to a spin system (see [91]). Summarizing, we map agents to gas particles in order to represent their 'physical' property of motion, and we map agents to spins for representing their 'information' property (i.e., their strategy). Remarkably, these two mappings can be viewed as two different layers for studying how the agent population evolves over time. Although the physical property

(i.e., the motion) affects the agent strategy (i.e., its spin), the equilibrium can be reached in both layers/domains independently. This last observation is important since we are interested in evaluating only the final equilibrium reached in the 'information' domain. Then, as stated before, agents interact only with those belonging to the same group, so the evolution of the mixed group G^b can be described by following equations

$$\begin{cases} \frac{d\rho_c^b(t)}{dt} = p_c^b(t) \cdot \rho_c^b(t) \cdot \rho_d^b(t) - p_d^b(t) \cdot \rho_d^b(t) \cdot \rho_c^b(t) \\ \frac{d\rho_d^b(t)}{dt} = p_d^b(t) \cdot \rho_d^b(t) \cdot \rho_c^b(t) - p_c^b(t) \cdot \rho_c^b(t) \cdot \rho_d^b(t) \\ \rho_c^b(t) + \rho_d^b(t) = 1 \end{cases} \tag{3.3}$$

with $p_c^b(t)$ probability that cooperators prevail on defectors (at time t), and $p_d^b(t)$ probability that defectors prevail on cooperators (at time t). These probabilities are computed according to the payoffs obtained, at each time step, by cooperators and defectors

$$\begin{cases} p_c^b(t) = \frac{\pi_c^b(t)}{\pi_c^b(t)+\pi_d^b(t)} \\ p_d^b(t) = 1 - p_c^b(t) \end{cases} \tag{3.4}$$

The system 3.3 can be analytically solved provided that, at each time step, values of $p_c^b(t)$ and $p_d^b(t)$ be updated. So, the density of cooperators reads

$$\rho_c^b(t) = \frac{\rho_c^b(0)}{\rho_c^b(0) - [(\rho_c^b(0) - 1) \cdot e^{\frac{\tau t}{N^b}}]} \tag{3.5}$$

with $\rho_c^b(0)$ initial density of cooperators in G^b, $\tau = p_d^b(t) - p_c^b(t)$, and N^b number of agents in G^b. Recall that setting $T_s = 0$, not allowed in a thermodynamic system, corresponds to a motionless case, leading to the Nash equilibrium in G^b. Instead, for $T_s > 0$ we can find more interesting scenarios. Now we suppose that, at time $t = 0$, particles of G^a are much closer to the wall than those of G^b (later we will relax this constraint); for instance, let us consider a particle of G^a that, during its random motion, it is following a trajectory of length d (in the n-dimensional physical space) towards the wall. Assuming this particle is moving with speed equal to $< v >$, we can compute the instant of crossing $t_c = \frac{d}{<v>}$, i.e., the instant when it moves from G^a to G^b. Thus, on varying the temperature T_s, we can vary t_c.
Let us consider the payoff of cooperators in the two groups. Each cooperator in G^a gains

$$\pi_c^a = (\rho_c^a \cdot N^a - 1) \cdot t \tag{3.6}$$

On the other hand, the situation for cooperators in G^b is much more different as, according to the Nash equilibrium, their amount decreases over time. Therefore, we can consider how changes the payoff of the last cooperator survived in G^b

$$\pi_c^b = \sum_{i=0}^{t} [(\rho_c^b \cdot N^b - 1) + (\rho_d^b \cdot N^b)S]_i \tag{3.7}$$

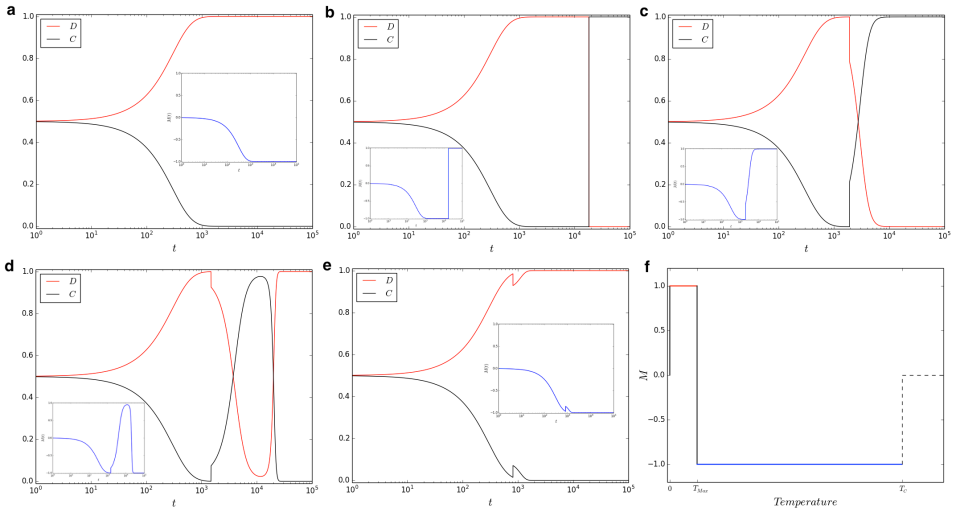

Figure 3.1: From **a** to **e**: Evolution of the group G^b, with $N = 100$ and $\epsilon = 1$, on varying the temperature: **a.** $T_s = 0$. **b.** $T_s = 0.1$. **c.** $T_s = 9$. **d.** $T_s = 15$. **e.** $T_s = 50$. Insets show the system magnetization over time. The istant $t = t_c$, can be detected in plots **c,d,e** as a discontinuity of the two lines (i.e., red and black). **f.** Final magnetization M, of G^b, for different temperatures (T_c indicates the 'critical temperature').

moreover, $\pi_c^b \to 0$ as $\rho_c^b \to 0$. At $t = t_c$, a new cooperator reaches G^b, with a payoff computed with equation 3.6.

3.3 Results

The analytical solution 4.3 allows to analyze the evolution of the system and to evaluate how initial conditions affects the outcomes of the model. Let us observe that, if $\pi_c^a(t_c)$ is enough big, the new cooperator may modify the equilibrium of G^b, turning defectors to cooperators. Notably, the payoff considered to compute p_c^b, after t_c, corresponds to $\pi_c^a(t_c)$, as the newcomer is the richest cooperator in G^b. Furthermore, we note that $\pi_c^a(t_c)$ depends on N^a, hence we study the evolution of the system on varying the parameter $\epsilon = \frac{N^a}{N^b}$, i.e., the ratio between particles in the two groups. Eventually, for numerical convenience, we set $k_b = 1 \cdot 10^{-8}$, $m_p = 1$, and $d = 1$.
Figure 3.1 shows the evolution of G^b, for $\epsilon = 1$ on varying T_s and, depicted in the inner insets, the variation of system magnetization over time (always inside G^b) (see [92]). As discussed before, in the physical domain of particles, heating the system entails the average speed of particles increases. Thus, under the assumption that two agents play together if they stay close (i.e., in the same group) for a long enough time, we hypothesize that exists a maximum speed such that for greater values interactions do not occur (in

terms of game). This hypothesis requires a critical temperature T_c, above which no interactions, in the 'information' domain, are possible. As shown in plot **f** of figure 3.1, for temperatures in range $0 < T_s < T_{max}$ the system converges to a cooperation phase (i.e., $M = +1$), for $T_{max} < T_s < T_c$ the system follows the Nash equilibrium (i.e., $M = -1$), and for $T > T_c$ a disordered phase emerges at equilibrium. Remarkably, results of our model suggest that it is always possible to compute a range of temperatures to obtain an equilibrium of full cooperation —see figure 3.2. Moreover, we

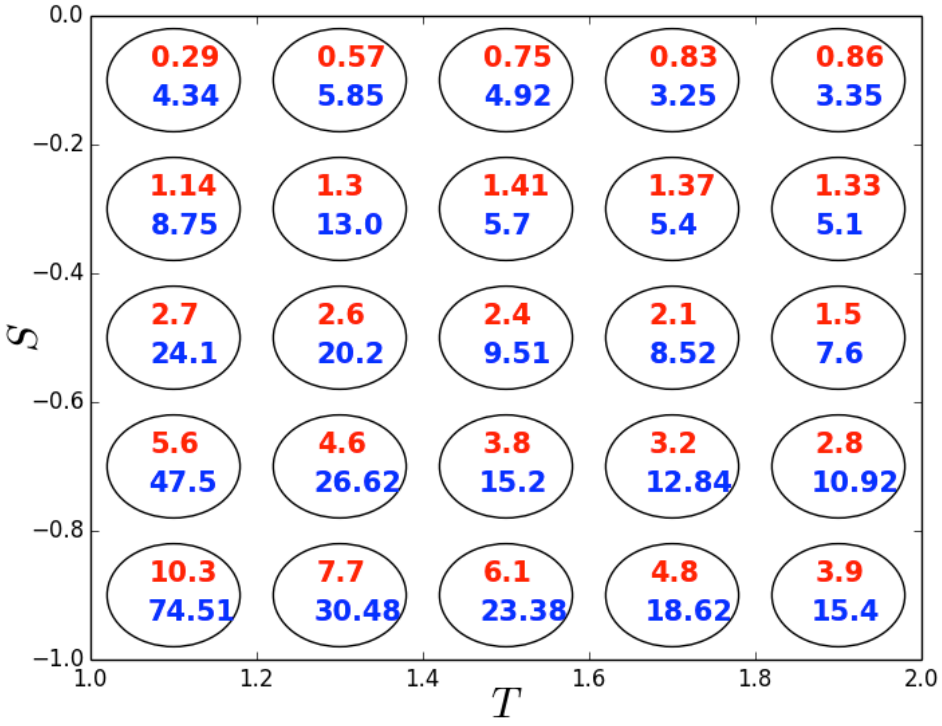

Figure 3.2: Maximum values of temperature T_s that allow the group G^b to converge to cooperation. Red values correspond to results computed with $\epsilon = 0.5$, while blue values to those computed with $\epsilon = 1$. Circles are placed in the TS diagram indicating values of T and S, of the payoff matrix, used for each case. Even for high values of T, and small values of S, it is possible to achieve cooperation.

study the variation of T_{max} on varying ϵ (see figure 3.3) showing that, even for low ϵ, it is possible to obtain a time t_c that allows the system to converge towards cooperation. Eventually, we investigate the relation between the maximum value of T_s that allows a population to become cooperative and its size N (i.e., the number of agents). Remarkably, as shown in figure 3.4, the maximum T_s scales with N following a power-law function characterized by a scaling parameter (i.e., an exponent) $\gamma \sim 2$. The value of γ has been computed by considering values of T_s shown in figure 3.2 for the case $\epsilon = 2$.

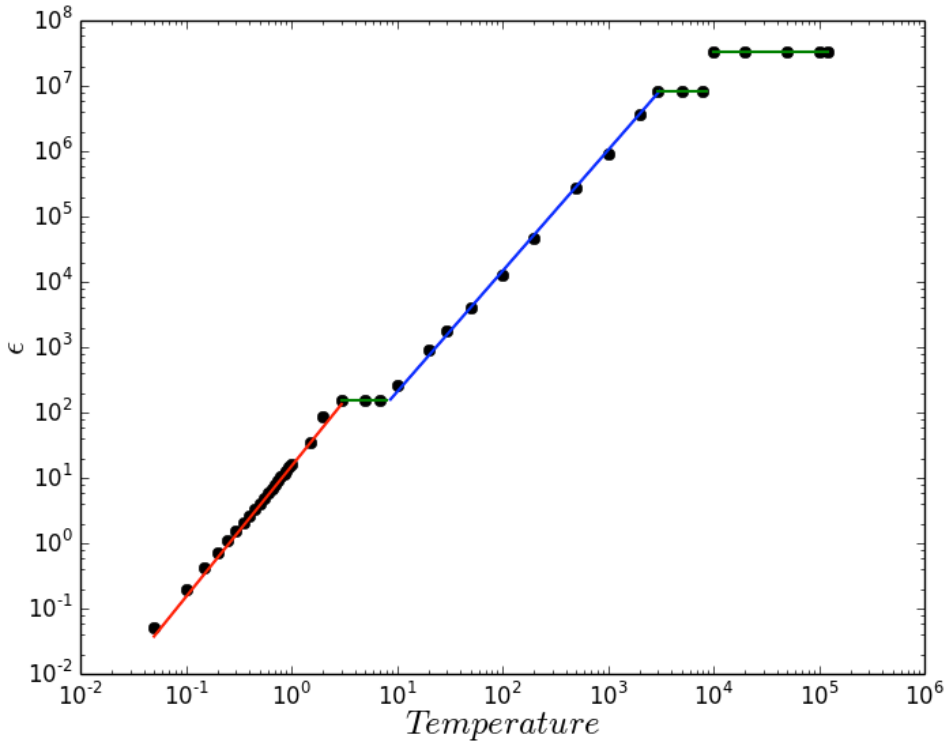

Figure 3.3: Maximum value of system temperature that allows to achieve cooperation at equilibrium versus ϵ (i.e., the ratio between particles in the two groups). Different colors identify different trends, fitted by power-law functions. After the final green plateau, temperatures are too high to play the spatial PD.

Eventually, it is worth to highlight that all analytical results let emerge a link between the system temperature and its final equilibrium. Recalling that we are not considering the equilibrium of the gas, i.e., it does not thermalize in the proposed model, we emphasize that the equilibrium is considered only in the information domain.

Phase Transitions in the spatial PD

As discussed before, in the information domain we can study the system by mapping agents to spins, whose value represents their strategy. In addition, we can map the difference between winning probabilities, of cooperators and defectors, to an external magnetic field: $h = p_c^b - p_d^b$. In doing so, by the Landau theory [24], we can analytically identify an order-disorder phase transition. Notably, we analyze the free energy F of the spin system on varying the control parameter m [73] (corresponding to the magnetization M)

$$F(m) = -hm \pm \frac{m^2}{2} + \frac{m^4}{4} \tag{3.8}$$

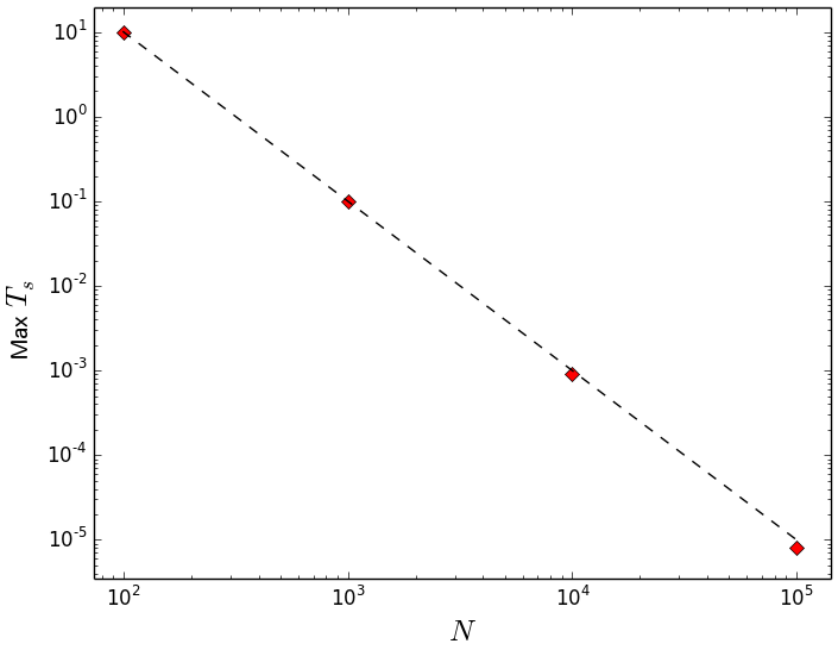

Figure 3.4: Maximum value of T_s to achieve full cooperation at equilibrium in function of N, i.e., the size of the population. The fitting function (dotted line) is a power-law characterized by a scaling parameter equal to 2.

where the sign of the second term depends on the temperature, i.e., positive for $T_s > T_c$ and negative for $T_s < T_c$; recalling that T_c represents the temperature beyond which it is not possible to play the PD due to the high particles speed (according to the condition before discussed). For the sake of clarity, we want to emphasize that the free energy is introduced in order to evaluate the nature of the final equilibrium achieved by the system. In particular, looking for the minima of F allows to investigate if our population reaches the Nash equilibrium, or different configurations (e.g., full cooperation). Figure 3.5 shows a pictorial representation of the phase transitions that occur in our system, on varying T_s and the external field h. Finally, the constraints related to the average speed of particles, and to the distance between each group and the permeable wall, can in principle be relaxed as we can imagine to extend this description to a wider system with several groups (as done in previous investigations, e.g. [54]), where agents are uniformly spread in the whole space. It is worth to highlight that our results are completely in agreement with those achieved by authors who studied the role of motion in the PD (as [52, 54]), explaining why clusters of cooperators emerge in their simulations [54]. We also recall that, in the proposed model, we are using memory-aware agents, while in previous computational

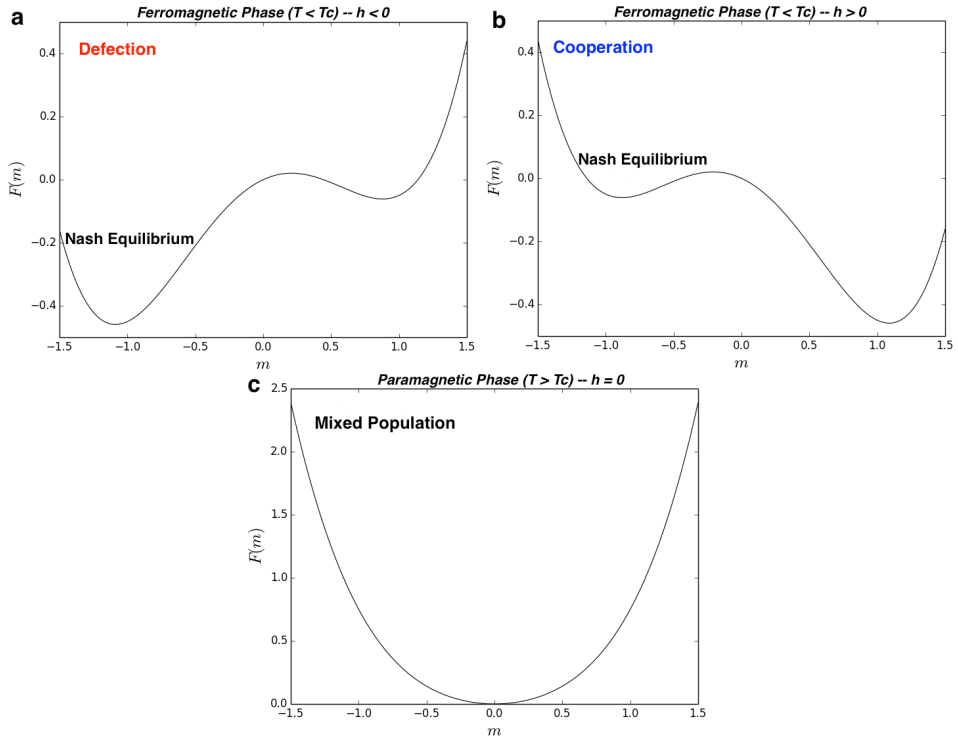

Figure 3.5: Order-disorder phase transitions in the population. For $T_s < T_c$, the population is in a ferromagnetic phase: **a.** Applying an external negative field, the system converges to the Nash equilibrium, corresponding to $m = -1$ (as $\sigma = -1$ represents defection); **b.** Applying an external positive field, the population converges to cooperation ($\sigma = +1$), corresponding to $m = +1$. **c.** For temperatures higher than T_c, a disordered paramagnetic phase emerges.

investigations agents reset their payoff at each step, i.e., before to start new interactions.

3.4 Conclusion

To conclude, in this chapter we provide an analytical description of the spatial Prisoner's Dilemma, by using the framework of statistical physics, studying the particular case of agents provided with memory of their payoff (defined memory-aware agents). This condition entails that their payoff is not reset at each time step, so that they can increase it over time. In particular, we propose a model based on the kinetic theory of gases, showing how motion may lead a population towards an equilibrium far from the expected one (i.e. the Nash Equilibrium). Remarkably, the final equilibrium depends on the system temperature, so that we have been able to identify a range of temperatures that triggers cooperation for all values of the payoff

matrix (related to the PD). In addition, we found an interesting relation between the maximum temperature that foster cooperation and the size of the system. Notably, a scaling parameter in that relation has been computed by investigating different orders of magnitude of the size of the system. Furthermore, the dynamics of the resulting model have been also described in terms of order-disorder phase transitions.

Chapter 4

The Role of the Temperature in the Public Goods Game

In this chapter, we aim to analyze the role of the temperature in the spatial PGG [93], one of the most famous games in EGT. The dynamics of this game is affected by a number of parameters and processes, namely the topology of interactions among the agents, the synergy factor, and the strategy revision phase. The latter is a process that allows agents to change their strategy. Notably, rational agents tend to imitate richer neighbors, in order to increase the probability to maximize their payoff. By implementing a stochastic revision process, it is possible to control the level of noise in the system, so that even irrational updates may occur. In particular, we study the effect of noise on the macroscopic behavior of a finite structured population playing the Public Goods Game. We consider both the case of a homogeneous population, where the noise in the system is controlled by tuning a parameter representing the level of stochasticity in the strategy revision phase, and a heterogeneous population composed of a variable proportion of rational and irrational agents. In both cases numerical investigations show that the Public Goods Game has a very rich behavior which strongly depends on the amount of noise in the system and on the value of the synergy factor. To conclude, our investigation sheds a new light on the relations between the microscopic dynamics of the Public Goods Game and its macroscopic behavior.

4.1 Introduction

Here, we aim to provide a description of the PGG by the lens of statistical physics, focusing in particular on the impact of noise in the population dynamics. Notably, for each individual the noise is controlled by a parameter adopted in the strategy revision phase (SRP), i.e., the process allowing the agent to update their strategy. The SRP can be implemented in several

ways, e.g. considering rational agents that aim to increase their payoff. Usually, rational agents tend to imitate their richer neighbors, while irrational agents are those that randomly change their strategy. Remarkably, tuning the level of noise to interpolate between configurations where agents fully utilize payoff information (low noise) to those where they behave at random (high noise), strongly affects the macroscopic behavior of a population. Although previous works (e.g. [94, 95, 96, 13]) focused on this topic (i.e. the role of noise) in this game, a complete analysis is still missing. In particular, we study the effect of noise in two different scenarios. We first consider the case of a homogeneous population, where the intensity of noise in the system is controlled by tuning the level of stochasticity of all agents during the SRP, by means of a global parameter. The latter is usually indicated by K, and defined as temperature or as an inverse degree of rationality [34]. Then, we consider a heterogeneous population, characterized by two types of agents, rational and irrational ones. While the former take their decision considering the payoff of their neighbors, the latter take decisions randomly. In the second case, the noise is controlled by tuning the density of irrational agents in the population. In both cases, we study the macroscopic dynamics of the population and the related steady states, achieved for different amount of noise and values of the synergy factor. It is worth to emphasize that the synergy factor, before mentioned, is a parameter of absolute relevance in the PGG, as it supports cooperative behaviors by enhancing the value of the total contributions provided by cooperators. Eventually, we recall that the influence of rationality in the PGG has been studied, by a probabilistic approach, in [97] where authors implemented agents able to select (with a given probability) between a rational and an irrational behavior.

4.2 Model

The PGG is a simple game involving N agents that can adopt one of the following strategies: cooperation and defection. Those playing as cooperators contribute with a coin c (representing the individual effort in favor of the collectivity) to a common pool, while those playing as defectors do not contribute. Then, the amount of coins in the pool is enhanced by a synergy factor r, and eventually equally divided among all agents. The cooperators' payoff (i.e. π^c) and that of defectors (i.e. π^d) read

$$\begin{cases} \pi^c = r\frac{N^c}{G} - c \\ \pi^d = r\frac{N^c}{G} \end{cases} \tag{4.1}$$

where N^c is the number of cooperators among the G agents involved in the game, r synergy factor, and c agents' contribution. Without loss of generality, we set $c = 1$ for all agents.

We now discuss the main properties and processes that characterize a population playing the PGG.

The Structure of the population

In the case of well-mixed populations of infinite size, the behavior of the system behavior can be predicted as a function of the synergy factor r [34] by studying the related Nash equilibria. In particular, when agents play in groups of G players, two different absorbing states appear separated at a critical point $r_{\mathrm{wm}} = G$. The population falls into full defection for $r < r_{\mathrm{wm}}$ and into full cooperation for $r > r_{\mathrm{wm}}$. Conversely, when agents are placed in the nodes of a network, surprisingly some cooperators can survive for values of r lower than r_{wm}. This effect is known as *network reciprocity* [22, 13, 98], since a cooperative behavior emerges as a result of the same mutualistic interactions taking place repeatedly over time. At the same time, the network structure allows a limited number of defectors to survive also beyond $r = r_{\mathrm{wm}}$. We refer to the two critical values of r at which cooperators first appear, and defectors eventually disappear from the population, respectively as r_{c1} and r_{c2}. It is worth mentioning that most investigations in EGT are performed by numerical simulations and an analytical definition of the critical thresholds (i.e. r_{c1} and r_{c2}) identified in networked topologies is missing. As a result, when studying EGT models by arranging agents in different spaces, the values of critical thresholds are achieved by Monte Carlo simulations. In a networked population, depending on the values of r and on how agents are allowed to update their strategy, it is possible to observe different regimes: two ordered equilibrium absorbing phases, where only one strategy survives (either cooperation or defection), and an active but macroscopically stable disordered phase [56] corresponding to the coexistence between the two species (i.e. cooperators and defectors).

The noise and the general set up of the model

A crucial parameter appearing in equation 8.1 is K_y, which plays the role of noise and then parametrizes the uncertainty in adopting a strategy. Notably, a low noise entails agents to strongly consider the difference in payoff $\Delta p = \pi_y - \pi_x$ while deciding their next strategy, whereas increasing the noise the payoff difference plays a more marginal role. In the case of a homogeneous population K is equal for all individuals, such that by tuning the value of this global variable we are able to control the level of noise in the system. In the limit of $K = 0$, the y-th agent will imitate the strategy of the x-th agent with probability $W = 1$ if $\pi_x > \pi_y$, and $W = 0$ otherwise. Conversely, in the limit $K \to \infty$ the SRP becomes a coin flip, and the imitation occurs with probability $W = 1/2$ no matter the value of the synergy factor. In the latter case the behavior of the PGG is analogous to that of a

classical voter model [99] where imitation between a pair of selected agents takes place with probability $W = 1/2$. Our study aims to confirm computationally results reported in [95, 35], and to evaluate the relation between r and K, in order to provide a complete description of the PGG, from the microscopic dynamics to the global behavior of the population. According to previous investigations, setting $K = 0.5$ is often considered as a good choice to describe a rational population with a moderate level of noise and where only a limited number of irrational updates may occur. In the case of bidimensional lattices with periodic boundary conditions —see Figure 4.1, since each agent has four neighbors, group interactions involve $G = 5$ players at a time. It has been shown in [3] that for such K the values of r_{c1}, at which cooperators emerge, and r_{c2}, where defectors completely disappears from the population, are respectively equal to 3.75 and 5.5. Instead, a coexistence between cooperators and defectors occurs for intermediate values of r between the two thresholds (i.e. r_{c1} and r_{c2}). Conversely, in the corresponding PGG on well-mixed populations, where games are organized in groups of the same size $G = 5$, the full defection and full cooperation regimes are separated at the critical point $r_{\mathrm{wm}} = 5$. It is also possible to consider the case of heterogenous populations where agents are characterized by different values K. In such scenario, the simplest set up is the one where only two different sets of agents exist: one endowed with K^1 and one with $K^2 > K^1$. Recalling that a higher value of K implies lower rationality in the SRP, by varying the density f of one species, with $0 \leq f \leq 1$, it is possible to control the level of noise in the system and study the outcomes of the model in different conditions. For instance, setting $K^1 = 0.5$ and $K^2 = \infty$, it is possible to evaluate the influence of a density f of rational agents in driving the population towards a particular state. This is particularly useful to analyze the behavior of a population whose agents have a different sensibility to their payoff and, from a social point of view, it allows to study the influence of rationality in driving the population towards an equilibrium (or steady state). As shown in related works from the sociophysics literature [64, 60], random imitation is not the only relevant non-rational behavior able to impact the way in which agents choose their next strategy. Just to cite few, investigations driven on simple principles such as social conformity [100] (see also Appendix A) or nonconformity [101], extremism [88], stubbornness [102] or multiplexity [103] showed how simple changes in the microscopic dynamics of the agents can significantly affect the social dynamics of a given population [64, 104, 105, 106, 107, 108, 109, 110, 111, 112]. Eventually, we note that in a heterogeneous population it could be interesting to consider more complicated cases where agents are characterized by a broad distribution of values of K, and can possibly change their own degree of rationality, for instance by thermalization-like processes (i.e. when two agents play, they modify their degree of rationality taking the average value of their current K). Since in the PGG, the strategy of the x-th agent can be described

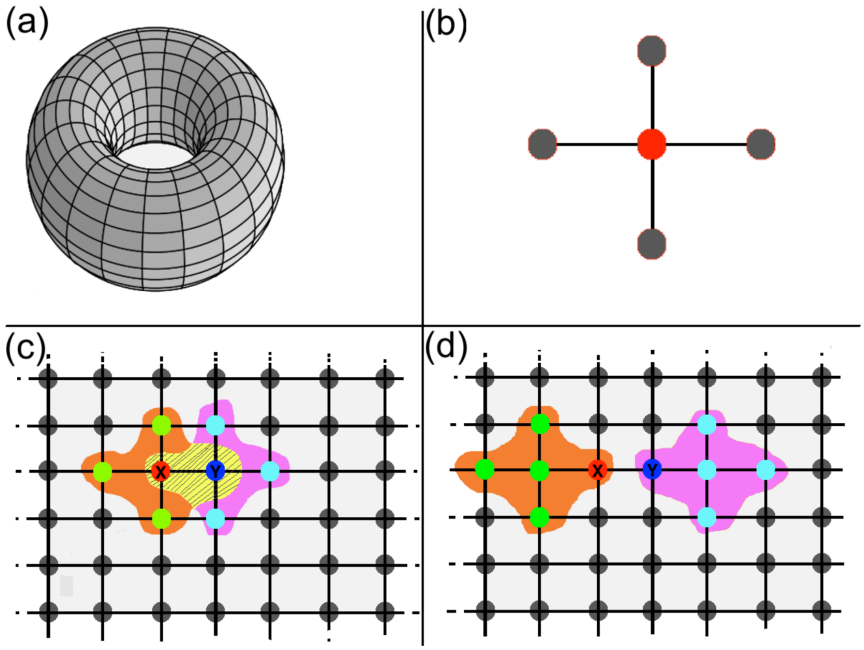

Figure 4.1: (Color online). Pictorial representation of the PGG on the considered topology. Agents are arranged in bidimensional square lattice with continuous boundary conditions, forming a toroid as shown in **(a)**. Each agent belongs to five groups of size $G = 5$: one where he is the central player, in red, and four as a peripheral node, in black **(b)**. At each time step, two agents x and y are randomly selected and they play the PGG with all the players in their groups for all groups of belonging. In **(c)**, we show the group where x and y are central: the green nodes are neighbors of node x, and this group has a orange shadow; while neighbors of agent y are cyan and this group has a violet shadow. The dotted lines in the area between x and y indicate the intersection between the groups formed by x and y. Notably, y belongs to the group formed by x and vice versa. In **(d)** we show for both x and y one of the possible groups where they are peripheral.

by a binary variable $s_x = \pm 1$, with $+1$ representing cooperation and -1 defection, the average magnetization [92] reads

$$M = \frac{1}{N} \sum_{i=1}^{N} s_i, \tag{4.2}$$

where $M = 1$ corresponds to full cooperation, while $M = -1$ to full defection. Since we are not interested in the sign of the prevalent strategy, but only to which extent the system is ordered, we consider the absolute value of the magnetization $|M|$. From equation A.1 it is straightforward to derive the density ρ of cooperators in the population

$$\rho = \frac{M + 1}{2} \tag{4.3}$$

so that we can identify the two (ordered, i.e. $|M| = 1$) absorbing states corresponding to $\rho = 1$ (i.e. full cooperation) and $\rho = 0$ (i.e. full defection). At last, another interesting order parameter useful to detect fluctuations in the system's behavior is the standard deviation of the fraction of cooperator $\sigma(\rho)$ obtained over the different runs. In the following section, we describe the macroscopic state of the system by reporting the average value of ρ, $\sigma(\rho)$, $|M|$ and T averaged over 100 simulations for all the considered configurations.

4.3 Results

We performed several numerical simulations of the PGG, for different values of the synergy factor r and the noise (measured either in terms of K or density of irrational agents $1 - f$), in a population of $N = 10^4$ agents distributed on a bidimensional lattice with periodic boundary conditions.

Homogeneous Populations. Let us here show results for the homogeneous case, where the level of noise in the system is controlled by the global variable K used in the SRP. We first analyze the strategy distribution diagram, which reports the average density of cooperators $\langle\rho\rangle$ as a function of r and K —Figure 4.2. Here, we observe that the PGG has a very rich behavior. For instance, plot **a** of Figure 4.2 shows 5 different regions (below described) of interest when studying the density of cooperators at equilibrium. Notably, low values of K (i.e., $K < 10$) let emerge three phases as a function of r in the considered range (i.e., from 3.4 to 6.0): two ordered phases (i.e., full defection and full cooperation) for low and high values of r, and a mixed phase (i.e., coexistence) for intermediate values of r. Therefore, at a first glance, an order-disorder phase transition of second kind emerges crossing the region labeled (1) in the first strategy distribution diagram (i.e., **(a)** of Figure 4.2). For higher values of K, next to $K = 10$, the active phase vanishes and the population always reaches an ordered phase. A more abrupt phase transition between the two ordered phases, separating region $(2A)$ (full defection) and $(2B)$ (full cooperation), appears, resembling analytical results obtained for the well-mixed approximation, even if fluctuations are possible near the critical point $r = 5$. For greater values of K, the region of r around $r = 5$ such that both ordered states are attainable increases. In such range of values the system behaves as a biased voter model, where the absorbing states of cooperation (defection) is favored for $r > 5$ ($r < 5$). In the limit $K \to \infty$, the behavior of the system approaches that of a classical unbiased voter model, no matter the value of the adopted synergy factor. Plots **(b)** and **(c)** of Figure 4.2 confirm the main differences among the five regions of plot **(a)**. The former shows that the population does not reach an ordered phase for intermediate values of r around $r = 5$ and low K, and the simulation is only stopped

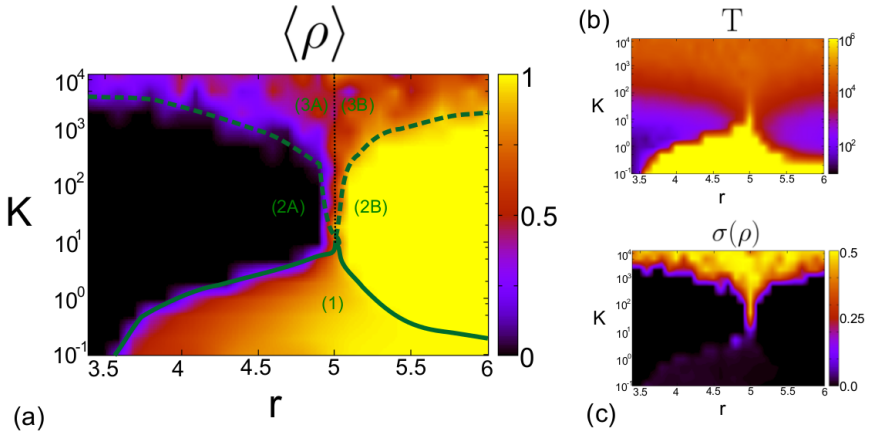

Figure 4.2: (Color online). Strategy distribution diagram showing the average density of cooperators $\langle\rho\rangle$ at the steady state (a), time to reach the absorbing state T (b) and standard deviation of the density of cooperators $\langle\rho\rangle$ at the steady state (c) as a function of the synergy factor r and the rationality K. Different regions are highlighted. In region (1) the system is stuck in a metastable active phase, macroscopically at the equilibrium, with coexistence of cooperators and defectors due to network reciprocity (the simulations have been stopped after $T = 10^6$ updates per agent). In region (2) the system always reaches the absorbing state predicted by the well-mixed population approximation, i.e. full defection for $r < r_{\rm wm} = 5$ and full cooperation for $r > r_{\rm wm}$. In region (3) both steady states become accessible with different probability, as in a biased voter model. Results are averaged over 100 simulation runs.

once the average number of updates is equal to the considered maximum number $T = 10^6$ with the system macroscopically at the steady state. Conversely, for different parameters the population reaches an absorbing state (i.e. full defection or cooperation) relatively quickly. Instead, plot **c** shows that the variance reaches a maximum value (as expected), $\sigma(\rho) = 1/2$, when the PGG behaves like a voter model, while smaller non-null values are also obtained for the active phase, due to the existence of fluctuations. In order to obtain a deeper characterization of the phase transitions occurring in the PGG, we study the average absolute value of the magnetization $|M|$, as a function of the synergy factor for different K values. As shown in plot **(a)** of Figure 4.3, only for values of $K < 10$ there are values of the synergy factors r such that $\langle|M|\rangle \neq 1$, since at $K \approx 10$ a more abrupt phase transition between full defection and full cooperation emerges, resembling the first-order first transition predicted analytically in the case of well-mixed population of infinite size. Then, we note that for all K values in the range $[0 \leq K \leq 10]$, it is possible to find a synergy factor r such that $|M(r)| = 0$. Notably, as K increases, the difference between the two critical thresholds r_{c1} and r_{c2} goes to zero as both converge quickly towards $r_{\rm wm} = 5$, eventually hitting such value at $K \approx 10$ —see plot **(b)** of Figure 4.3. Furthermore, we also

observe that the value of r_0, for which cooperators and defectors coexist in equal number in the active phase, is always smaller than $r_{\rm wm}$ —see plot **(b)** of Figure 4.3. Here, we remark that r_0 separates the active phase in two regions, where either defectors (1A) or cooperators (1B) are predominant. Eventually, both plots **(c)** and **(d)** of Figure 4.3 clearly confirms the previous investigations. For instance, for $K = 10000$ the density of cooperators becomes almost flat as in a Voter model (see plot **(c)** of Figure 4.3).

Heterogeneous Populations. We now consider the case of a heterogenous population, where a density of agents f ($0 \leq f \leq 1$) with $K^1 = 0.5$ is inserted, spatially at random, in a population of irrational individuals which perform coin flips to decide their strategy. In this configuration, the level of noise is controlled by the variable f, and the lower its value the higher the stochasticity in the population. As shown in Figure 4.4, the strategy distribution diagram obtained as a function of the different values of noise is qualitatively comparable to the previously considered case. As f goes to 1 the PGG turns its behavior to the expected one for a population composed of only rational individuals (i.e., $r_{c1} = 3.75$ and $r_{c2} = 5.5$). Remarkably, the outcomes shown in Figure 4.4 suggest that for values as small as $f \sim 3\%$, the PGG shows an active phase (i.e., the network reciprocity still holds). Thus, very few rational agents are able to provide the population an overall rational behavior at equilibrium. See plot **(b)** of Figure 4.4 to observe the scaling for the critical values of the synergy factor: r_{c1} (at which cooperators first appear), r_{c2} (at which defectors disappears), and r_0 (where cooperators and defectors coexist in equal proportion). Finally, considering both the homogenous and heterogenous case here presented, it is important to highlight that our analyses do not study the evolution of a population over time, but focus on the final equilibria (or steady-state). Therefore, further investigations of the proposed models could be related to this aspect (i.e. a time-dependent investigation). For instance, it would be of absolute interest studying the emergence of clusters in the population, as in the theory of percolation [24].

4.4 Conclusion

The aim of this work is to provide a detailed study of the role of noise in the PGG by the lens of statistical physics. Notably, the proposed model allows to define a clear relation between the noise introduced in the microscopic individual behavior and the macroscopic properties of a population. To achieve this goal, we start from the theoretical considerations presented in [94, 95], then considering a richer scenario and controlling the noise in two different cases: a homogeneous population (i.e. all agents have the same degree of rationality) and a heterogeneous one (i.e. more degrees of rationality are considered). The phase diagram resulting from numerical simulations shows

the influence of the synergy factor r and of the noise in the macroscopic behavior of the population. So, beyond confirming results reported in works as [94, 13], our investigation extends to further insights. Notably, the phase diagram (see Figure 4.2) shows many interesting regions. For a finite range of values of low noise, there exists a second order phase transition between two absorbing states as a function of r, with the presence of a metastable regime between them (region (1) —see plot **(a)** of Figure 4.2). For higher values of noise the active phase and network reciprocity disappears (regions $(2A)$ and $(2B)$ —see plot **(a)** of Figure 4.2) and the system always reaches an ordered state. In particular, cooperation (defection) is usually reached if r is greater (smaller) than the group size $G = 5$, even if fluctuations are possible next to the critical point due to the finite size of the system. As the level of noise increases, the system approaches the behavior of a classical voter model (region (3) —see plot **(a)** of Figure 4.2), where either one of the two ordered phase is reached no matter the value of the synergy factor. From the analysis of the heterogenous population case, we note that even a very small density f of rational agents, $f \approx 3\%$, allows to observe a network reciprocity effect. In such sense, beyond the physical interpretation of our results, we deem important to highlight that, from the perspective of EGT and from that of sociophysics, the PGG is a system that 'correctly works' even in the presence of few rational players. Here, saying that the system 'correctly works' means that the equilibrium predicted for given a r by the analysis of the Nash equilibria of the system in the well-mixed approximation is achieved. Finally, it might be interesting to investigate the behavior of the PGG for populations with greater heterogeneity in the rationality of the agents, and possibly change it over time. For instance, we think that investigating a model where agents modify their K due to simple interactions, as in thermalization-like contact processes, might be relevant to get further insights on these dynamics. In particular, even if the average value of K in the population is constant, we reckon that differences might emerge with regard to the final steady state of the corresponding homogeneous population, due to the existence of a different initial transient where the distribution of K is non-trivial. To conclude, this work extends results reported in previous analyses on the role of noise in the spatial PGG and aims to link evolutionary game theory to other spin models, such as the voter model, more rigorously studied in the context of statistical physics.

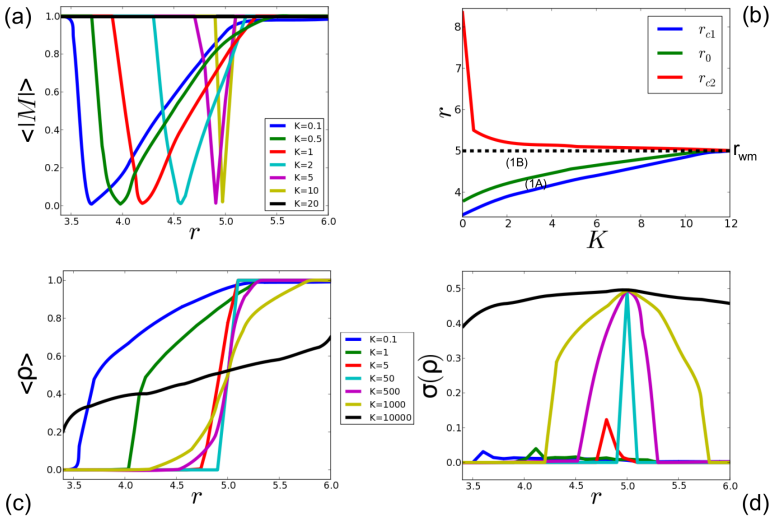

Figure 4.3: (Color online) In the top panels we focus on the transition from the active phase towards the ordered phase. In **(a)** we show the average absolute value of the magnetization $\langle |M| \rangle$ as a function of the synergy factor r for different K. As the temperature K increases, the range of r giving rise to an active phase shrinks around $r = r_{\rm wm} = 5$ up to a critical value beyond which network reciprocity disappears. The scaling as a function of K of the two extreme points of the active range, r_{c1} and r_{c2}, as well as the value of r_0 for which $|M| = 0$, are shown in **(b)**. In the bottom panels we show the average density of cooperators $\langle \rho \rangle$ **(c)** and the standard deviation $\sigma(\rho)$ for selected values of K **(d)**. For the three smallest temperatures the system crosses region (1), marked by a second order transition in $\langle \rho \rangle$ and small values of σ. For $K = 50$, on each single run the system always reaches one of the two absorbing states. $\langle \rho \rangle$ is equal to 0 (1) for low (high) values of r, but takes intermediate values around $r = 5$. The transition is quite steep and $\sigma(\rho) = 0$ unless around $r = 5$. For higher values of K, for even a greater range of values of r around $r = 5$ both full defection or cooperation are achievable, $0 < \langle \rho \rangle < 1$ and $\sigma > 0$. In such regime the system behaves as a biased voter model under the external field $r - r_{\rm wm}$. As K increases, the behavior of an unbiased voter model, no matter the value of r, is approached. Results are averaged over 100 simulation runs.

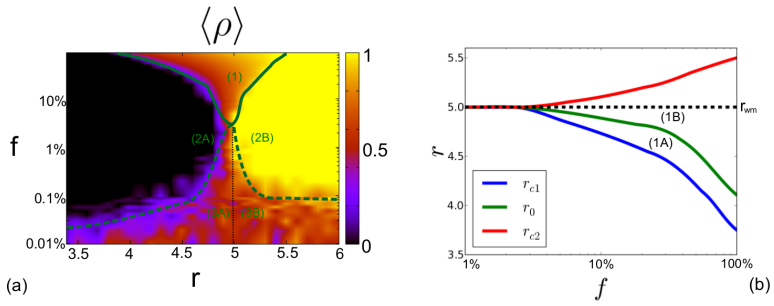

Figure 4.4: (Color online) **(a)** Strategy distribution diagram showing the average density of cooperators $\langle\rho\rangle$ as a function of the synergy factor r and the fraction of rational agents in the population f, i.e., those provided with $K^1 = 0.5$.(**b** Critical thresholds r_{c1}, r_{c2} of synergy factors, and the value r_0 for which cooperators and defectors coexist in equal number as function of the fraction f of rational agents. Results are averaged over 100 simulation runs.

Chapter 5

Collective Influence in the Public Goods Game

In this chapter, we investigate the spatial PGG considering the presence of agents susceptible to the local field generated by their nearest neighbors [106]. Notably, in the PGG, agents can be usually defined as fitness-driven agents when modify their strategy according to payoff-based rules. At the same time, representing strategies as spins, allows to investigate the role of local fields in the process of strategy selection (or 'strategy revision phase'). In particular, some agents can be susceptible to their local fields, while others are susceptible to their payoff. So, in social terms, agents susceptible to local fields can be considered as conformist agents. As result, here we study a population composed of two kinds of agents: fitness-driven agents and conformity-driven agents. The relevance of this investigation is related to the number of behaviors we may observe in real social systems as stubbornness, altruism, and selfishness. In particular, the fitness is mapped to the agents' payoff, so that richer agents are those most imitated by fitness-driven agents, while conformity-driven agents tend to imitate the strategy assumed by the majority of their neighbors. Numerical simulations aim to identify the nature of the transition, on varying the amount of the relative density of conformity-driven agents in the population, and to study the nature of related equilibria. Finally, we found that the susceptibility to local fields generally fosters ordered cooperative phases, and may also lead to bistable behaviors (see also Appendix A for further details on the role of conformity in social processes).

5.1 Introduction

Here, we study the spatial PGG considering a population with agents susceptible to local fields. Notably, since strategies are mapped to spins, local fields are generated by the strategy of a set of agents. Therefore, in social

terms, being susceptible to local fields entails to behave as a conformist. As result our population is composed of conformity-driven agents and fitness-driven agents. Thus, while the former tend to update their strategy with the most adopted one in their neighborhood, the latter tend to imitate their richest neighbor (i.e., the most fitted). In physical terms, conformity-driven agents correspond to agents susceptible to the influence of a local field, i.e. that generated by their nearest-neighbors. Notably, a field results from a number of spins, and the latter corresponds to the strategy of our agents. Although the PGG exhibits a theoretically predicted Nash Equilibrium of defection, previous works identified several strategies to support cooperation, spanning from awarding mechanisms (e.g. [34]) to optimal game settings. Notably, in [34] authors report that the synergy factor, usually indicated as r, adopted to compute the agents' payoff, can be opportunely tuned in order to support cooperation on bi-dimensional regular lattices. This result is very important as it entails that if the payoff of cooperators reaches, or overtakes, a minimum value, all agents turn their strategy to cooperation. As below, the minimum threshold of the synergy factor depends on the topology of the population (i.e., the way agents are arranged). Therefore, adding a social influence in the PGG implies dealing with two degrees of freedom: the synergy factor r (whose individual effect is known) and the density of conformist agents ρ_c. The proposed model is studied by means of numerical simulations and performed by arranging agents that play a spatial PGG on a bi-dimensional regular lattice with periodic boundary conditions.

5.2 Model

In general, the PGG considers a population of N agents that can adopt two different strategies: cooperation and defection. At each time step, cooperators provide a unitary contribution to a common pool, whereas defectors do the opposite, i.e., not contribute. After all agents have made a decision and accumulated their corresponding payoff, they undergo a round of strategy revision phase, i.e. they can change their strategy from cooperation to defection, or vice versa. In doing so, the population evolves until it reaches a final equilibrium (or steady-state). The synergy factor plays a key role in this dynamics [34], as it promotes cooperation. Notably, it is possible to compute, for a given topology (e.g. square lattice), the minimal value of r, here denoted as r_m, for which any $r > r_m$ allows cooperators to survive, or even to dominate. From a statistical physics perspective, in particular referring to the Curie-Weiss model [135], we can now identify two different phases (or equilibria) [24]: a paramagnetic equilibrium in which we observe the coexistence of cooperators and defectors, and a ferromagnetic equilibrium, implying that one species prevails. Typically, the basic dynamics of the PGG let agents change their strategy according to rules

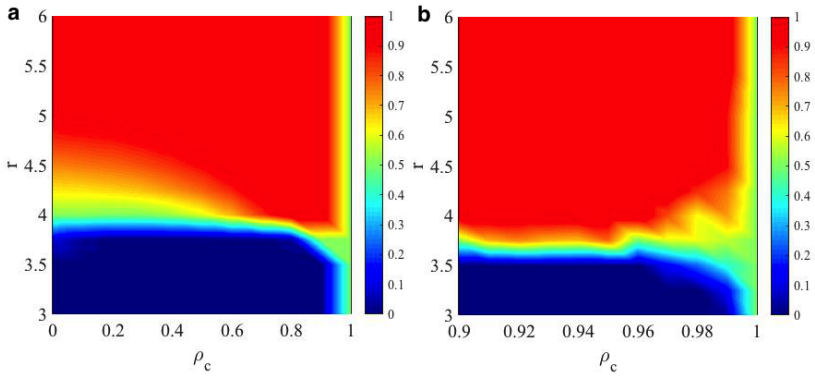

Figure 5.1: (Color online) Cooperation diagram on varying ρ_c in a population with $N = 10^4$. **a** ρ_c in range $\in [0.0, 1.0]$. **b** ρ_c in range $\in [0.9, 1.0]$. Red corresponds to areas of cooperation, while blue to those of defection. Results are averaged over 50 simulation runs and have been computed using 11×11 parameter values.

based on the payoff [1], e.g. agents imitate their richest neighbor, which is our definition of rational thinking [113]. In our model we aim to investigate the outcomes of the PGG in heterogeneous populations, i.e. composed of fitness-driven agents (FDAs) and conformity-driven agents (CDAs). Specifically, we map the fitness to the agents's payoff, so that the richest one is the fittest one. This assumption is far from general, as the fitness might be related to various factors, but we believe to be anyhow characterizing several realistic economic systems. Thus, in our model, FDAs tend imitate the richest neighbors, while CDAs tend imitate the most adopted strategy. So the imitation process, in particular for CDAs, depends on the local connectivity of the underlying interaction structure (i.e. the adopted topology). As result our population is composed of $N = N_f + N_c$ agents, with N_f is the number of FDAs and N_c that of CDAs. Thus, we can introduce $\rho_f = N_f/N$ and $\rho_c = N_c/N$ to identify the density of FDAs and CDAs, respectively. For the sake of clarity, we use the convention in which upper indices refer to the strategy (i.e. cooperation and defection), while lower indices to the agent's nature (i.e. conformity-driven and fitness-driven). Both FDAs and CDAs change strategy by a stochastic rule. In particular, we implement a Fermi rule [34] to compute the transition probability between two different strategies for FDAs. CDAs adopt a simple majority voting [60] rule to decide their next strategy: an agent computes the transition probability according to the density of neighbors having the strategy of majority. In doing so, FDAs act rationally, while CDAs follow a social behavior (i.e. conformism). Following the prescription of [34], we arrange agents in a bi-dimensional regular lattice of degree 4 with periodic boundary conditions (a torus). Summarizing, our population evolves according to the following steps:

1. At $t = 0$, set an equal number of cooperators and defectors, and the

density of conformists $\rho_c \in [0, 1]$;

2. select randomly one agent x, and select randomly one of its neighbors y;
3. each selected agent plays the PGG with all its five communities, then computes its payoff;
4. agent y performs the strategy revision phase according to its nature;
5. repeat from (2) until an ordered phase is reached, or up to a limited number of time steps elapsed.

We remark that the neighborhood for each agent has always 4 agents. Therefore, one agent plays in 5 different groups at a time, all composed of 5 members. Finally, we remind that agents may change strategy, i.e. from cooperation to defection (and vice versa), but they cannot change their nature (i.e. fitness-driven and conformity-driven). Although in real social systems individuals might change also their behavior (e.g. from CDA to FDA), in this work we aim to analyze the relation between the density of CDAs and the outcomes of the PGG. Therefore, we need to assume agents keep constant their behavior.

5.3 Results

We investigate the behavior of the proposed model for different values of ρ_c, from 0 to 1, and of r. The latter assumes values in the range $[3, 6]$ since, in this topology, it is known from [34] that the two thresholds for different equilibria are $r_m = 3.74$ and $r_M = 5.49$ in a FDA population. The threshold r_m indicates that lower values of r lead the population towards a phase of full defection at equilibrium. For intermediate values of r, i.e. $r_m \leq r \leq r_M$, the population reaches a disordered phase, i.e. a mixed phase characterized by the coexistence of both species at equilibrium; eventually, for values of $r > r_M$ cooperators succeed, i.e. the population reaches an ordered phase of full cooperation. In order to investigate the proposed model, we perform numerical simulations with populations of different size, from $N = 10^2$ to $N = 10^4$. The first analysis is related to the distribution of strategies, at equilibrium, on varying the synergy factor r and the density of conformists ρ_c — see figure 5.1. It is worth noting that the disordered phase becomes narrower as ρ_c increases. Notably, we observe that r_m and r_M are strongly affected by ρ_c. At a first glance, as also reported in [4], conformism fosters cooperation, as r_M strongly reduces while increasing ρ_c. On the other hand, for $\rho_c = 1$ a bistable behavior is expected as agents change strategy without considering the payoff. In particular, the minimal threshold of synergy factor to avoid cooperators disappear reduces to values smaller than $r = 3.75$

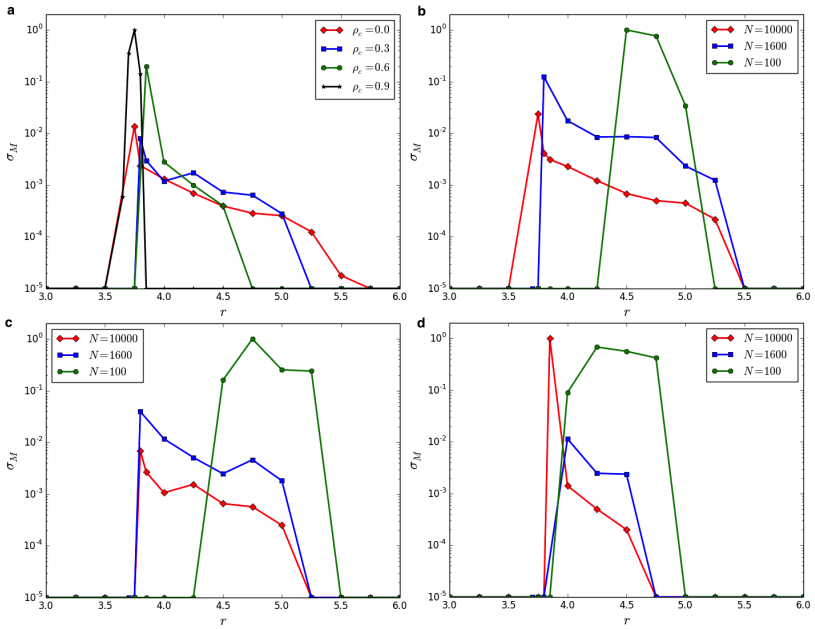

Figure 5.2: (Color online) Variance (σ_M) of the order parameter M as a function of the synergy factor r, for different configurations: **a** $N = 10^4$. **b** $\rho_c = 0.0$. **c** $\rho_c = 0.3$. **d** $\rho_c = 0.6$. Since we adopted a logarithmic scale for the y-axis, we highlight that all values equal to 10^{-5} correspond to 0.

(computed in [34] and confirmed here for $\rho_c = 0.0$) when ρ_c is greater than 0.85. Moreover, considering the higher threshold r_M (i.e. that to obtain full cooperation for $\rho_c = 0.0$), we observe that even with low density of conformist agents, r_M decreases, up to reach a value slightly smaller than 4.0. In the range $\rho_c \in [0.9, 1.0]$, a closer look allows to note a richer behavior of our model — see plot **b** of figure 5.1. We notice that defectors succeed only for values of r smaller than 3.6, while cooperators succeed for values of r greater than 3.78. As result the mixed phase is obtained only in a narrow range between the two listed values (i.e. $3.6 \leq r \leq 3.78$). For values of $\rho_c \geq 0.97$ a bistable behavior can be observed: sometimes cooperators succeed, while other times fail (i.e. defectors succeed). Thus, since our results are computed as average values of different simulation runs, the colors represented in both plots of figure 5.1 in some cases reflect the probability to find the final population in a given status starting with those initial conditions (i.e. r and ρ_c).

In order to characterize the transition at fixed ρ_c, since we observe qualitatively different phases, we tentatively try to identify the transition lines by studying the behavior of the variance as a function of r, which as we will see play the role of inverse 'temperature'. Here, the variance σ_M is referred to the magnetization of the system [92], which we identify as our

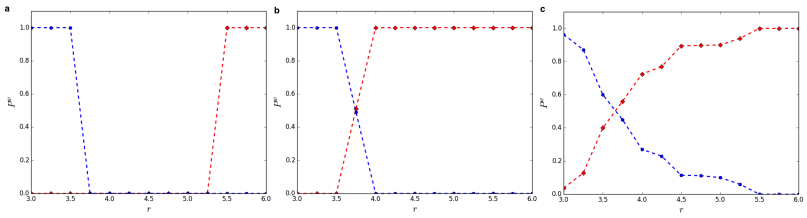

Figure 5.3: (Color online) Probability to succeed as a function of the synergy factor r, in a population with $N = 10^4$, for the two species: cooperators, i.e., red dotted line (Diamonds $\diamond$), and defectors, i.e., blue dotted line (Circles $\circ$). **a** $\rho_c = 0.0$. **b** $\rho_c = 0.9$. **c** $\rho_c = 0.99$.

order parameter (as discussed in chapter 2), and given by

$$M = \frac{1}{N}\sum_{i=1}^{N} s_i \tag{5.1}$$

with s_i strategy of the i-th agent, i.e. $s = \pm 1$. Hence, the variance σ_M is computed numerically, but can be easily identified as the susceptibility of the order parameter χ,

$$\sigma_M = \frac{1}{Z}\sum_{i=1}^{Z}(M_i - \langle M\rangle)^2 \equiv \chi \tag{5.2}$$

with Z number of simulations performed under the same conditions (i.e. fixed r and ρ_c) and $\langle M\rangle$ average magnetization (computed in the same conditions). Plot **a** of figure 5.2 (a) shows the variance σ_M for different values of ρ_c: $0, 0.3, 0.6, 0.9$, as a function of the synergy factor r. As expected, we found that for $\rho_c = 0.0$ the variance is maximum at $r_m \sim 3.75$. Plots **b, c, d** of figure 5.2 illustrate how these curves scale as we increase the number of agents for $\rho_c = 0.0$, $\rho_c = 0.3$ and $\rho_c = 0.6$, respectively. We observe that in the case $\rho_c = 0.6$, the limit $N \to \infty$ is critical, i.e. we find that there seem to exist a r_{crit} for which $\lim_{N\to\infty} \chi_N \equiv \chi \approx (r - r_{crit})^{-\alpha}$ for some exponent $\alpha > 0$. The universality class will be studied elsewhere.

Then, in order to characterize the bistable behavior shown in Figure 5.1, we study the probability for the system of being in the defecting or in the cooperating phase at the end of the simulation, as a function of r (see figure 5.3) and of ρ_c (see figure 5.4). In figure 5.3 the two dotted lines refer to the winning probabilities of defectors (i.e., blue) and of cooperators (i.e., red). Therefore, for $\rho_c = 0.0$, the two curves are zero in the intermediate range of r, i.e., $3.75 \leq r \leq r_M$, as none is expected to completely succeed. Remarkably, increasing ρ_c we found a decreasing paramagnetic range of r, disappearing for values $\rho_c \geq 0.8$. As shown in plots **b** and **c** of figure 5.3, at least one curve is always greater than zero. Although we are dealing

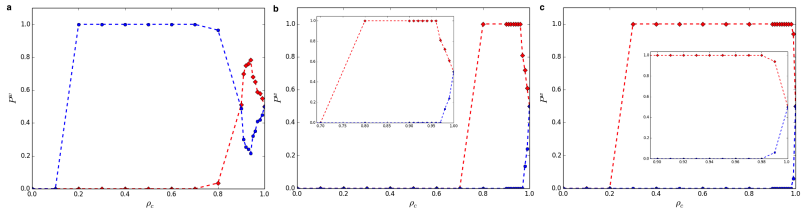

Figure 5.4: (Color online) Probability to succeed as a function of the density of conformists ρ_c, in a population with $N = 10^4$, for the two species: cooperators, i.e., red dotted line (Diamonds $\diamond$), and defectors, i.e., blue dotted line (Circles $\circ$). **a** $r = 3.75$. **b** $r = 4.0$. **c** $r = 5.25$.

with success probabilities, it is worth noting that the summation of values taken by the two curves has to be ≤ 1, thus even zero as it means that none succeeds once the disordered phase is reached. Moreover, figure 5.3 allows to observe the emergence of a bistable behavior, e.g. for $\rho_c = 0.9$ at $r = 3.75$ we have both curves having the same P^w, i.e., about 50% of cases defectors prevail, while in the remaining cases cooperators succeed. Figure 5.4 aims to characterize the same bistable behavior on varying ρ_c and keeping fixed r. Plot **a** of Figure 5.4 refers to $r = 3.75$ and it lets emerge an interesting result: in the range $0.2 \leq \rho_c \leq 0.7$ defectors prevail. This indicates that in this region conformism promotes defection, being 0 the expected value of P^w for both species. Moreover, the bistable behavior emerges as $\rho_c \geq 0.8$. Plot **b** of figure 5.4 refers to $r = 4.0$ and shows that the upper bound of the paramagnetic phase (i.e., r_M) is reduced to 4.0 as $\rho_c \geq 0.8$. Then, a bistable behavior emerges for $\rho_c \geq 0.92$. Eventually, in plot **c** of figure 5.4 referred to $r = 5.25$, we see that even for lower values of ρ_c cooperators succeed, and the bistable behavior emerges for $\rho_c \geq 0.93$. In the light of these results, we can state that when r is close to the lower bound of the paramagnetic phase, i.e., r_m, conformism supports defection until the emergence of a bistable behavior. While, for higher values of r, conformism supports cooperation, and only for high values of ρ_c the system becomes bistable.

Finally, we construct an approximate phase diagram of our system — see figure 5.5. In the top part we have the domination of cooperation (i.e., red), and in the lower one that of defection (i.e., blue). Along the line separating the two parts above identified (at fixed r), we find an important point indicated as ρ^* below described. In an area of the left diagram between defection and cooperation, for $\rho_c < \rho^*$ and $r_m < r < r_M(\rho_c)$, defectors and cooperators coexist, with the prevalence of the former. In this region, it is possible to change the parameters to reach smoothly the cooperation region. For $\rho_c > \rho^*$ we have the coexistence of cooperation and defection on the transition line $r = r_m$, due to the fact that r_M approaches r_m as an increasing function of ρ_c. The point in which $r_M = r_m$ is a triple point.

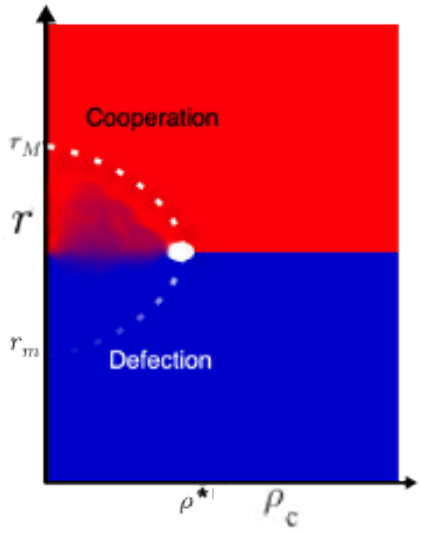

Figure 5.5: (Color online) For $r_m < r < r_M$ and $\rho_c < \rho^*$, we observe a phase where defection and cooperation coexist, represented in the dashed white line, where the variance is continuous. For $\rho_c > \rho^*$, the transition from defection to cooperation is sharper at r_c. This picture gives the idea of the existence of a triple point at $r = r_m$, $\rho_c = \rho^*$ where three different behaviors coexist.

5.4 Conclusion

Summarizing, we studied the spatial PGG in the presence of agents susceptible to local fields, i.e. to the influence of their nearest neighbors. In particular, we considered two different kinds of agents: conformity-driven agents (CDAs) and fitness-driven agents (FDAs). The former are those that tend imitate the strategy of majority, while the latter are those that tend to imitate the richest players. In both cases, CDAs and FDAs update their strategy by considering only their neighborhood. Previous studies [98, 114, 115] reported that social influences strongly affect evolutionary games. The proposed model is different from those implemented in previous investigations (e.g. [98, 115]), results are similar and, on a quality level, further extends their findings. Here, we highlight the prominent role of conformism in the spatial PGG: it seems that this social influence may lead the population towards different phases and behaviors, as full cooperation and bistable equilibria. In particular, conformism promotes the population to reach an ordered phase, even when a disordered one is expected. For intermediate densities of conformists (e.g. 0.5), the final equilibrium is that closer to that one would expect considering only FDAs, at a given r. Therefore, our investigations suggest that conformism drives the system towards ordered states, with a prevalence for cooperative equilibria. Eventually, we

focused on the identification of an order-disorder transition [24, 116] that characterizes the behavior of our population on varying the degrees of freedom. To conclude, we found that the spatial PGG under social influences has a very rich behavior, characterized by different final states.

Part III

Applications

Chapter 6

Solving Optimization Problems by the Public Goods Game

As first application, we introduce a method based on the Public Goods Game for solving optimization tasks [117]. In particular, we focus on the Traveling Salesman Problem, i.e. a problem whose search space exponentially grows increasing the number of cities, then becoming NP-hard. The proposed method considers a population whose agents are provided with a random solution to the given problem. In doing so, agents interact by playing the Public Goods Game using the fitness of their solution as currency of the game. Notably, agents with better solutions provide higher contributions, while those with lower ones tend to imitate the solution of richer agents for increasing their fitness. Numerical simulations show that the proposed method allows to compute exact solutions, and suboptimal ones, in the considered search spaces. As result, beyond to propose a new heuristic for combinatorial optimization problems, our work aims to highlight the potentiality of evolutionary game theory beyond its current horizons.

6.1 Introduction

Here, we propose a method based on the Public Goods Game for solving combinatorial optimization problems. In the last years, many evolutionary algorithms [118, 119] have been proposed for solving optimization problems [120, 121, 122], as for instance genetic algorithms [118] and ant colonies heuristics [123]. Remarkably, optimization problems have been widely investigated also within the realm of statistical physics [124, 125, 126, 127, 128, 129, 130, 131], where theoretical physics and information theory meet forming a powerful framework for studying complex systems [23, 132]. For instance, a statistical physics mindset approach in combinatorial optimiza-

tion problems emerges when the set of feasible solutions, of a problem like the Traveling Salesman Problem [133, 134] (TSP hereinafter), is represented in terms of an energetic landscape. In doing so, the searching of a solution corresponds to the searching of a minimum of free energy, in a landscape whose global minimum, i.e. the deepest valley, corresponds to the optimal solution of the problem. Different models as the Curie-Weiss [135] and spin glasses [136, 137] have an energy that can be studied by the Landau formulation of phase transitions [24]. These models are successfully adopted for facing different issues as opinion dynamics [27], information retrieval [128, 138], optimization tasks [124, 139] and learning processes [128]. Using the metaphor of the energy, heuristics like genetic algorithms [118] and swarm logics [123], implement strategies as genetic recombination, mutation, and collective motions, for surfing the energetic landscape with the aim to reach one of the deepest valleys in a finite time, i.e. a good suboptimal solution of a problem. Therefore, parameters as the mutation rate used in genetic algorithms can be compared to physical parameters as the system temperature. In the proposed model, we adopt a mechanism based on partial imitation [139]: when an agent interacts with another one having a higher fitness, the former imitates a part of the latter's solution. For example, in the TSP, the weaker agent imitates only a part of the path traveled by a stronger opponent. In doing so, agents are able to generate solutions over time, with the aim to achieve the optimal one. In physical terms, a partial imitation can be interpreted as a slow cooling process of a spin particle system, where the slowness comes from an imitative dynamics that is only 'partial' (i.e. only few entries of a solution array are imitated). Our model considers an agent population, whose interactions are based on the Public Goods Game (PGG hereinafter). As we know from evolutionary game theory (EGT hereinafter) [34], the outcomes of the classical PGG are affected by a parameter defined synergy factor r, used for supporting cooperators. Here, as shown below, this parameter (i.e. r) has a marginal interest, however what is relevant for our investigations is that an ordered phase (i.e. the prevalence of a species in the population) can be reached by an opportune tuning of its value. Usually, in EGT models, a species indicates a set of agents with the same strategy, e.g. cooperation, whereas in the proposed model a species corresponds to a set of agents having the same solution of a TSP. In general, ordered phases entail all agents have the same state (or strategy in EGT), i.e. in physical terms all spins are aligned in the same direction. The system magnetization allows to measure the state of order of a system, and its value equals to ± 1 in the ordered cases. Dealing with neural networks, and in general with spin glasses, it is possible to introduce a gauge for the magnetization so that its value goes to ± 1 when the spin alignments (i.e. agent states) follow particular patterns. For instance, in the case of the TSP, a pattern can be a specific sequence of cities. The mentioned gauge is defined Mattis magnetization [128], and it reads $M_m = \frac{1}{n}\sum_i \epsilon_i s_i$ with ϵ_i

value in the i-th position of the pattern, s_i value of the spin in the same position of a signal S of length n. As we can observe, when spins are perfectly aligned with a pattern ϵ, the Mattis magnetization is 1. In the proposed model, we introduce a similar approach. In particular, each agent is provided with a random solution of the TSP (i.e. an array of cities representing a possible solution), and the order is reached when all agents hold the same solution. Therefore, in our case, the value of M_m is computed assigning the value of $+1$ when a city has the same position both in the pattern of reference (i.e. the known optimal solution of a TSP problem), and in the solution array computed by an agent, otherwise the value is -1. It is worth to recall that the utilization of the Mattis magnetization, as measure for the performance of our model, can be adopted only when the optimal solution of a TSP is known in advance. Since our agents interact by the PGG, the modification of their solution occurs during the phase of the game usually defined as 'strategy revision phase' (previously described), that in our case is renamed as 'solution revision phase'. Furthermore, our agents use their fitness as currency of the game, so that their payoff depends on the quality of their solution and on those of their opponents. We performed several numerical simulations to evaluate the quality of our method considering the TSP as reference, i.e. a famous NP-hard problem. Results show that the PGG can be successfully adopted for developing new heuristics, opening the way to investigations that cross the current fences of EGT.

6.2 Model

Before introducing the proposed model we recall the basic dynamics of the PGG. The latter considers a population with N agents and two possible strategies: cooperation and defection. Cooperators contribute to a common pool with a coin (usually of unitary value), while defectors contribute nothing or, as in our case, provide a partial contribution (i.e. a coin whose value is lower than that of coins provided by cooperators). Then, the total amount of coins is enhanced by a synergy factor r (whose value is greater than 1), and the resulting value is equally divided among all agents (no matter their strategy). In doing so, each agent receives a payoff which reads

$$\begin{cases} \pi^c = r\frac{\sum_{i=1}^{N^c} c_i}{G} - c \\ \pi^d = r\frac{\sum_{i=1}^{N^c} c_i}{G} \end{cases} \tag{6.1}$$

with N^c number of cooperators, G amount of agents involved in the game (i.e. size of groups considered at each iteration that, in most EGT models, is much smaller than N), c_i unitary contribution (we set, without loss of generality, equal for all agents, i.e. $c_i = c = 1$), and π^c and π^d payoff of cooperators and defectors, respectively. As the quantitative definition of the

payoff suggests, defection is more convenient than cooperation, and it also represents the Nash Equilibrium of this game. The role of the synergy factor r is promoting cooperation and, as demonstrated in previous investigations, its value may strongly affect the evolution of a population [34]. Remarkably, in square lattices, values of r smaller than 3.75 entail all agents become defectors, whereas higher values allow cooperators to survive and even to succeed (for $r \geq 5.49$). As previously mentioned, the evolution of a population results from the process defined as 'strategy revision phase'. Notably, after each iteration, an agent has the opportunity to change its strategy by imitating that of a richer opponent (considering the gained payoff). In the proposed model we consider a well-mixed population (in Appendix II the model is briefly analyzed on structured populations), so that agents may freely interact with their opponents. Moreover, agents are provided with a random solution of a TSP (i.e. an array of cities). Notably, each solution is evaluated by a fitness η computed as follows

$$\eta = \frac{Z-1}{D} \tag{6.2}$$

with Z number of cities and D, total distance of a path. In doing so, its range is $\eta \in [0, 1]$. At each time step, one agent is randomly selected (say the xth) and plays the PGG with 4 (randomly chosen) opponents, forming a group with $G = 5$ agents. Now, every agent of the group contributes with its fitness; then, as in the PGG before summarized, the total summation of contributions is enhanced by a synergy factor r, and eventually equally distributed among all agents of the group. It is worth noting that, in the proposed model, all agents always contribute. However, some agents provide a contribution higher/smaller than that of others. Therefore, 'below average contributors' (i.e. those having a low quality solution) can be considered as defectors [140]. According to this setting, the payoff reduces to one equation

$$\pi_x = r\frac{\sum_{i=1}^{5}\eta_i}{G} - \eta_x \tag{6.3}$$

with π_x indicating the payoff of the xth agent, and η_x its fitness (i.e. that corresponding to its solution). Finally, the 'strategy revision phase' is substituted with a 'solution revision phase': the randomly selected agent computes the probability Π_s to modify each entry of its solution by imitating that of its best opponent (if exists)

$$\Pi_s = \frac{1}{1 + e^{\frac{\eta_x - \pi_x}{K}}} \tag{6.4}$$

As in the PGG, K represents the uncertainty in imitating an opponent (i.e. plays the role of temperature). Hence, setting $K = 0.5$ we implement a rational approach during the revision phase [34]. In doing so, the xth

agent imitates with probability Π_s each entry of the solution of its best opponent, if the latter has a greater or, at least, equal fitness (otherwise the xth agent does not revise its solution). Summarizing, given a TSP, we define a population whose agents at the beginning receive a random solution of the problem. Then, local interactions, based on the PGG, allow the population to converge towards a shared solution. From a local point of view, at each time step, a randomly selected agent (say x) plays the PGG with 4 (randomly chosen) opponents, and computes its payoff (i.e. by Eq.(6.3)). So, according to its fitness η_x and to the gained payoff π_x, the xth agent computes the probability Π_s to imitate the solution of its best opponent (say y, if exists). In particular, if $\eta_y \geq \eta_x$, the xth agent revises its solution, i.e. it imitates each entry of the solution of the yth agent with probability Π_s (i.e. each entry is modified according to Π_s). The whole process is repeated until the population reaches an ordered phase (i.e. all agent share the same solution), or up to a limited number of time steps elapsed. It is worth observing that as Π_s goes to 1, the imitation process tends to become full (not partial) as each entry can be imitated, provided that the best agent has a greater (or an equal) fitness. Eventually, we remark that when an agent performs a 'partial imitation', to modifying for instance one city along its path, the same city is never visited twice. In order to clarify this point we provide a simple example. Let us consider an agent having the following solution: [Paris, New York, London, Miami, Rome, Madrid], that has to put in the third cell (now containing London) the city of Rome. Since currently Rome is in the fifth cell, the algorithm swaps the values for the third and fifth cells so that, after the whole process, the resulting array is: [Paris, New York, Rome, Miami, London, Madrid]. Thus, repetitions are completely avoided, and all solutions generated according to the proposed heuristic are suitable solutions.

6.3 Results

Numerical simulations have been performed considering a number of cities up to $Z = 50$ for defining the TSP. Agents know the starting city and the landing one so, since each city can be visited only once, the number of feasible solutions is $(Z-2)!$. Moreover, without loss of generality, we consider that the distance between two close cities is always equal to one —see Fig. 6.1. Eventually, we set the synergy factor to $r = 2$. We remind that in the present work we are not interested in studying phenomena as the evolution of cooperation, but we aim to evaluate if agents are able to converge towards an ordered phase, characterized by the existence of only one shared solution of a TSP problem. Thus, the choice of setting $r = 2$ reflects this requirements, i.e. to use a value that in the PGG leads to an ordered phase (i.e. full defection in the specific case). As illustrated

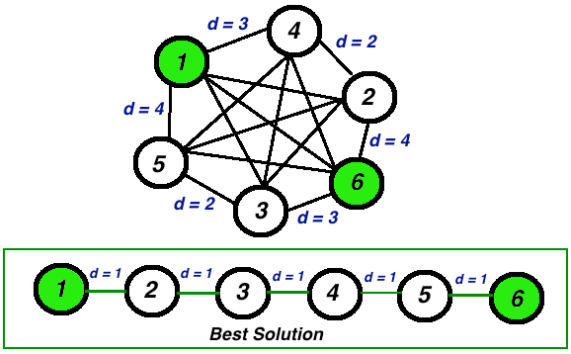

Figure 6.1: General setting of the TSP considering $Z = 6$ cities forming a complete graph. Each node represents a city, and some distances are reported in blue, close to the related link. Then, the best solution is shown. Green nodes represent the starting and the landing ones.

in Fig. 6.2, the ergodicity of the process always allows agents to converge to one common solution. Moreover, we are able to verify the quality of solutions both considering the related fitness and the Mattis magnetization (see the inset of Fig. 6.2). In particular, the latter can be used when the solution of a problem is known in advance, as in our case. An important

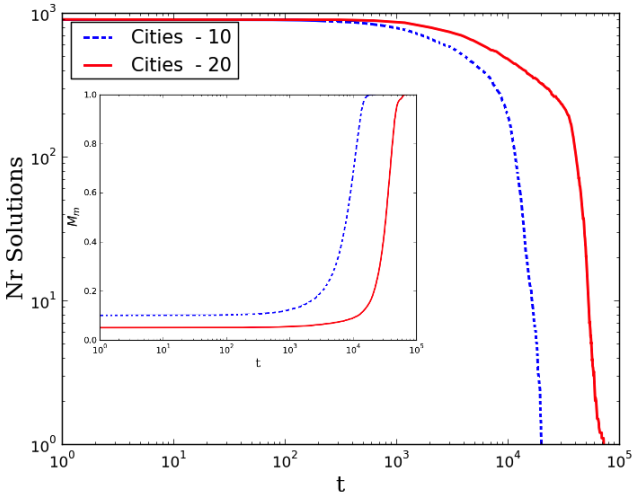

Figure 6.2: Number of solutions over time in a population of $N = 900$ agents while solving a TSP with 10 cities (blue dotted line) and 20 cities (red line). The inset shows the related Mattis magnetization for the two cases (both successful). Results are averaged over different simulation runs.

relation to be considered is the one defined between the final average fitness and the size of the population N, studied on varying the amount of cities

Z —see plot **a** of Fig. 6.3. Moreover, as shown in plot **b** of Fig. 6.3, it is

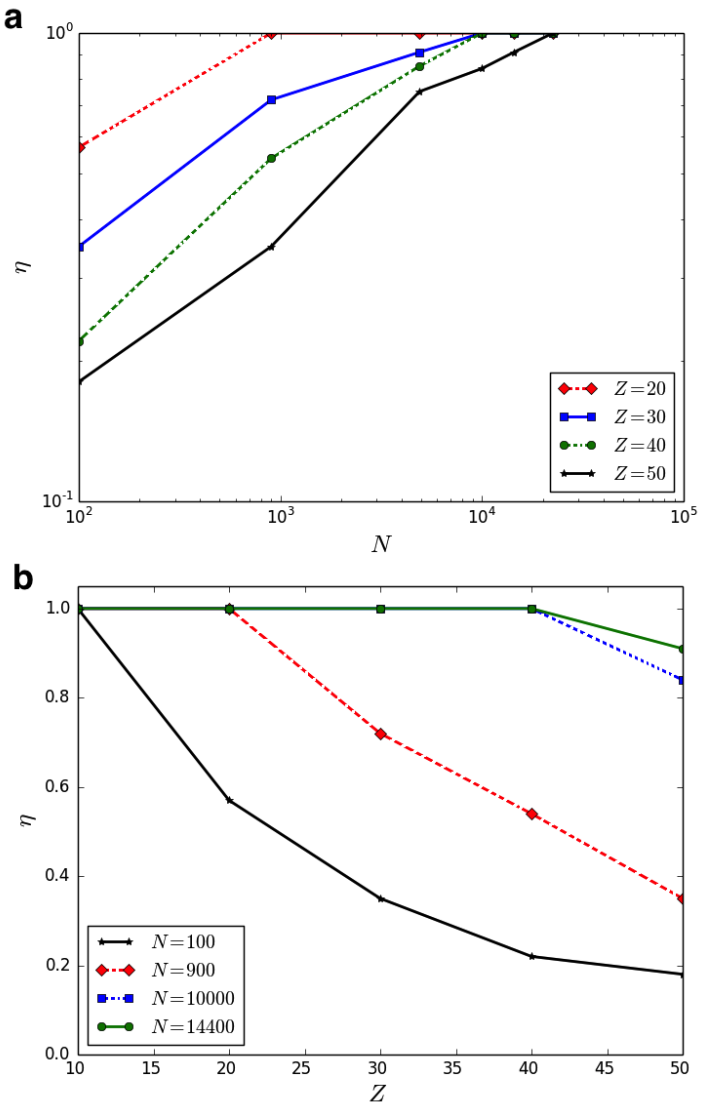

Figure 6.3: **a)** Average fitness of final solution in function of N (i.e. the number of agents), for different values of Z (i.e. the number of cities). **b)** Average fitness of the final solution on varying the number of cities, for different agents N. Results are averaged over different simulation runs.

worth noting that also good suboptimal solutions may be computed using a number of agents N smaller than that required to compute the optimal one. As expected, increasing Z the average value of η reduces (keeping fixed the number of agents N). On the other hand, as shown in Fig. 6.4, it is worth highlighting that it is possible to find an opportune N for each considered Z in order to achieve the highest fitness (i.e. $\eta = 1$). We deem

relevant to note that the number of agents to compute the best solution, i.e. $N(\eta = 1)$, is much smaller than the number of feasible solutions for each problem, therefore our method can be considered a viable heuristic for facing combinatorial optimization problems. Eventually, we focused on the number

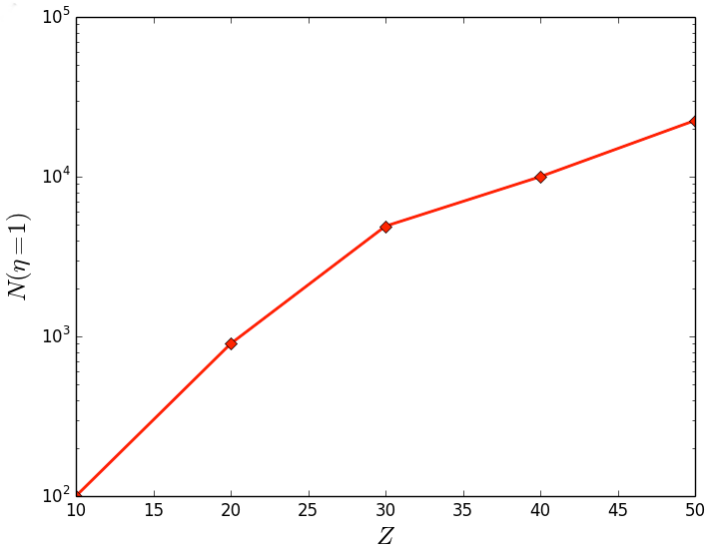

Figure 6.4: Minimum number of agents to compute the optimal solution of a TSP on varying the number of cities Z. Results are averaged over different simulation runs.

of time steps to let the population converge, considering in particular the successful cases, i.e. those leading to the optimal solution —see Fig. 6.5. As expected, wide search spaces (e.g. $Z = 50$) require more time steps to let the population converge to the same final (and optimal) solution. Moreover, increasing N the number of time steps T increases accordingly for the same problem (i.e. keeping fixed Z). These results are in full agreement with converging processes that can be observed in generic agent-based models, e.g. increasing the size of a population the number of time steps, required to let agents converge towards the same state, increases [141].

6.4 Conclusion

In this work we show that evolutionary games as the PGG can be, in principle, applied also for solving combinatorial optimization problems. In particular, the order-disorder phase transition occurring in a population interacting by the PGG can be adopted for letting the population converge towards a common solution of a given problem. Notably, the solution plays the same role of the strategy in the classical PGG, and the order is reached by implementing a mechanism of 'partial imitation' [139]. The latter allows

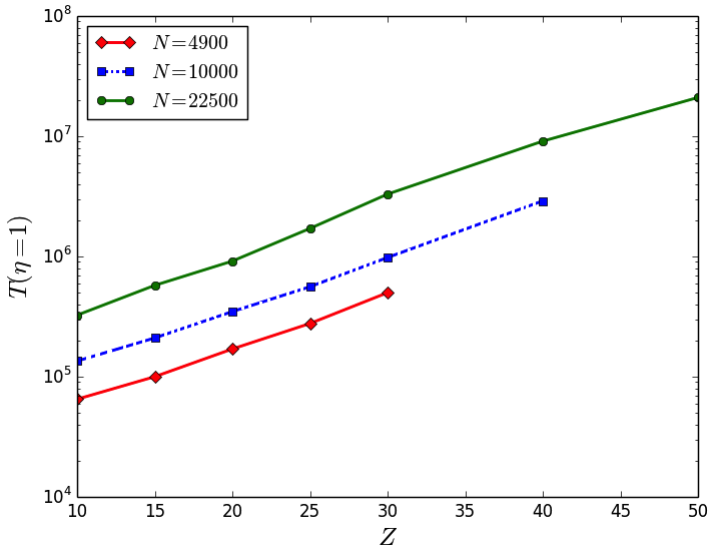

Figure 6.5: Number time steps required for converging to the final (optimal) state on varying Z, for different population sizes N. Results are averaged over different simulation runs.

agents with a weak solution to partially imitate stronger (i.e. richer) opponents. From a physical perspective, this mechanism corresponds to a slow cooling process that triggers the emergence of solutions over time, whereas the ergodicity of the process allows the population to reach an absorbing state of full order. In doing so, an ordered phase entails all agents share the same solution. Under the hypothesis that an evolutionary dynamics driven by the payoff, i.e. rational, may constitute the base for solving difficult problems as the TSP, we performed several numerical simulations by considering a well-mixed population. Although we implemented a simplified version of the TSP, with a limited number of cities, it is worth highlighting that results indicate that the proposed model allows to compute the optimal solution in all considered search spaces. Moreover, even using a reduced number of agents, it is possible to compute a good suboptimal solution. Furthermore, we note that even introducing spatial constraints in the TSP definition, the algorithm is able to face the problem, once the driveability of the graph is known (as shown in Fig. 6.1). Therefore, in the light of the achieved outcomes, we deem relevant to further investigate the potential of evolutionary games in optimization problems, then enlarging the domain of applications of EGT. However, it is important to emphasize that in order to really appreciate the quality of the proposed model as algorithm for solving the TSP, further investigations are required. In particular, those for comparing the performances with other heuristics, as genetic algorithms (see Appendix I). On the other hand, we remark that our results indicate

a clear relation between the size of a population and the complexity of the faced problem. This last observation constitutes a first, even if theoretical, advantage of our method respect to the others because, as far as we know, similar relations are not available for other strategies. Now, from the point of view of EGT, there are two important observations. First, the synergy factor has a marginal role in the proposed model. We recall that, for the aims of our work, we are interested in allowing the population to converge towards an ordered state. On studying the PGG, the synergy factor is fundamental because, as before mentioned, some values may lead a population towards a steady-state of coexistence between cooperators and defectors. Therefore, since here we have to avoid similar outcomes, in principle, every value of the synergy factor that supports a generic state of full order can be adopted. At the same time, we think that the synergy factor should not be too high, otherwise it might generate problems when computing transition probabilities during the 'solution revision phase'. In particular, as indicated in Eq.(6.4), the fitness and the payoff are compared when evaluating whether one agent has to change its strategy. Thus, we suggest to use small values, like the one we adopted (i.e. $r = 2$). The second observation is related to the identification of defectors. Notably, here we refer to the PGG, i.e. a simple game with two strategies: cooperation and defection. In the classical version, cooperators contribute with a coin, while defectors do not contribute. However, as reported in [140], when the amount of contributions is not set to a specific value (e.g. a coin of unitary value), those agents that contribute with a below-average contribution can be considered as defectors. To conclude, the proposed heuristic shows that cooperative dynamics, leading from disordered to ordered states, may constitute the basic mechanism for implementing optimization algorithms.

Appendix I

Here, we report results of a comparative analysis between the proposed method and two heuristics: a genetic algorithm [119] (GA hereinafter) and a strategy based on social imitation (SI hereinafter) [139]. Notably, although GAs have been proposed several years ago, they currently constitute one of more interesting methods in optimization (e.g. [142]). In addition, comparing the outcomes of the proposed model with those achieved by the SI method (i.e. [139]) allows to evaluate the influence of the game dynamics (i.e. of the PGG). Before showing a comparative table, we briefly summarize how the GA has been implemented:

1. Define a population with N genes, assign each one a random solution for the considered TSP, and define a maximum number of iterations I;

2. While the best fitness in the population is smaller than 1, or the number of iterations is smaller than I:
3. _ Compute the fitness η of each gene (i.e. the goodness of its solution);
4. _ Select the best half of the population according to fitness;
5. _ Generate two new solutions for each couple of genes, defined among the set computed at the previous step;
6. _ Apply the random mutation, to each gene, with probability p_m;

We set to 0.1 the probability p_m (i.e. the random mutation), and to $30k$ the maximum number of iterations I. In addition, we emphasize that the crossover operator has been defined by cutting each gene parent (i.e. solution) in two different points, so generating an offspring by using the central part of one parent and the side parts of the other parent. In the case this process generates not viable solutions (e.g. in the presence of repetitions), the duplicates are removed for adding the missing cities. In addition, we briefly describe the SI method: given a TSP, start with a population composed of agents having a random solution (i.e. an array of cities). At each time step, randomly select two agents: the agent having the lower fitness imitates one entry of the solution of the other selected agent. Then, repeat this process until the population converges towards a shared solution (or a maximum number of time steps elapses). Further details are described in [139]. Table 6.1 shows the number of agents (or genes for the GA) for computing the optimal solution on varying the number of cities, the average number of time steps required to complete a simulation (computed on 20 different attempts) and, when smaller than 1, the average fitness.

Table 6.1: Performance comparison, on varying the number of cities (Z), between the proposed method (PGG) and two heuristics: GA and SI. N indicates the minimum number of agents (genes for GA) used to solve the problem, and $< T >$ indicates the average number of time steps required. The average fitness $< \eta >$ is indicated only when smaller than 1, although the best value computed considering all attempts is 1 (i.e. the optimal solution has not been always computed).

Z	PGG	SI	GA
10	$N = 100 \mid < T >= 1K$	$N = 60 \mid < T >= 8K$	$N = 100 \mid < T >= 27$
20	$N = 900 \mid < T >= 29K$	$N = 270 \mid < T >= 500K$	$N = 100 \mid < T >= 1.3k$
30	$N = 4900 \mid < T >= 500K$	$N = 700 \mid < T >= 5.5M$	$N = 100 \mid < T >= 13.2k$
40	$N = 10000 \mid < T >= 3M$	$N = 1200 \mid < T >= 40M$	$N = 200 \mid < T >= 23k \mid < \eta >= 0.76$
50	$N = 22500 \mid < T >= 21M$	$N = 1600 \mid < T >= 360M$	$N = 200 \mid < T >= 28.5k \mid < \eta >= 0.61$

According to these results, we observe that the proposed method requires the highest number of agents to solve a TSP. However, if compared to the SI algorithm, our approach is much more faster (see the average number of time steps $< T >$). Instead, the GA requires a smaller amount of agents than PGG, and it is also faster. At the same time, it is important to observe that the GA has a synchronous dynamics (while our method is asynchronous), i.e. during the same time step, all agents are involved for generating offsprings and updating their solution (according to the random mutation mechanism). Therefore, further analyses are required for a complete time comparison. Nevertheless we found that, considering 20 different simulation runs, the average fitness of the best solution (found in the gene population) is smaller than 1 when $Z \geq 40$. Hence, the GA must be run several times for each task, saving the best solution. To conclude, according to this analysis, we report that a GA constitutes the best choice for solving simple problems (i.e. with few cities), or for computing a good suboptimal solution in a short time. On the other hand, when the number of cities increases, the proposed method allows to reach a higher fitness in a smaller number of attempts than that required by a GA.

Appendix II

Here, we present a brief analysis of the proposed model performed by using a structured population, i.e. agents arranged on a network. Notably, we considered regular square lattices (with periodic boundary conditions), and small-world networks implemented according to the Watts-Strogatz model [81]. In particular, small-world networks have been defined starting with a 2-dimensional ring with 8 neighbors per node, and then rewiring with probability β each edge at random. Thus, using values of β higher than 0, we obtained small-world networks. Figure 6.6 shows results of the comparative analysis. For each type of network, we considered different realizations. So, we observe that the amount of agents to solve a TSP increases using structured populations, in particular in small-world networks. Therefore, the most convenient choice for solving a TSP remains the well-mixed population. Now, we discuss a possible explanation of this result. Notably, small-world networks contain few nodes with a number of connections (i.e. degree) higher than the average value. These nodes are usually defined hubs. On one hand, their role is fundamental in spreading processes, since they make them faster than those implemented by using regular topologies. On the other hand, when hubs are provided with a solution having a fitness higher than that of their neighbors, they may constitute a limit during the definition of new solutions. Notably, in this case all neighbors tend to imitate the solution of hubs thus, given a TSP with defined conditions (e.g. number of cities), small-world networks require a number of agents higher

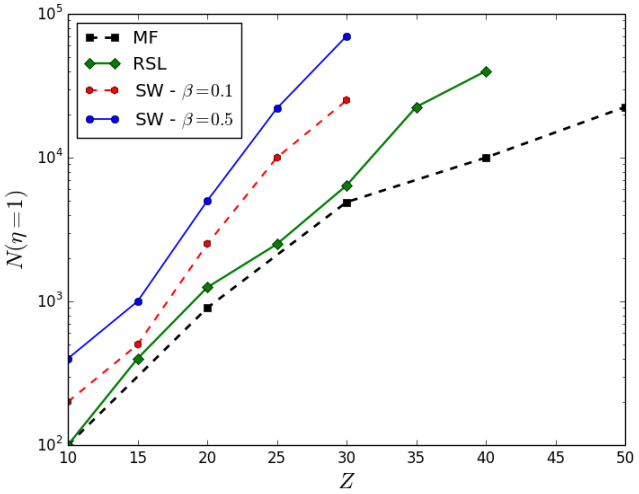

Figure 6.6: Minimum number of agents to compute the optimal solution of a TSP on varying the number of cities Z. As indicated in the legend, the (dotted) black line refers to results obtained in the well-mixed population. The (continuous) green line refers to the regular square lattice, with periodic boundary conditions. The (dotted) red line refers to small-word networks achieved with $\beta = 0.1$, and the blue (continuous) line to those obtained in small-world networks achieved with $\beta = 0.5$. Results are averaged over different simulation runs.

than that required in regular networks for solving the same problem. In few words, hubs are able to affect the solution of too many opponents, reducing the innovative potential of the whole population. Eventually, our observation is corroborated by comparing results obtained in small-world networks generated with different β. In particular, increasing β the number of hubs increases, and networks generated with $\beta = 0.5$ resulted less convenient than those generated with $\beta = 0.1$. To conclude, in the light of results, we deem that topologies containing hubs may reduce the computational power and the innovative potential of an agent population.

Chapter 7

Modeling Poker as an Evolutionary Game

This second application is focused on the evolutionary dynamics of Poker [143, 91, 113]. Notably, despite its wide diffusion and the raised scientific interest around it, Poker still represents an open challenge. Recent attempts for uncovering its real nature, based on statistical physics, showed that Poker in some conditions can be considered as a skill game. In addition, preliminary investigations reported a neat difference between tournaments and 'cash game' challenges, i.e. between the two main configurations for playing Poker. Notably, these previous models analyzed populations composed of rational and irrational agents, identifying in the former those that play Poker by using a mathematical strategy, while in the latter those playing randomly. Remarkably, tournaments require very few rational agents to make Poker a skill game, while 'cash game' may require several rational agents for not being classified as gambling. In addition, when the agent interactions are based on the 'cash game' configuration, the population shows an interesting bistable behavior that deserves further attention. In the proposed model, we aim to study the evolutionary dynamics of Poker by using the framework of Evolutionary Game Theory, in order to get further insights on its nature, and for better clarifying those points that remained open in the previous works (as the mentioned bistable behavior). In particular, we analyze the dynamics of an agent population composed of rational and irrational agents, that modify their behavior driven by two possible mechanisms: self-evaluation of the gained payoff, and social imitation. Results allow to identify a relation between the mechanisms for update the agents' behavior and the final equilibrium of the population. Moreover, the proposed model provides further details on the bistable behavior observed in the 'cash game' configuration.

7.1 Introduction

Poker is one of the most famous card games and constitutes also an open challenge for artificial intelligence and game theory [144, 145, 146, 147]. In last years, mainly due to the advent of online gaming platforms, Poker has widely increased its popularity and its prestige, up to be considered even as a profession. However, in this scenario, an important question is still feeding an old debate: 'Is Poker a Skill Game?'. This question has not yet a clear and shared answer, and its relevance is given by the related implications, spanning from legal aspects to healthcare problems [148, 149, 150]. For instance, considering Poker as gambling would entail the need to include it in the list of dangerous activities, i.e. those that can lead to the emergence of an addiction, and that can require clinical treatments. It is worth to emphasize that the utilization of money and the influence of luck, barely measurable, represent two main elements that support its classification as 'gambling'. On the other hand, the possibility to apply a rational strategy (e.g. based on mathematics) for improving the success probabilities, suggests that Poker can be really considered as a 'skill game', e.g. like Chess. In order to shed some light on this issue, two recent works [113, 91] analyzed the dynamics of an agent population, whose interactions were based on a simplified version of Poker. In particular, these mentioned models consider agents behaving in two possible ways: 'rational' and 'irrational'. Rational agents are those that play Poker following a mathematical strategy, while irrational agents are those that play randomly. In particular, in the model presented in [91] agents can modify their strategy and the whole dynamics has been studied by a compartmental approach. The latter, as some models defined in epidemiology (e.g. SIS model [151]), allows to provide a macroscopical description of the population, and it has been named RIR model (i.e. Rational-Irrational-Rational). It is worth noting that the RIR model [91] (see Appendix A for a full description) has been studied in two different configurations: full challenge and one-round challenge. Full challenges entail each interaction lasts until the winner gains all the money of its opponent, thus different rounds can be required. Instead, the second configuration (i.e. one-round challenge) entails each interaction lasts for only one betting round. After each interaction, in both configurations, the amount of money of each player is set to the initial value. In addition, each interaction considers only two agents at time, i.e. it is a pairwise interaction defined 'heads-up' in the Poker jargon. Here, the full challenge configuration can be related to Poker tournaments, while the one-round challenge can be related to the 'cash game' variant. Since agents modify their behavior by imitating that of the winner, after each challenge a well mixed population reaches an ordered phase, i.e. after a number of interactions all agents share the same strategy. Remarkably, the full challenge configuration indicates that even with very few rational agents in the population, at $t = 0$, the

final ordered phase is always composed of rational agents. A more complex situation is observed in the case of one-round challenges, since a bistable behavior emerges. In particular, considering the same initial density of rational agents, it is possible to reach both equilibria, i.e. full rational and full irrational. Clearly, increasing the amount of rational agents at the beginning of the challenge, increases the number of final equilibria corresponding to full rational. As result the emergence of the bistable behavior described in [91] still deserves attention. It is also worth to highlight that the statistical physics approach to Poker, presented in these models [113, 91], leads to two main conclusions: 1) the nature of Poker strongly depends on the player's behavior and 2) Poker tournaments can be classified as 'skill game', while 'cash-game' challenges composed of few rounds make Poker similar to gambling. Here, we aim to obtain further insights on Poker by using an approach based on EGT. The proposed model aims to study the equilibria that can be reached in a population, considering rational and irrational agents, by focusing on two degrees of freedom: the imitation probability p_i and the success probability of rational agents p_r. The first degree (i.e. p_i) indicates the probability to modify a behavior (e.g. from rational to irrational) by imitating the opponent, while p_r indicates the success probability of rational agents when play against irrational ones. Thus, as below explained, we can avoid to focus on full challenges or on one-round challenges, because on varying the value of p_r we are able to consider different cases, i.e. from short to long-lasting challenges. Here, it is important to evaluate the influence of the imitation probability since in real Poker challenges, it is not always possible to imitate the winner (e.g. players can decide to hide the own cards when the opponent folds). In addition, cash-game challenges can last few or many rounds, therefore the success probability p_r varies over time. In order to take into account also the second observation, we studied also the case with a variable value of p_r (during the same challenge). In doing so, we observed the same bistable behavior found in one-round challenges of [91]. Then, we compared the outcomes of the two models, i.e. the new one and the previous one presented in [91]. To conclude, it is worth to note that the proposed model constitutes a new application of EGT (see also [152]), and allows to reach further insights for understanding the nature of Poker. In addition, our results shed more light on the bistable behavior reported in [91].

7.2 Model

In this section, we present the proposed model. We considered an agent population whose interactions are based on a simple game inspired from Poker (in particular focusing on the variant named Texas Hold'em —see [153]). The agents may follow two different strategies: rational and irrational. Ra-

tional agents are those that take actions according to a mathematical strategy, i.e. those that aim to maximize the probability to succeed by a 'rational' mindset. Irrational agents, on the contrary, are those that take actions randomly, i.e. without to consider the value of their own cards nor other strategies. According to results achieved in previous works [113, 91], the winning probability of rational agents depends on the duration of a challenge. Notably, rational agents have high probability to succeed against irrational agents when the amount of rounds that constitute a challenge increases. For instance, if challenges terminate when one agent wins all the money of its opponent, the success probability of rational agents increases up to 80%. At the same time, when a challenge is composed of only one round, a rational agent succeeds against an irrational one with a probability close to 20%. In the case the agents modify their strategy, imitating that of their winning opponent, a mixed population (i.e. composed of 50% of rational agents at $t = 0$) can reach two different equilibria: full rational and full irrational. As previously discussed, in real scenarios the behavior of the winner is not always disclosed. Thus, the imitation probability, on average, is much smaller than 1. In order to analyze a system, taking into account this last observation, we introduce a model inspired from EGT where agents play Poker and modify their strategy according to the following mechanisms: imitation and payoff evaluation. The former can be adopted when the winning opponent reveals its strategy, while the latter entails to modify a behavior according to the amount of the gained payoff. Thus, if after an iteration the agent's payoff decreases, it is more likely a rational agent becomes irrational, and vice versa. From the EGT perspective, the two updating mechanisms allow to implement a 'strategy revision phase'. Notably, in the case a losing agent (say y) decides to imitate its opponent (say x), it computes the transition probability (from rational to irrational, and vice versa) by using the Fermi-like equation presented in Chapter 1. Instead, when an agent does not imitate its opponent, it changes its strategy according to the following probability

$$W(T_y) = (1.0 - \frac{\pi^y}{4.0})/2.0 \tag{7.1}$$

where T_y indicates the transition probability of the y-th agent to modify its strategy (from rational to irrational, and vice versa), π^y indicates its payoff divided by constant equal to 4. In particular, at each iteration, the two agents are randomly selected and they play with 4 opponents. In addition, since we studied both the well-mixed configuration and the spatially structured configuration, we highlight that in the second case the two randomly selected agents, and their opponents, are nearest neighbors.

Now, it is worth to highlight that the payoff of this game is very simple: when an agent wins a challenge, its payoff increases of 1, whereas each time it loses a challenge the payoff decreases of 1. Thus, the mathematical definition of the payoff reads: $\pi = \sum_{i=0}^{3} c_i$, with c_i outcome of the i-th challenge and

equal to $c_i \pm 1$, i.e. $+1$ if successful, otherwise -1. According to these rules, we considered the evolution of a population on varying p_i and p_r (i.e. imitation probability and success probability of rational agents). We recall that when two agents of the same kind face each other, both have the same probability to succeed (i.e. 50%). Eventually, it is worth to emphasize that the strategy imitation takes place only after comparing the payoffs of the two considered agents. For example, if the agent y is undergoing a strategy revision phase with $p_i = 1$, it will imitate the agent x only after evaluating the payoff difference, as defined in 8.1. For instance, if y wins 3 out of 4 challenges, losing only against the agent x that, in turn, wins only against y and loses all the other challenges, π_y is clearly bigger than π_x. Accordingly, the probability that the agent y imitates x is very low even if $p_i = 1$. Finally, we highlight that the well-mixed configuration allows to perform a mean field analysis of the system, while the other one allows to evaluate the role of an interaction topology (e.g. [154]). Remarkably, even a simple topology, like a regular square lattice, can be strongly relevant in in the dynamics of some games, a for instance the Public Goods Game (see [34]). Summarizing, our population evolves according to the following steps:

1. At $t = 0$, set a number of rational and irrational agents in the population;
2. select randomly one agent x, and select randomly one opponent y (being a neighbor in the case of the lattice topology);
3. each selected agent plays the game with all its four opponents (randomly composed in the well mixed case), then computes its payoff;
4. agent y performs the strategy revision phase according p_i, then adopting eq 8.1 or eq. 7.1, to compute the weight probability to change its behavior/strategy;
5. repeat from (2) until an ordered phase is reached, or up to a limited number of time steps elapsed.

Then, before to show results of numerical simulations, we highlight that the maximum number of time steps has been set to 10^8.

7.3 Results

Let us start considering the results achieved in [91], where a well-mixed population played both full and one-round challenges —see figure 7.1. In particular, considering the same starting conditions, as the initial density of rational agents in the population, figure 7.1 clearly indicates that full challenges support rational agents (i.e. all agents become rational after a number of time steps), while one-round challenges entail sometimes rational

succeed, other times all the population turns to irrational (i.e. irrational succeed). As previously discussed, the bistable behavior of the population playing one-round challenges needs further attention, in order to better understand the related motivation. According to the investigations performed in [113, 91], rational agents have about 80% to succeed in full challenges, and about 20% in one-round challenges. Therefore, increasing the number of rounds from 1 to ∞ entails to support rationals. In addition, the model presented in [91] considers that agents modify their behavior by imitating the winning opponents. So, in order to represent scenarios closer to real challenges, it is important to observe that players are not always able to imitate their opponent because the latter can also keep hidden her/his own cards (notably, only in particular conditions players have to show their cards). Accordingly, here we analyze the evolutionary model of Poker on varying two relevant parameters: the imitation probability (i.e. p_i) and the success probability of rational agents (i.e. p_r). Figure 7.2 shows results of numerical simulations performed on a well mixed population with $N = 10000$ agents. Since some games, as the Public Goods Game, show a different behavior in networked topologies (as discussed in Chapter 1), we studied the proposed model also in a regular square lattice with periodic boundary conditions. Remarkably, we did not find any particular difference between the the well-mixed case and the lattice topology, as reported in Figure 7.3 that shows very small and non-correlated values. Then, we considered different initial densities of rational agents (i.e. $\rho(0)$) and, as for games like the Public Goods Game, we found that the process is independent from the value of $\rho(0)$, i.e. the latter does not affect the outcomes. Eventually, as anticipated before, in order to make the model closer to real scenarios we analyzed it on varying the value of p_r during the same simulation (showing in the plot the average result, as for the other cases) —see Figure 7.4. In particular, at each time step, the value of p_r can be 0.2, or 0.8, both with equal probability (i.e. 50%). It is worth to observe that results achieved with one-round challenges in [91] are very similar to those achieved on varying p_r during the same simulation. Therefore, in our view, the bistable behavior is due to the variation, along the same challenge, of the success probability of rational agents. In particular, the bistable behavior reported in [91], may reflect the fact that strong card combinations, being opportunities for those that play by using a mathematical strategy (i.e. rational agents), are not very frequent (as real Poker players usually know from direct experience, and as the theory of probability suggests given the structure of 'playing cards' used in Poker). Thus, several times rational agents fold without to participate. So, since one-round challenges entail a loser imitates the winner, a rational agent many times becomes irrational for this reason, i.e. for the low rate of good own cards (defined as *hand* in the Poker jargon). Finally, it is worth to point out that this last observation can be, in principle, provided only considering the probability laws, and the dynamics of the model described

in [91]. However, the evolutionary model here presented is able to prove it by the numerical simulation.

7.4 Conclusion

In this work we propose a model based on EGT for studying the dynamics of Poker, considering a simplified version of this game. In particular, our agents are provided with two behaviors (or strategies), i.e. rational and irrational, and we analyze the evolution of the population in function of two degrees of freedom: the imitation probability and the success probability of rational agents. We remind that rational agents represent players that take decisions using a mathematical based strategy, while irrational agents are those that play randomly. In addition, since our agents can modify their strategy over time, they undergo a 'strategy revision phase', whose aim is to increase their payoff. In particular, according to an imitation probability, losing agents may assume the strategy of their opponents, or they evaluate to change strategy considering the trend of their payoff. In the first case, they know the strategy of their opponent, while in the second case they do not. Before to discuss about the achieved results, we deem relevant to clarify an important conceptual point: even if the proposed model is based on EGT, it does not constitute a dilemma game, like for instance the Prisoner's dilemma [2, 12, 56, 57] and the Public Goods Game [6, 34, 106]. Notably, agents do not have to chose between their own benefit and that of their community of belonging. So, we analyzed the equilibria reached by the population, both in the mean-field and in a structured configuration, on varying the degrees of freedom before illustrated. In general, we found only two final equilibria: full rational and full irrational, even with an imitation probability equal to zero. It is worth to point out that when p_i is equal to 1, an absorbing state characterized by a full order is highly expected, as demonstrated in a number of models embodying an imitative mechanism (the most simple example is the voter model [99]). According to this observation, and as shown in 7.2, the transition between full irrational to full rational appears quite smooth for p_i close to zero, and becomes more sharp increasing p_i up to 1, where a critical threshold, i.e. $p_r = 0.5$, between the two regimes can be clearly identified. Although further analyzes are mandatory for classifying the observed phase transition, on a quality level we can state that for low p_i a second order phase transition occurs, while for high p_i emerges a first order phase transition. Now, we recall that in the proposed model setting p_i to 1 does not ensure that, during an iteration, one agent imitates another one. The motivation is that the imitation takes place with a probability depending on the payoff difference between the selected agents. For instance, if $p_i = 1$ and the agent undergoing the 'strategy revision phase' achieved a payoff higher than that of its opponent, the imitation process does not take

place. The role of a pure imitative mechanism has been investigated in [93], where authors analyzed the link between the Public Goods Game and the voter model. Notably, a voter model like mechanism emerges in the Public Goods Game at high temperature, i.e. when agents change strategy without to consider the payoff differences. Moreover, it is worth to recall that results shown in 7.2 are independent from the initial density of rational agents. Eventually, considering the results achieved on varying the p_r during each challenge, we found that they are very similar to those achieved by the 'one-round' configuration of the model presented in [91]. Therefore, the observed bistable behavior of the population can be explained by the fact that during a challenge, rational agents fold weak *hands* and, according to the theory of probability (see also the Sklansky tables [153]), there are many more weak *hands* than strong ones. To conclude, results achieved by numerical simulations allow to get further insights on the game of Poker, showing the relevance of models based on EGT and, in addition, allow to shed light on the bistable behavior reported in [91].

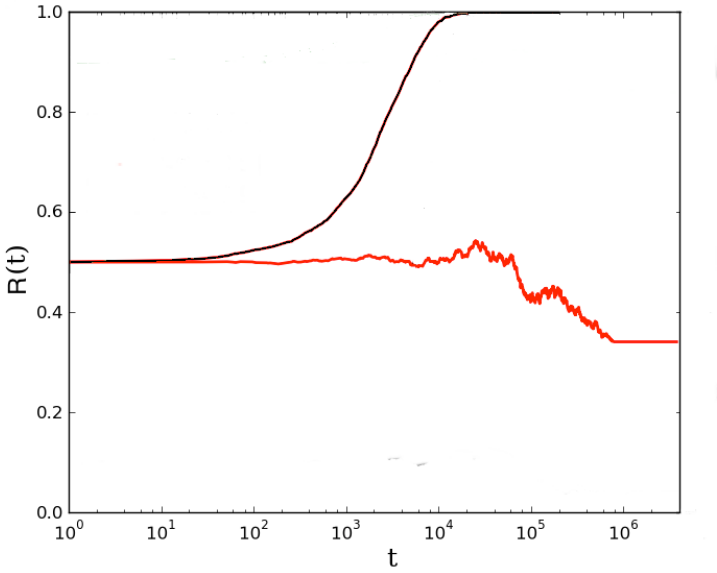

Figure 7.1: Mean field analysis of a population playing Poker. Amount of rational agents over time $R(t)$ ($+1$ indicates rational, -1 irrational) in the two different configurations analyzed in [88], for the case with an equal starting density of rational and irrational agents. Black line indicates the result achieved with full challenges. Red line indicates the result achieved with one-round challenges. Results have been averaged over different simulation runs.

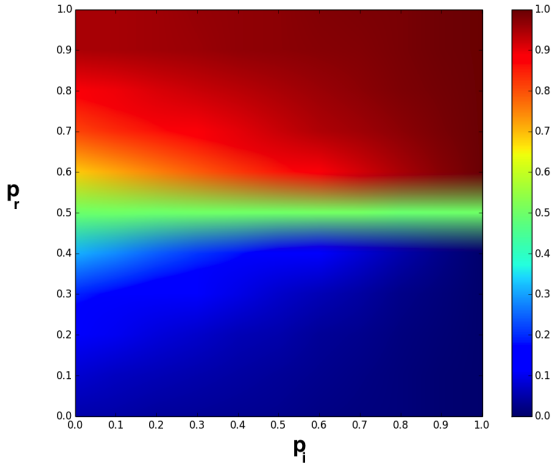

Figure 7.2: Strategy distribution in the proposed model, on varying the degrees of freedom p_i and p_r, i.e. the imitation probability and the probability a rational agent succeeds over an irrational one, respectively. Red indicates full rational, while blue full irrational. Results have been averaged over 100 simulation runs.

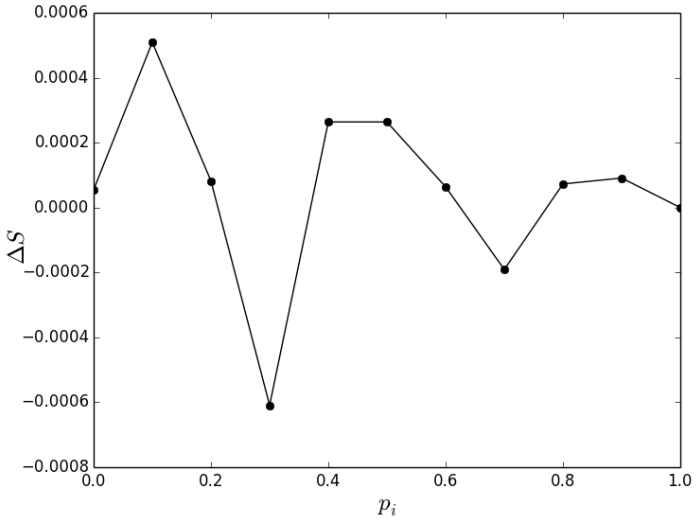

Figure 7.3: Average difference, in the summation of states (+1 indicates rational, −1 irrational), obtained on varying the imitation probability, between results achieved in a well mixed population and in a structured population (i.e. regular square lattice with periodic boundary conditions). Results have been averaged over 100 simulation runs.

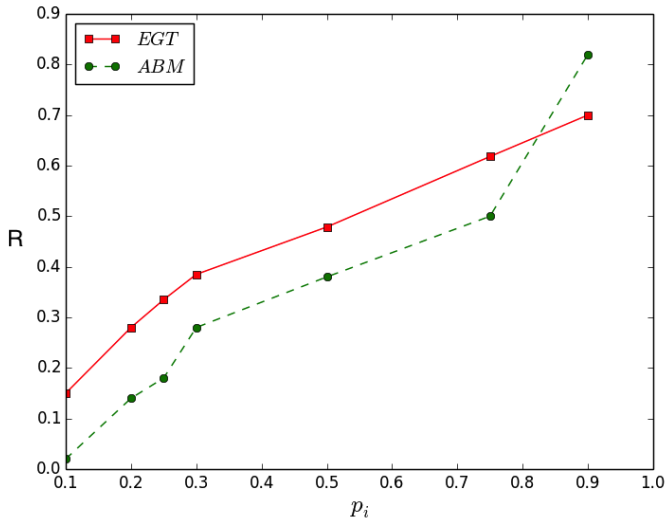

Figure 7.4: Comparison between the outcomes achieved in the model described in [91], defined as ABM in the legend, and those achieved in this work, defined as EGT in the legend. Amount of rational agents R ($+1$ indicates rational, -1 irrational). In particular, this analysis aims to evaluate if one-round challenges analyzed in [88] behave like an EGT based model with a varying p_r (i.e. probability of success of rational agents). Results have been averaged over 100 simulation runs.

Chapter 8

Modeling the Evolutionary Dynamics of Group Formation

Finally, we propose a model for studying the dynamics of group formation [155]. The latter constitutes a relevant phenomenon observed in different animal species, whose individuals tend to cluster together forming groups of different size. Results of previous investigations suggest that this phenomenon might have similar reasons across different species, such as improving the individual safety, and increasing the probability to get food resources. Remarkably, the group size might strongly vary from species to species, and sometimes even within the same species. In the proposed model, an agent population tries to form homogeneous groups. The homogeneity is computed according to a spin vector, that characterizes each agent, and represents a set of features (e.g. physical traits). Therefore, we analyze the formation of groups of different size, on varying a parameter named 'individual payoff', representing the gain that agents receive acting individually. In particular, agents can form a group (receiving a 'group payoff'), or can act individually (receiving an 'individual payoff'). Remarkably, the phase diagram of our population shows a sharp transition between the 'group phase' and the 'individual phase', in correspondence of a critical 'individual payoff'. To conclude, our results support the hypothesis that the phenomenon of group formation has evolutionary roots.

8.1 Introduction

The dynamics of group formation constitutes a topic of interest for a wide number of researchers, spanning from anthropologists to zoologists [156, 157, 158, 159, 160, 161, 162], and from social psychologists to economists [163, 164, 165, 166, 167, 168]. In general, the formation of a group can be viewed

as an emergent phenomenon [165, 169] where a number of individuals cluster together for performing one or more actions. Accordingly, the lifespan (as well as other characteristics) of a group can vary from case to case, and individuals can change group over time [170, 171, 172]. In an ecological system, many times being part of a group allows to receive benefits [171], both being a predator and being a prey. For instance, the former can be advantaged during a hunt, e.g. surrounding a prey, while the latter can improve her/his safety staying inside a group [173]. Here, we remark that the previous example, referring to predators and preys, can be considered outdated in the case of the human species. However, we should remind that millions of years ago, and maybe even in more recent times, humans have played both roles in their ecosystem. Different studies suggest that the formation of social groups has evolutionary roots [156, 174, 175, 176, 9, 177, 178], shared among animals belonging to different species. For instance, we can observe groups of fishes (generally named as shoals), of mammalians (named herds or families/tribes in the case of humans), and of birds (named flocks) [175].

What differs, from species to species, is the average size of a group [179, 180, 181, 182, 183], e.g. shoals are usually much bigger than herds, herds are bigger than families, and so on and so forth. In addition, even within the same species, groups of different size can be observed. The formation of groups is a phenomenon of interest also beyond the domain of evolutionary biology, as we can mention the formation of sport teams, of business organizations [166], and of scientific communities. Even if the motivations that lead to the formation of this kind of groups can be quite different from those that trigger the emergence of groups in nature, in both cases individuals cluster together driven by a rational mindset, i.e. aimed to increase their wealth. Therefore, we think that the framework of EGT might be a suitable choice for studying this phenomenon, since it embodies both the rationality and the evolutionary aspect of group formation [13, 184]. When studying the dynamics of group formation, it is important to evaluate the role of similarity. In particular, the heterogeneity of a group can be an advantage, or a disadvantage, depending on the context of reference. Indeed, heterogeneity might refers to different aspects, as physical traits, genetic makeup, or skills. Previous studies (e.g. [185]) reported that social networks show a positive value of assortativity [76], i.e. it seems individuals be more likely to generate links with their own similar, while other kinds of complex networks [75] are more likely to be disassortative (according to an entropic principle [185]). Thus, in the proposed model, we consider an agent population that forms and breaks groups over time, according to the gain agents receive acting in group or individually. The agent's gain comes from the difference between benefits and costs, in taking a particular action (i.e. group or individual). The gain achieved in group is defined as 'group payoff', while that achieved singularly is defined 'individual payoff'. According to

results reported in [185], here the 'group payoff' is maximized for homogeneous groups. Results of numerical simulations indicate that for each group size G, there is a critical 'individual payoff' between a 'group phase' and an 'individual phase' of the population, i.e. the formation of groups or the individual action. In addition, forming groups of big size is more difficult than forming small groups. To conclude, in our view, the achieved results support the hypothesis of an evolutionary mechanism underlying the formation of groups in nature. Notably, we speculate that each animal species has its 'individual payoff', i.e. a kind of gain its individuals receive when they act as single members, and that this parameter might depend also on the considered environment. In addition, in the case of human beings, we suppose that the 'individual payoff' might be related also to socio-cultural conditions, leading to the formation of very small groups in the modern civilization, and to the formation of bigger groups (i.e. tribes) in more archaic systems (see [186, 187, 188]). Notably, two important differences between the modern civilization and the archaic ones are the living environment and the cultural structure (e.g. relations, laws, etc) of a society, both making a city more suitable than a forest for individual life styles.

8.2 Model

In the proposed model, we consider a population with N agents that can cluster together forming groups of size G. Each agent is represented by a spin vector S, of length L, e.g. for $L = 6$ the i-th agent can be represented as $S_i = [+1, -1, -1, -1, +1, +1]$. Here, each entry of the spin vector can be viewed as a feature, so the homogeneity of a group is measured considering the distance between spin vectors of its members. It is worth to note that we refer to the concept of feature with its more general meaning, since it may vary from species to species. For instance, for many animals (including humans) a feature can be a physical trait, and in the case of humans it can represent also a hobby, or a specific skill, and so on (i.e. not only physical features). The dynamics of the proposed model is very simple. At each time step a number G of agents, not belonging to any group, is randomly selected. So, selected agents compute the potential payoff they could gain acting together (depending on the homogeneity of the potential group). In particular, the 'group payoff' π_g decreases when members have different spin vectors. Then, the value of π_g is compared to that of π_i, i.e. the payoff that agents would gain acting individually. In doing so, π_i and π_g are used to compute the probability of forming a group of size G, with the selected agents, which reads

$$W(G) = \left(1 + \exp\left[\frac{\pi_g - \pi_i}{K}\right]\right)^{-1} \tag{8.1}$$

where the constant K parametrizes the uncertainty in taking a decision (i.e. to form, or not, the group). By using $K = 0.5$, we implement a rational approach [3, 91]. After processing a new potential group, the model evaluates if a previous one, randomly selected among those formed at previous time steps, might be broken. The breaking process is performed according to the same equation adopted to generate a group (i.e. Eq. 8.1). As mentioned before, the homogeneity of a group is computed according to the spin vector of its members. Accordingly, the group payoff π_g is defined as length of the normalized average summation of each spin vector (composing the considered group). In particular, since each entry can be positive (i.e. $+1$) or negative (i.e. -1), after computing the average value of a single spin we take its absolute value. So, given spin vectors of length L, the 'group payoff' for a group of size G reads

$$\pi_g = \frac{1}{L}\frac{1}{G}\sum_{j=1}^{L}|\sum_{i=1}^{G} v_{ij}| \tag{8.2}$$

with v_i elements of the spin vector of each agent. Eventually, it is worth noting that the range of π_g is $[0, +1]$, while that of the 'individual payoff' π_i spans the interval $[-1, +1]$. In doing so, we represent scenarios where acting individually can be very risky (i.e. $\pi_i = -1$), and very convenient (i.e. $\pi_i = +1$). At the same time, we assume that acting in group cannot never lead to a negative payoff. Finally, we remark that during each simulation, the value of π_i remains constant. Summarizing, the proposed model can be described as follows:

1. At $t = 0$ generate a population providing each agent with a random spin array;
2. While the number of time step is smaller than T:
3. ____ Randomly select G agents, not belonging to other groups;
4. ____ Compute the probability the selected agents form a new group;
5. ____ Randomly select a group among those previously formed, and compute the probability to break it;

Since we consider an asynchronous dynamics, i.e. only a subset of agents plays at a given time step, the value of T must be big enough in relation to the population size.

8.3 Results

Numerical simulations have been performed in a population with $N = 1000$ agents, considering different conditions related to the 'group payoff' and

to the 'individual payoff', i.e. π_i in the range $[-1, +1]$, and π_g in the range $[0, +1]$. In addition, we study the dynamics of the population for different length of the spin vector characterizing our agents. Due to the value of N, we analyzed the emergence of groups of the following size: $[2, 4, 5, 10, 25, 50, 100]$. Figure 8.1 shows the phase diagram of our population. Figure 8.2 indicates the density of the groups in function of the

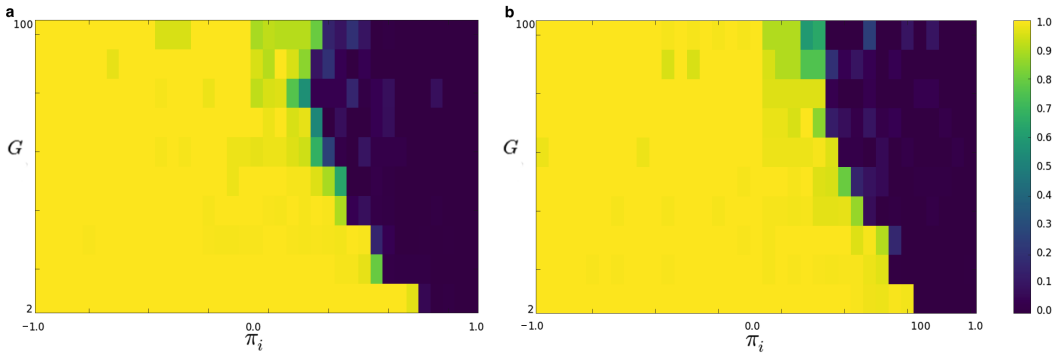

Figure 8.1: Strategy distribution diagram of the population, group size G versus the 'individual payoff' π_i, on varying the length of the spin vector L. Yellow indicates the 'group phase', while Blue the 'individual phase'. **a** $L = 3$ and **b** $L = 10$. Results have been averaged over different simulation runs.

'individual payoff', on varying the length of the spin vector L. It is then

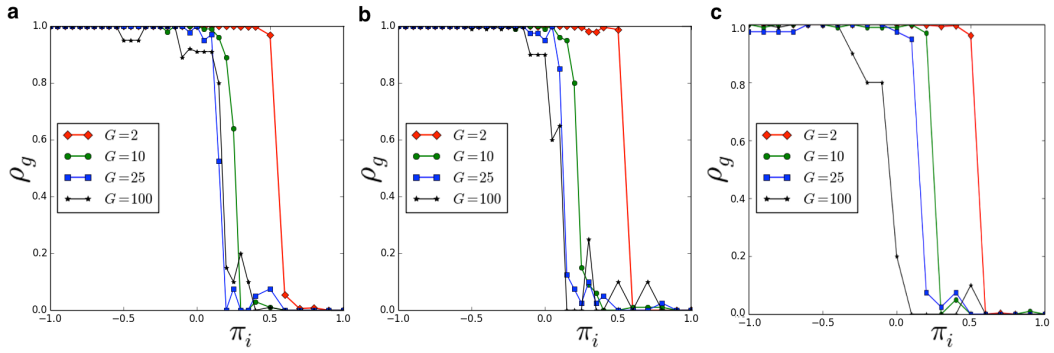

Figure 8.2: Density of groups ρ_g in function of the 'individual payoff' π_i, on varying the length of the spin vector L: **a** $L = 3$. **b**$L = 10$. **c** $L = 25$. Results have been averaged over different simulation runs.

possible to find the critical thresholds $\hat{\pi}_i$, on varying the group size G. For instance, in the case $L = 3$, we observe $\hat{\pi}_i = 0.55$ for $G = 2$, $\hat{\pi}_i = 0.15$ for $G = 10$, and $\hat{\pi}_i = 0.05$ for $G = 25$. It is then worth to evaluate if the length L (i.e. the length of the spin vector) affects the outcomes of the model —see Figure 8.3. In particular, one can observe that L does not influence the

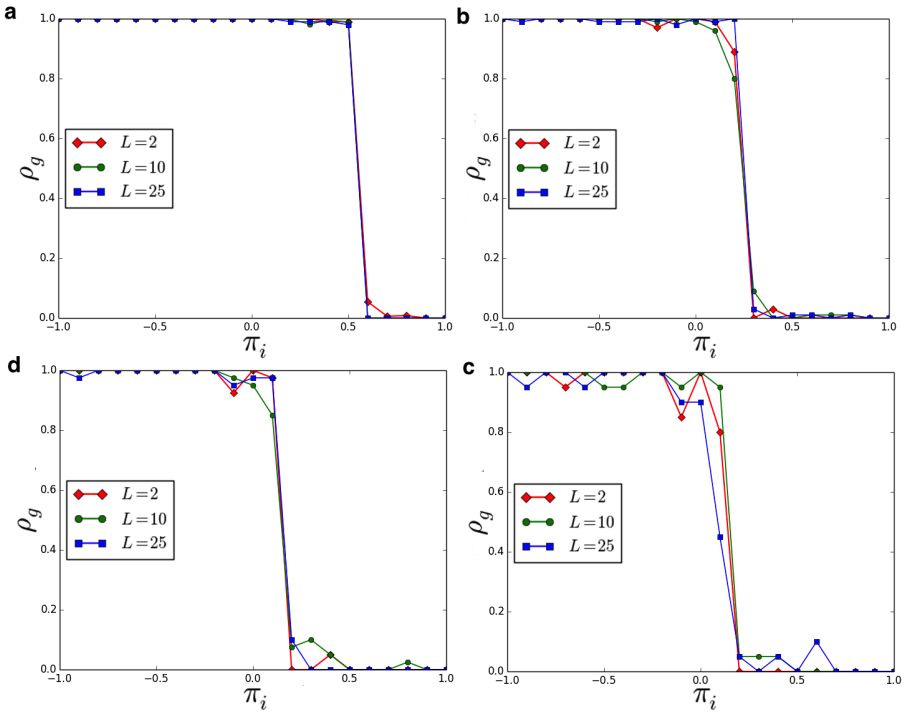

Figure 8.3: Density of groups ρ_g in function of the 'individual payoff' π_i, for different vector spin length L, on varying the group size G. **a**) $G = 2$. **b**) $G = 10$. **c**) $G = 25$. **d**) $G = 50$. Results have been averaged over different simulation runs.

density of groups at equilibrium. Eventually, as reported in Figure 8.4, we analyze the number of breaking groups ($B(t)$) over time. In particular, we consider different group sizes G, and spin vector lengths L, on varying the individual payoff.

8.4 Conclusion

In this work, we study the phenomenon of group formation using the framework of EGT. In particular, we introduce a simple model where agents evaluate if clustering together, or acting individually, according to a payoff they may receive if acting in group (named 'group payoff'), or individually (named 'individual payoff'). Under the assumption that the 'group payoff' increases while increasing the homogeneity of a group, we study the formation and the breaking of groups. Even if further investigations would be required in order to evaluate the outcomes on varying the definition of the 'group payoff', we suppose that the achieved results can be considered general enough for envisioning some interesting speculation related to the evolutionary aspects of group formation in nature. Notably, observing that

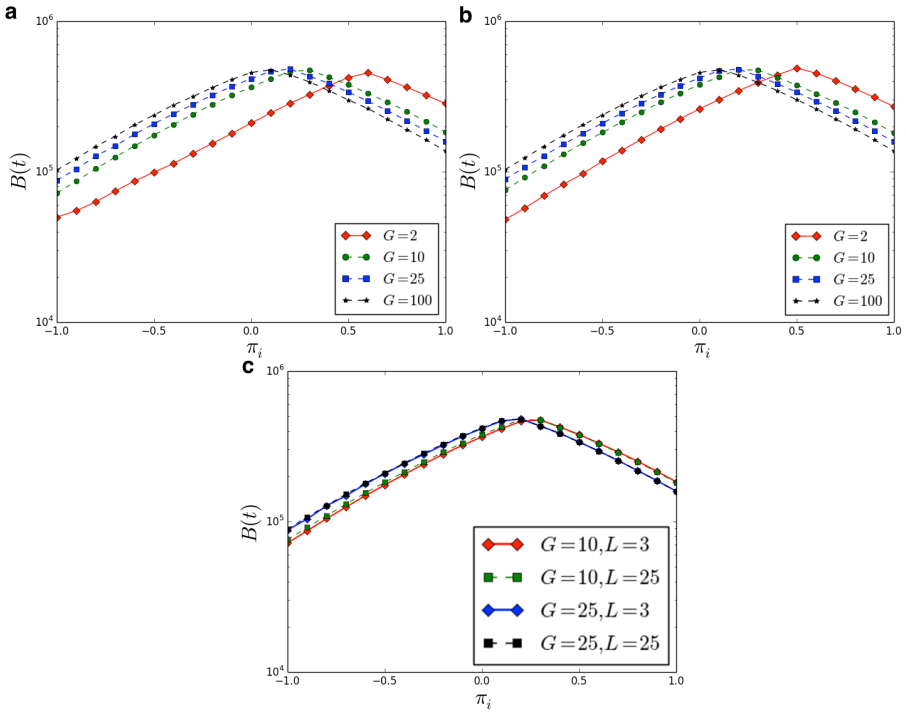

Figure 8.4: Breaking groups over time (i.e. $B(t)$). The legend indicates, for each line, the considered group size G. **a**) Results achieved with $L = 3$. **b**) Results achieved with $L = 25$. **c**) Comparison between results achieved with $L = 3$ and $L = 25$. Results have been averaged over different simulation runs.

groups form in species ranging from ants to birds, and from lions to human beings, we support the hypothesis that this process has evolutionary roots [161, 175]. In addition, we suggest that the 'individual payoff' is a relevant parameter representing the ensemble of genetic traits, skills, living environments, and even socio-cultural conditions one can observe in real systems. For instance, we hypothesize that being part of a group is more advantageous in a hostile environment than in a relaxed one, as suggested by some theories related to the formation of shoals of fishes. So, even considering the same species, we can have individuals acting in very small groups and others in big groups. For example, in the modern civilization [188, 186], small groups named families are, nowadays, composed of very few members, while tribes living in wilder environments are more copious. We deem relevant to emphasize that the proposed model suggests the existence of a critical threshold in the 'individual payoff', leading to a sharp transition in the phase diagram (see Figure 8.1), from a 'group phase' achieved for low values of π_i to an 'individual phase' achieved for high values of π_g. Notably, for high values of the critical π_i the group formation is scarcely observed.

Here, 'group phase' and 'individual phase' correspond to the two states our population can achieve at equilibrium, i.e. with agents forming groups or acting individually. Finally, results reported in figure 8.4 confirm previous findings and provide a further detail. In particular, analyzing the average number of breaking groups $B(t)$, we observe that small groups are more robust than big ones, and the maximum number of breaking groups is in correspondence with the critical threshold $\hat{\pi}_i$. Furthermore, for very high 'individual payoffs' big groups are more robust than small ones (i.e. the opposite of the case with low π_i). To conclude, we highlight that the proposed model represents an application of EGT besides its classical domain, providing results that remarkably corroborate the hypothesis that the emergence of groups in animal species has evolutionary roots.

Part IV

Conclusions

Chapter 9

Conclusions

In this thesis, we presented the results of some investigations in Evolutionary Game Theory, i.e. a modern research area in the field of complex systems, with two major aims: developing a statistical physics description of EGT, and showing some applications of evolutionary games beyond the current fences of EGT. The work is composed of four main parts. The first part of the work is focused on a general introduction to EGT, and on the main mathematical methods used for developing the models presented in the following chapters. For instance, we provided a brief introduction to phase transitions, illustrating the Ising model and the Mean Field approximation, and to some analytical approaches to population dynamics, with a focus on applications in sociophysics. The second part is composed of chapters that illustrate statistical physics models for studying some relevant phenomena in EGT. In particular, we proposed a mathematical model for understanding the relation between the emergence of cooperation in the Prisoner's Dilemma and a random motion in continuous spaces, the connection between the Public Goods Game and the classical Voter Model and, eventually, the influence of local fields in the Public Goods Game. It is worth to remind that in all these three chapters, of the second part, the proposed models have a direct connections with social and biological phenomena, as for instance the role of rationality and of conformity in the strategy selection. Notably, we deem important to highlight that EGT aims to understand the equilibria and the dynamics of social and ecological systems, as well as of many complex biological processes, therefore the definition of new models is often inspired from real scenarios belonging to the mentioned areas. Then, the third part of the work shows three different applications: a heuristic for solving combinatorial optimization problems, an evolutionary game for understanding the dynamics and the nature of Poker games and, finally, an evolutionary game for representing the dynamics of group formation. Like for the second part, two applications (i.e. Poker and group formation) have a direct relation with social and biological phenomena. In particular, the

emergence of groups constitutes an open problem in different scientific communities, and nowadays, is of great interest for anthropologists, ethologists, and theoretical biologists. Eventually, an appendix presents an investigation of the role of conformity in a famous model used in social dynamics, i.e. the q-voter model. Notably, since we presented some results related to the role of conformism in the Public Goods Game, we deem useful (and hopefully interesting) to compare the outcomes achieved by the two different approaches (i.e. q-voter model and PGG). Let us now briefly discuss about potential further developments of the presented works. In the first model, we propose an analytical approach for studying the emergence of cooperation in the Prisoner's Dilemma, by considering memory-aware agents, i.e. agents able to increase their payoff over time. Therefore, a further step in this direction would be to solve the problem without the adopted constraint (i.e. the memory), in order to apply the method to models usually implemented in EGT. In addition, many aspects related to the geometry of the agent space might be investigated. In the second model, we studied the role of rationality in the Public Goods Game, and the relation between this game and the classical voter model. Here, further investigations might consider more complex topologies, and different updating rules. Then, the third model, i.e. the influence of local fields in the Public Goods Game, can be analyzed in other games, since it constitutes a topic of special interest in sociophysics. Then, considering the presented applications, we believe that they constitute a preliminary attempt toward the utilization of EGT in different fields. In particular, the optimization strategy requires to be improved for solving more complex problems (e.g TSP with more cities), the model on Poker needs to find confirmation from analyses performed on real dataset and, eventually, the model on group formation requires further studies for a deeper comprehension of its outcomes, and for further extensions to specific cases. Summarizing, in this work we tried to highlight the link between Evolutionary Game Theory and Statistical Physics, in order to get more insights on evolutionary dynamics and to envision new applications in different scientific areas, as combinatorial optimization problems. Therefore, in the light of the achieved results, we believe important to perform further investigations, for instance according to the ideas above reported. To conclude, we deem that a combined approach of EGT and Statistical Physics may lead to relevant results in different scientific fields.

Appendices

Appendix A

Conformism-driven phases in the Q-Voter Model

In Chapter 5, we presented the results of an investigation focused on the role of local fields in the dynamics of the spatial PGG. Since the susceptibility to local fields might correspond to the social behavior known as conformity, here we show a further investigation on a different model, based on this behavior. In particular, we study the q-voter model, by considering agents arranged on complex topologies (e.g. small-world networks) [100]. Notably, we approach the problem of understanding how conformity affects opinion dynamics by implementing the q-voter model [64, 189, 190, 191, 192], i.e. a variant of the classic voter model [141], on heterogeneous networks. In fact, while it is already known that conformity enhances the reaching of consensus (i.e. an opinion shared by *all* agents) [194] the details of this process are still questioned [191]. Moreover, systems like the voter model and the q-voter model are often simulated over fully connected networks [190, 193, 195], and only to a lesser extent on more complex topologies (see for instance [196, 197, 198]). If, on one hand, this allows to analytically model the system under the mean-field approximation, on the other strongly limits the validity of results to unrealistic scenarios as it has been proven that social systems show highly heterogeneous structures [79]. Thus, our analysis aims at exploring the behavior of the q-voter model by considering more realistic network topologies with the aim to understand the extent to which 1) varying the amount of conformist agents and 2) varying the network structure affects the consensus reaching process. In order to do so, we heavily rest upon numerical simulations.

Results of our simulations indicate the presence of different opinion-formation regimes, driven by the density of conformist agents and varying across different network configurations. Threshold values separating different regimes vary as well. Moreover, the system seems to undergo a spontaneous symmetry-breaking, by (stochastically) choosing states with the same

'net' opinion but opposite signs. The remainder of the paper is organized as follows: Section A introduces the proposed model. Section A shows results of numerical simulations. Finally, Section A ends the paper.

Model

In order to study the role of conformity in the q-voter model, we defined a simple agent-based model by considering N agents, provided with an opinion and a social character.

Opinions are mapped to states $s_i = \pm 1$, $i = 1 \dots N$ and are assigned to each agent of the population stochastically, i.e. according to the probability coefficients $P_+ = P_- = 1/2$; thus, our initial expected number of opinions $+1$ is $\langle N_+^0 \rangle = N/2$. Moreover, agents are provided with an individual behavior, i.e. either conformist or non-conformist. In what follows, we will adopt the definition according to which a conformist agent adopts the opinion of the majority of its neighbors, whereas a non-conformist one adopts the opposite. As for the opinion, the behavior is assigned stochastically too, according to the coefficients P_c and $P_a \equiv 1 - P_c$, i.e. the probability to behave as a conformist or a non-conformist, respectively. As before, the initial expected number of conformist agents is $\langle N_c^0 \rangle = P_c \cdot N$. The two processes of assigning opinions and behaviors are independent: so, each agent's initial probability of being both conformist and having opinion $+1$ is $p_{c,+}^0 \equiv P_c \cdot P_+ = \frac{P_c}{2}$. We will consider agents interacting on different configurations: while the probabilities P_+ and P_- will remain fixed, P_c and P_a will vary, in order to achieve different densities of conformist (and non-conformist) agents in the population. Naturally, opinions vary as a result of the system dynamics.

The q-voter model extends the classic voter model, letting each agent adopt the opinion shared by a subset of neighbors of arbitrary dimension [190]. This model is described by two parameters: q and ϵ. The former represents the number of neighbors each agent has to consider to have its opinion defined, whereas the latter represents the probability for each agent to change its state anyway, even if not all the q chosen neighbors agree. We implement the q-voter model setting $q = 4$ and $\epsilon = 0$. Therefore, agents choose $q = 4$ neighbors at random: if they all share the same opinion, a conformist agent adopts it, whereas a non-conformist agent adopts the opposite one. Otherwise, the agent keeps its precedent opinion: in fact, setting $\epsilon = 0$ means setting to zero the probability of changing opinion stochastically, in the event the q neighbors disagree.

It is worth emphasizing that the implemented updating rule has been chosen to be synchronous; this means that every agent updates its state simultaneously, on the basis of neighbors's opinion at the previous time step. In fact, we believe asynchronous updating does not adequately capture the real dynamics of a social experiment. For instance, let us imagine many

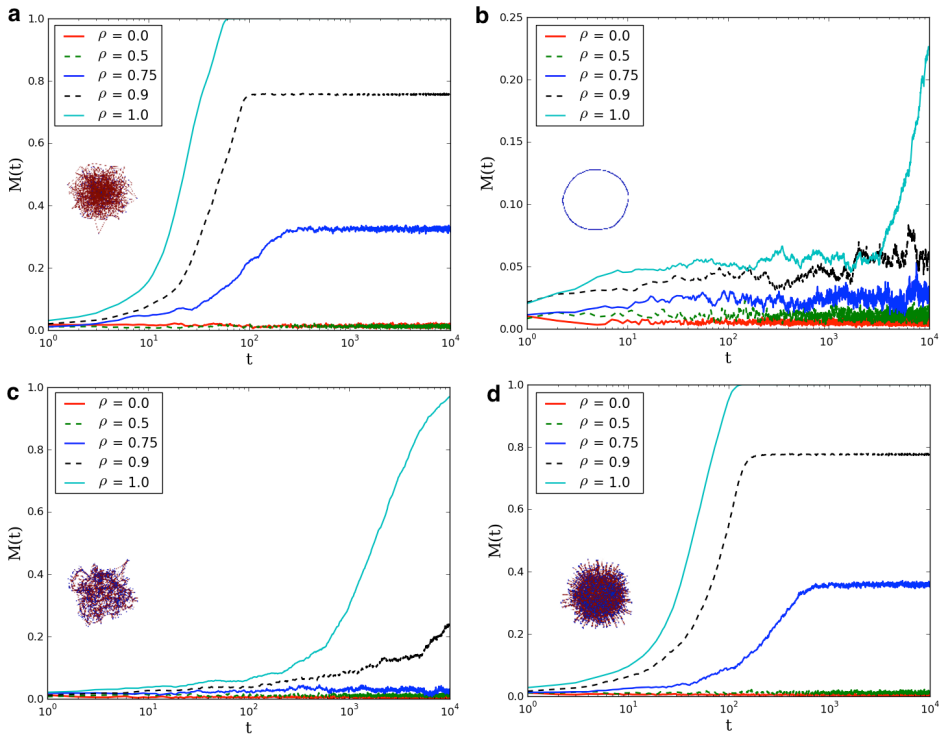

Figure A.1: Evolution of the magnetization for different values of ρ and different configurations: **a** scale-free network; **b** regular lattice; **c** small-world network ($\beta = 0.1$); **d** small-world network ($\beta = 0.5$). Small pictorial representations are shown for each network.

people forming groups to discuss about politics: it is hard to imagine participants discussing and changing their opinion 'sequentially'. Persons interacts with their neighbors simultaneously, updating their opinion in 'real time', i.e. *before* being engaged in a new discussion with a different group. Another example is provided by voting scenarios, where people express their opinion at the same time. Moreover, even if asynchronous updating were applicable, it would cause the system dynamics to be dependent on the particular sequence of agents chosen.

Results

Numerical simulations of the proposed model have been carried on by chosing $N = 5000$ agents, embedded on different network topologies as scale-free networks, regular lattices, small world networks and completely random networks. While scale-free networks have been generated via the Barabasi-Albert model [75], the other kinds of networks have been generated via the Watts-Strogatz model [81]. The latter allows to obtain different network

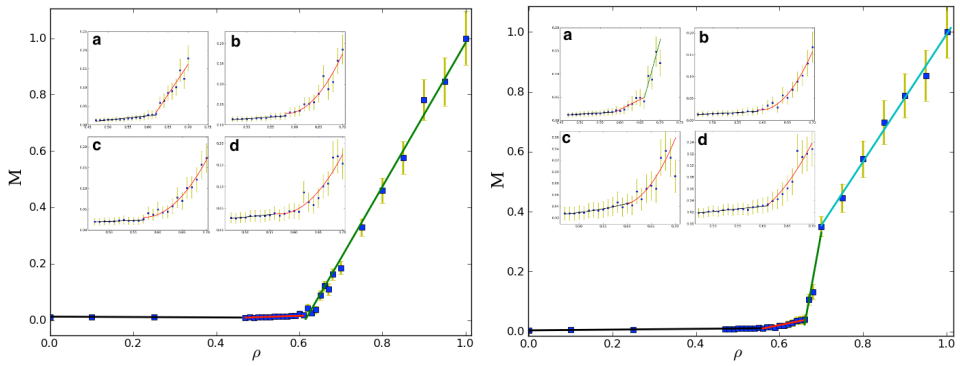

Figure A.2: Phase-diagram plotting M versus ρ for two network configurations (left: scale-free; right: small-world with $\beta = 0.5$): different phases are visible, separated by threshold values of ρ. Insets show the same analysis for networks with (**a**) $N = 2500$, (**b**) $N = 2000$, (**c**) $N = 1000$ and (**d**) $N = 500$. Error bars represent the standard deviation over the simulations run. The average R^2 of the fits is: scale-free - (main panel) 0.9, (**a**) 0.88, (**b**) 0.88, (**c**) 0.8, (**d**) 0.86; Watts-Strogatz - (main panel) 0.92, (**a**) 0.85, (**b**) 0.92, (**c**) 0.9, (**d**) 0.86.

configurations by varying the value of the rewiring probability β: regular lattices are achieved by setting $\beta = 0$, small-world networks by setting $0 < \beta < 1$ and completely random networks by setting $\beta = 1$. In this work, we have considered the following values: $\beta \in [0, 0.01, 0.1, 0.5, 1]$. Moreover, all the considered networks have an average degree equal to $\sum_{i=1}^{N} k_i/N = 8$ (i.e. agents have, on average, eight neighbors). Now, it is worth to highlight that, since these network models are stochastic, we decided to generate and to use a single network for each configuration and for each size. Each simulation has been performed with a different amount of conformist agents $\rho \in [0, 0.1, 0.25, 0.5, 0.6, 0.65, 0.7, 0.75, 0.9, 1]$ - notice that the expected value of ρ coincides with the expected fraction of conformist agents, i.e. $\langle \rho \rangle = \langle N_c^0/N \rangle = P_c$ - and it has been run for 10^4 time steps. For the vast majority of cases this temporal limit was long enough to reach a steady-state, as only few network configurations required more time. However, in the latter scenarios (e.g. regular lattices) we performed longer simulations. We first consider the evolution of the system magnetization over time, i.e. the absolute value of the difference between the number of agents in the two states [92], normalized to N:

$$M = \frac{|N_+ - N_-|}{N}. \tag{A.1}$$

The magnetization ranges between 0 and 1 ($0 \leq M \leq 1$), with $M = 0$ indicating the equipartition of the two opinions (i.e. the maximally disordered

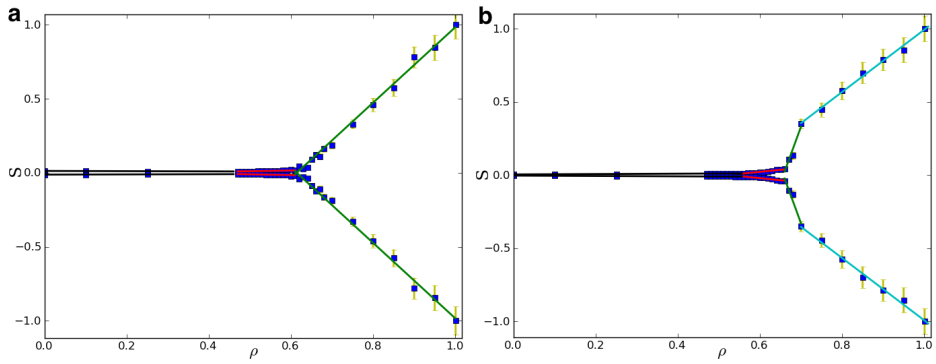

Figure A.3: Symmetry-breaking diagram plotting S versus ρ for two network configurations (left: scale-free; right: small-world with $\beta = 0.5$): as ρ crosses one of the threshold values, the system can be found in one of two states, a priori equally probable, characterized by opposite values of S. Error bars represent the standard deviation over the simulations run.

phase), and $M = 1$ indicating that consensus has been reached. Notice that both situations $N_+ = 0$, $N_- = N$ and, vice-versa, $N_- = 0$, $N_+ = N$ are compatible with consensus, i.e. magnetization is uninformative about the dominant opinion sign.

Figure A.1 illustrates the evolution of the magnetization, upon varying the value of ρ for different network configurations. Remarkably, the density of conformist agents (i.e. ρ) strongly affects the process of consensus reaching; more detailedly, 1) values of $\rho \leq 0.5$ seem not to be sufficiently high to let the system escape the disordered phase where the two opinions coexist; 2) values of $0.5 < \rho < 1$ let the system escape the disordered phase but not to reach consensus: a steady-state is reached where one of the two opinions prevails on the other; 3) only the density value $\rho = 1$ allows the system to reach the consensus.

Remarkably, this is valid for all the considered configurations: what changes is the number of time steps after which the steady-state, or the consensus, is reached. In particular, the regular lattice (panel b of Figure A.1) is the configuration where the process is slowest. As the network is more and more rewired (panels c and d of Figure A.1), the process becomes faster. Interestingly, further rewiring the network ($\beta > 0.5$) does not lead to any appreciable change. Qualitatively speaking, the scale-free configuration (panel a of Figure A.1) does not show significant differences with respect to the small-world network with $\beta = 0.5$; however, the latter reaches the steady-state later, for all the values of ρ. It is maybe surprising that the presence of hubs does not speed up the process. However, this apparent paradox could be explained by considering that we are implementing a q-voter model, with an update rule involving only four neighbors at a time:

thus, the (potential) influence those hubs could have on large numbers of nodes is drastically reduced. Notice also that, for any given configuration, rising ρ shortens the time for reaching the steady-state. According to Figure A.1 the value $\rho = 0.5$ seems to play the role of a threshold, separating two phases of the system: the disordered one, characterized by $M = 0$, and the ordered one, with M gradually rising (as a function of ρ) until full consensus is reached. As we will show in a while, the behavior of the q-voter model on heterogeneous networks is far richer.

Figure A.2 shows the value of the magnetization at the steady-state (i.e. after 10^4 time steps), for two network configurations only (but the same holds true for all the others), as a function of ρ. Let us focus on the scale-free configuration (left panel of Figure A.2). At a first sight, two distinct phases are visible: the disordered one, characterized by $M = 0$ for all the values of $\rho \leq 0.5$, and the ordered one, characterized by a value $M \neq 0$ for $\rho > 0.5$. Thus, the magnetization seems to play the role of the order parameter of a continuous phase transition, while ρ plays the role of control parameter, which can be varied to change the system behavior smoothly. Actually, a closer inspection reveals three different opinion-formation regimes (indicated by different colors), with two distinct threshold values: $\rho_{c1} \simeq 0.45$ separating the flat behavior (in black) from the slowly-rising linear one (in red) and $\rho_{c2} \simeq 0.59$ separating the latter from the rapidly-rising linear one (in green). The insets (zooming on the second transition) reveal that the same qualitative behavior can be observed also for networks with a lower number of agents; what changes is the trend followed by points in the third phase (linear for $N \geq 2500$ and quadratic for $N < 2500$) with ρ_{c2} shifting towards lower values ($\simeq 0.56$ for $N = 500$ agents). Let us now comment our findings for the Watts-Strogatz configuration (right panel of Figure A.2). This time four phases are distinguishable, separated by three threshold values: $\rho_{c1} \simeq 0.55$, $\rho_{c2} \simeq 0.65$ and $\rho_{c3} \simeq 0.70$. However, as the insets reveal, the system loses two of the phases as the number of agents is lowered, showing three linear regimes for $N \geq 2500$ and only one quadratic regime for $N < 2500$. We also emphasize that all the aforementioned critical thresholds ρ_c represent average values computed over the simulations run for each kind of network (i.e. scale-free and small world), characterized by a standard deviation $\sigma_{\rho_c} \simeq 0.02$. However, the analysis of M is somehow limiting because the values of M cannot be negative: this means that the situations where agents reach consensus by adopting the opinions $+1$ and -1 are indistinguishable. Thus, we need a quantity able to distinguish the sign of the system final state. To achieve this, we use the *summation of states*

$$S = \frac{\sum_i s_i}{N} = \frac{N_+ - N_-}{N} \tag{A.2}$$

providing a complementary information with respect to M. Plotting the summation S versus the density of conformists ρ, it is possible to achieve

further information on the system dynamics. As shown in Figure A.3, as the density of conformists rises the system chooses one of two states, characterized by the same absolute value of S, but with opposite sign: remarkably, the two states revealed by crossing the thresholds are symmetrically distributed with respect to the horizontal axis. In other words, by rising the density ρ the system is induced to choose one out of two possible states, a priori equally probable, thus breaking its symmetry.

Each point of the phase diagram is the result of an average over more simulations: the obtained values show very small numerical differences, amounting to few percents in the vast majority of cases. When considering the summation of states, to not wash away the information provided by the sign of S, the symmetry-breaking diagram has been obtained by averaging the negative and the positive values separately, maintaining the bi-stable character of the system.

We have already noticed that the behavior of our system, distinguishing the disordered state with $M = 0$ from the ordered state with $M > 0$, can be interpreted, in more physical terms, as a phase transition with ρ playing the role of control parameter and M playing the role of order parameter. Such an evidence can be better described upon recalling the behavior of a system of spins as the temperature is varied. In other words, our population of agents behaves like a spin system [24], which is found to be in a paramagnetic phase for the values $\rho < \rho_c$. The latter plays the role of the critical temperature in the usual spin case. In order to describe the phase transition of our system, we move from the well known relation $M \propto \left(1 - \frac{T}{T_c}\right)^{\gamma}$. A similar relation can be shown to hold true for our agents.

Let us start by highlighting that the role of temperature T is played, in our case, by the parameter $(1-\rho)$, therefore the critical temperature T_c can be mapped to $(1-\rho_c)$. In order to find the value of the exponent γ describing the ferromagnetic phase of our system, we have plotted the magnetization M as a function of $(1-\rho)/(1-\rho_c)$. Fig. A.4 shows it for the scale-free configuration ($N = 5000$ nodes). The functional form is very well described by the analytical relation $M \propto \left(1 - \frac{(1-\rho)}{(1-\rho_c)}\right)^{\gamma}$ with $\gamma \simeq 1.45$ and $\rho_c = 0.59$.

However, while for a classical spin system the analytical relation described above separates *two* distinct phases (the paramagnetic one, for $\frac{T}{T_c} > 1$ and the ferromagnetic one, for $\frac{T}{T_c} < 1$), in our case the ferromagnetic phase $M > 0$ can be further subdivided into different subphases which have been called 'regimes' by us. Nevertheless, the formalism used in physics to describe a phase transition does not allow one to take into account the possibility of observing subphases; for this reason, the value $\rho_c = 0.59$ has been chosen by us to simply distinguish the phase with $M = 0$ from the phase with $M > 0$, completely ignoring the details of the latter.

The same line of reasoning holds true for the small-world configuration.

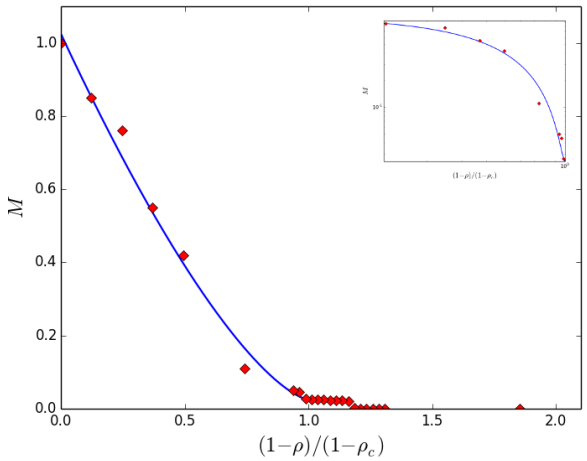

Figure A.4: Plot of M as a function of $(1-\rho)/(1-\rho_c)$, for the scale-free network with $N = 5000$. The blue curve represents the analytical relation $M \propto \left(1 - \frac{(1-\rho)}{(1-\rho_c)}\right)^{\gamma}$ which describes very accurately the functional dependence of M on the control parameter $(1-\rho)/(1-\rho_c)$. The best fitting procedure gives $\gamma \simeq 1.45$ once the value $\rho_c = 0.59$ has been inserted into the aforementioned formula. The inset shows the same fitting curve in a log-log scale.

Conclusion

The q-voter model shows a very rich behavior, even simply considering agents with two opinions and two characters only, as conformists and non-conformists. Notably, the density of conformist agents ρ strongly affects the consensus reaching process, defining threshold values separating different phases of opinion formation. For $\rho = 0$ the two original opinions equally coexist, i.e. 50% of agents remain in the $+1$ state and 50% of agents remain in the -1 state (with small fluctuations). Then, by progressively rising ρ, the system starts showing a non-zero magnetization, i.e. a larger number of agents starts sharing the same opinion. Indeed, our control parameter ρ can be mapped to the control parameter T (i.e. the temperature) of a spin system; following the same line of reasoning we have been able to identify a critical exponent γ that characterizes the phase transition occurring in our agent population, as the density of conformists exceeds the threshold ρ_c. More precisely, the system undergoes a sort of continuous phase transition, which can be further broken down in several regimes, suggesting different functional forms of $M(\rho)$, separated by different values of ρ.

Apart from the details of the process, the response of the q-voter model to changes of the conformist agent density is remarkably stable across different network topologies: Watts-Strogatz networks with $\beta \geq 0.5$ show similar phase-diagrams and symmetry-breaking processes, in turn very similar to

the ones observed for the scale-free configuration. The effect of considering heterogeneous topologies is mainly reflected in the speed of the process, which depends on the values of the parameter β: in particular, the more random the network, the faster the process.

In conclusion, what emerges indicates that different regimes of 'opinion growth' are identifiable, strongly affected by the density of conformists. Moreover, even if the percentage of conformists drives the society towards a 'prevalent' opinion (whose diffusion speed grows as more and more conformists are considered) in the case of agents with only two opinions (evenly distributed at $t = 0$), the prevalent one cannot be predicted *a priori*.

Bibliography

[1] Perc, M., Grigolini, P.: Collective behavior and evolutionary games - An introduction. *Chaos, Solitons & Fractals* **56** 1-5 (2013)

[2] Perc, M., Szolnoki, A.: Social diversity and promotion of cooperation in the spatial prisoner's dilemma. *Physical Review E* **77** 011904 (2008)

[3] Wang, Z., Szolnoki, A., and Perc, M.: Interdependent network reciprocity in evolutionary games. *Scientific Reports* **3** 1183 (2013)

[4] Szolnoki, A., Xie, N.-G., Wang, C. and Perc, M.: Imitating emotions instead of strategies in spatial games elevates social welfare. *Europhysics Letters* **96** 38002 (2011)

[5] Perc, M. and Szolnoki, A.: Self-organization of punishment in structured populations. *New Journal of Physics* **14** 043013 (2012)

[6] Szolnoki, A., Szabo, G., Perc, M.: Phase diagrams for the spatial public goods game with pool punishment. *Physical Review E* **83** 0361101 (2011)

[7] Friedman, D.: On economic applications of evolutionary game theory. *Journal of Evolutionary Economics* **8-1** 15–43 (1998)

[8] Schuster, S., de Figueiredo, L., Schroeter, A., and Kaleta, C.: Combining metabolic pathway analysis with evolutionary game theory. Explaining the occurrence of low-yield pathways by an analytic optimization approach. *BioSystems* **105** 147–153 (2011)

[9] Frey, E.: Evolutionary game theory: theoretical concepts and applications to microbial communities. *Physica A* **389** 4265–4298 (2010)

[10] Lieberman, E., Hauert, C., Nowak, M.A.: Evolutionary dynamics on graphs. *Nature* **433** (2004)

[11] Fu, F., Rosenbloom, D.I. Wang, L., Nowak, M.A.: Imitation dynamics of vaccination behaviour on social networks. *Proc. R. Soc. B* **278** 42–49 (2011)

[12] Poncela, J. et al.: Cooperation in the Prisoner's Dilemma game in random scale-free graphs. *International Journal of Bifurcation and Chaos* **20-3** 849–857 (2010)

[13] Gracia-Lazaro, C., Gomez-Gardenes, J., Floria, L.M., Moreno, Y.: Intergroup information exchange drives cooperation in the public goods game. *Physical Review E* **94** 042808 (2014)

[14] Szolnoki, A., and Perc, M.: Biodiversity in models of cyclic dominance is preserved by heterogeneity in site-specific invasion rates. *Scientific Reports forthcoming* (2016)

[15] Grujic, J., Fosco, C., Araujo, L., Cuesta, A.J., Sanchez, A.: Social experiments in the mesoscale: Humans playing a spatial prisoner's dilemma. *Plos One 5-11* e13749 (2010)

[16] Kaveh, K., Veller, C., Nowak, M.A.: Games of multicellularity. *Journal of Theoretical Biology*, **403** 143–158 (2016)

[17] Hauser, O.P., Rand, D.G., Peysakhovich, A., Nowak, M.A.: Cooperating with the future. *Nature* **511** (2014)

[18] Hauser, O.P., Hendriks, A., Rand, D.G., Nowak, M.A.: Think global, act local: Preserving the global commons. *Scientific Reports* **6** 36079 (2016)

[19] Nakajima, Y., Nowak, M.: Evolutionary dynamics in finite populations with zealots. *Journal of mathematical biology* **70-3** 465–484 (2015)

[20] Colman, A.M.: Game Theory and Its Applications *Routledge: New York, NY, USA*, (2008)

[21] Darwin, C.: On the origin of species, by means of natural selection, or the preservation of favoured races in the struggle for life. *LONDON: JOHN MURRAY ALBEMARLE STREET*, (1859)

[22] Nowak, M.A.: Evolutionary Dynamics. Exploring the Equations of Life. *Harvard University Press*, (2006)

[23] Anderson, P.W.: More is different. *Science* **177** 1–4 (1972)

[24] Huang, K.: Statistical Mechanics. *Wiley 2nd Ed.* (1987)

[25] Mussardo, G.: Statistical Field Theory: An Introduction to Exactly Solved Models in Statistical Physics. *Oxford University Press* (2010)

[26] Hauert, , Szabo, G.: Game Theory and Physics. *American Journal of Physics* **73-5** 405–414 (2005)

[27] Galam, S., Walliser, B.: Ising model versus normal form game. *Physica A* **389** 481–489 (2010)

[28] Taylor, P.D., Jonker, L.B.: Evolutionary Stable Strategies and Game Dynamics. *Math. Biosci.* **40** 145–156 (1978)

[29] Zeeman, E.C: Population Dynamics from Game Theory. *Lecture Notes in Mathematics - Springer Verlag* **819** (1980)

[30] Hofbauer, J., Shuster, P., Sigmund, K.: A note on evoutionary stable strategies and game dynamics. *Journal of Theoretical Biology* **81** 609–612 (1979)

[31] Sigmund, K.: Games of Life: Explorations in ecology, evolution and behavior. *Oxford University Press* (1993)

[32] Amaral, M.A., Wardil, L., Perc, M., da Silva, J.K.L.: Stochastic win-stay-lose-shift strategy with dynamic aspirations in evolutionary social dilemmas. *Physical Review E* **032317** (2016)

[33] Szolnoki, A., Perc, M.: Zealots tame oscillations in the spatial rock-paper-scissors game. *Physical Review E* **062307** (2016)

[34] Szolnoki, and Perc, M.: Reward and cooperation in the spatial public goods game. *Europhysics Letters* **92** 38003 (2010)

[35] Gracia-Lazaro, C., et al.: Heterogeneous networks do not promote cooperation when humans play a Prisoner's Dilemma. *PNAS* **109-32** 12922–12926 (2012)

[36] Santos, F.C., Pacheco, J.M., Lenaerts: Evolutionary dynamics of social dilemmas in structured heterogeneous populations. *PNAS* **103-9** 3490–3494 (2006)

[37] Julia, PC, Gomez-Gardenes, J., Traulsen, A., and Moreno, Y.: Evolutionary game dynamics in a growing structured population. *New Journal of Physics* **11** 083031 (2009)

[38] Wang, Z., Xia, C.-Y., Meloni, S., Zhou, C.-S., Moreno, Y.: Impact of social punishment on cooperative behavior in complex networks. *Scientific Reports* **3** 3055 (2013)

[39] Santos, F.C., Pacheco, J.M.: Scale-free networks provide a unifying framework for the emergence of cooperation. *Physical Review Letters* **95-9** 098104 (2005)

[40] Santos, F.C., Mantos, M.D., Pacheco, J.M.: Social diversity promotes the emergence of cooperation in public goods games. *Nature* **454-7201** 213–216 (2008)

[41] Santos, F.C., Rodrigues, J.F., Pacheco, J.M.: Graph topology plays a determinant role in the evolution of cooperation. *Proc. R. Soc. B* **273-1582** 51–55 (2006)

[42] Gomez-Gardenes, J., Gracia-Lazaro, C., Floria, L.M., Moreno, Y.: Evolutionary dynamics on interdependent populations. *Physical Review E* **86** 056113 (2012)

[43] Nicosia, V., Bianconi, G., Barthelemy, M.: Growing multiplex networks. *Physical Review Letters* **111** 058701 (2013)

[44] Battiston, F., Nicosia, V., Latora, V.: Structural measures for multiplex networks. *Physical Review E* **89** 032804 (2014)

[45] Bianconi, G.: Statistical mechanics of multiplex networks: Entropy and overlap. *Physical Review E* **87** 062806 (2013)

[46] Sole-Ribalta, A., De Domenico, M., Kouvaris, E., Diaz-Guilera, A., Gomex, S., Arenas, A.: Spectral properties of the Laplacian of multiplex networks. *Physical Review E* **88** 032807 (2013)

[47] Kouvaris, N.E., Hata, S., Diaz-Guilera, A.: Pattern formation in multiplex networks. *Scientific Reports* **5** 10840 (2015)

[48] De Domenico, M., Sole-Ribalta, Cozzo, E., Kivela, M., Moreno, Y., Porter, A.M., Gomex, S., Arenas, A.: Mathematical formulation of multilayer networks. *Physical Review X* **3** 041022 (2013)

[49] Gomez-Gardenes, J., Reinares, I., Floria, L.M.: Evolution of Cooperation in Multiplex Networks. *Scientific Reports* **2** 620 (2012)

[50] Wang, Z., Wang, L., Szolnoki, A., Perc, M.: Evolutionary games on multilayer networks: A colloquium. *EPJ-B* **88** 124 (2015)

[51] Nowak, M.A.: Five rules for the evolution of cooperation. **Science 314-5805** 1560–1563 (2006)

[52] Meloni, S., Buscarino, A., Fortuna, L., Frasca, M., Gomez-Gardenes, J., Latora, V., Moreno, Y.: Effects of mobility in a population of prisoner's dilemma players. *Physical Review E* **79-6** 067101 (2009)

[53] Cardillo, A., Meloni, S., Gomez-Gardenes, J., Moreno, Y.: Velocity-enhanced cooperation of moving agents playing public goods games. *Physical Review E* **85-6** 067101 (2012)

[54] Antonioni, A., Tomassini, M., Buesser, P.: Random diffusion and cooperation in continuous two-dimensional space. *Journal of Theoretical Biology* **344** 40–48 (2014)

[55] Tomassini, M., Antonioni, A.: Levy Flights and Cooperation among mobile individuals. *Journal of Theoretical Biology* **364** 154–161 (2015)

[56] Javarone, M.A.: Statistical Physics of the Spatial Prisoner's Dilemma with Memory-Aware Agents *EPJ-B* 89 (2016)

[57] Javarone, M.A., Atzeni, A.E.: The role of competitiveness in the Prisoner's Dilemma. *Computational Social Networks* **2** (2015)

[58] Nishimori, H.: Statistical Physics of Spin Glasses and Information Processing. An Introduction. *Clarendon Press Oxford* (2001)

[59] Galam, S.: Sociophysics: a physicist's modeling of psycho-political phenomena. *Springer Science* (2012)

[60] Galam, S.: Sociophysics: a review of Galam models. *Int. J. Mod. Phys. C* **19-03** 409–440 (2008)

[61] Galam, S.: A Renormalization Group Like Model for a Democratic Dictatorship. *Order, Disorder and Critically: Advanced Problems of Phase Transition Theory* **Volume 4** World Scientific Publishing (2015)

[62] Galam, S.: Modeling the Forming of Public Opinion: an approach from Sociophysics. *Global Economics and Management Review* **18-1** 2–11 (2013)

[63] Galam, S.: Terrorism and Passive Supporters: An Approach from Physics. *Complex Societal Dynamics: Security Challenges and Opportunities* **75** 175 (2010)

[64] Castellano, C., Fortunato, S., Loreto, V.: Statistical Physics of Social Dynamics. *Review of modern physics* **81-2** 591 (2009)

[65] Agliari, A., Barra, A., Contucci, P., Sandell, R. Vernia, C.: A stochastic approach for quantifying immigrant integration: the Spanish test case. *New Journal of Physics* **16-10** 103034 (2014)

[66] Barra, A., Galluzzi, A., Tantari, D., Agliari, E., Requena.Silvente, F.: Assessing the role of migration as trade-facilitator using the statistical mechanics of cooperative systems. *Palgrave Communications* **2** (2016)

[67] Agliari, E., Barra A., Galluzzi, A., Javarone, M.A., Pizzoferrato, A., Tantari, D.: Emerging heterogeneities in Italian customs and comparison with nearby countries. *PloS one* **10-12** e0144643 (2015)

[68] D'Orsogna, M.R., Perc, M.: Statistical Physics of crime: A review. *Physics of Life Reviews* **12** 1–21 (2015)

[69] Javarone, M.A.: Network strategies in election campaigns. *Journal of Statistical Mechanics: Theory and Experiment* P08013 (2014)

[70] Barra, A., Galluzzi, A., Guerra, F., Pizzoferrato, A., Tantari, D.: Mean field bipartite spin models treated with mechanical techniques. *EPJ-B* **87-3** 1–13 (2014)

[71] Di Biasio, A., Agliari, A., Barra, A., Burioni, R.: Mean-field cooperativity in chemical kinetics. *Theoretical Chemistry Accounts* **131-3** 1–14 (2012)

[72] Genovese, G., Barra, A.: A mechanical approach to mean field spin models. *Journal of Mathematical Physics* **50-5** 053303 (2009)

[73] Barra, A.: The mean field Ising model trough interpolating techniques. *Journal of Statistical Physics* **132-5** 787–809 (2008)

[74] Gallo, I., Barra, A., Contucci, P.: Parameter evaluation of a simple mean-field model of social interaction. *Mathematical Models and Methods in Applied Sciences* **19** 1427–1439 (2009)

[75] Albert, R., Barabasi, A.L.: Statistical mechanics of complex networks. *Review of modern physics* **74** 47–97 (2002)

[76] Newman, M.: The structure and function of complex networks. *SIAM Review* **45-2** 167–256 (2003)

[77] Boccaletti, S., Latora, V., Moreno, Y., Chavez, M., Hwang D.-U.: Complex Networks: Structure and Dynamics. *Physics Reports* **424-4** 175–308 (2006)

[78] Caldarelli, G.: Scale-free networks: complex webs in nature and technology. *Oxford University Press* (2007)

[79] Estrada, E.: The structure of complex networks: theory and applications. *Oxford University Press* (2012)

[80] Barrat, A., Barthelemy, M., Vespignani, A.: Dynamical Processes on Complex Networks. *Cambridge University Press* (2008)

[81] Watts, D.J., Strogatz, S.H.: Collective dynamics of 'small-world' networks. *Nature* (1998)

[82] Agliari, E., Barra A., Camboni, F.: Criticality in diluted ferromagnets. *Journal of Statistical Mechanics: Theory and Experiment* P10003 (2008)

[83] Barra A., Agliari, E.: Equilibrium statistical mechanics on correlated random graphs. *Journal of Statistical Mechanics: Theory and Experiment* P02027 (2011)

[84] Barra A., Agliari, E.: A statistical mechanics approach to Granovetter theory. *Physica A* **391-10** 30173026 (2012)

[85] Castellana, M., Barra, A., Guerra, F.: Free energy bounds for hierarchical spin models. *Journal of Statistical Physics* **155-211** (2013)

[86] Hartmann, A.K., Wight, M.: Phase Transitions in Combinatorial Optimization Problems: *WILEY-VCH*, (2005)

[87] Murray JD: Mathematical Biology. *Springer* (2002)

[88] Galam, S., Javarone, M.A.: Modeling Radicalization Phenomena in Heterogeneous Populations. *PloS One* **11-5** e0155407 (2016)

[89] Galam, S., Jacobs, F.: The role of inflexible minorities in the breaking of democratic opinion dynamics. *Physica A* **381** 366–376 (2007)

[90] Kelling GL, Coles CM. Fixing Broken Windows: Restoring Order and Reducing Crime in Our Communities. *Simon and Schuster*, (1997)

[91] Javarone, M.A.: Is Poker a Skill Game? New insights from Statistical Physics. *Europhysics Letters* **110** (2015)

[92] Mobilia, M. and Redner, S.: Majority versus minority dynamics: Phase transition in an interacting two-state spin system. *Physical Review E* **68-4** 046106 (2003)

[93] Javarone, M.A., Battiston, F.: The Role of Noise in the Spatial Public Goods Game. *Journal of Statistical Mechanics: Theory and Experiment* 073404(2016)

[94] Szolnoki, A., Perc, M., Szabo, G.: Topology-independent impact of noise on cooperation in the spatial public goods game. *Physical Review E* **80** (2009) 056109

[95] Szabo, G., Christoph, H.: Phase transitions and volunteering in spatial public goods games. *Physical Review Letters* **89-11** (2002) 118101

[96] Szolnoki, A., Vukov, J., Szabo, G.: Selection of noise in strategy adoption for spatial social dilemmas. *Physical Review E* **80-5** (2009) 056112

[97] Vilone, D., Ramasco, J.J., Sanchez, A., San Miguel, M.: Social and strategic imitation: the way to consensus. *Scientific Reports* **2-686** (2012)

[98] Szolnoki, A., Perc, M.: Conformity enhances network reciprocity in evolutionary social dilemmas. *J. R. Soc. Interface* **12** (2015) 20141299

[99] Liggett T.M.: Interacting Particle Systems. *Springer-Verlag, New York* (1985)

[100] Javarone, M.A., Squartini, T.: Conformism-driven phases of opinion formation on heterogeneous networks: the q-voter model case. *Journal of Statistical Mechanics: Theory and Experiment* P10002 (2015)

[101] Javarone, M.A.: Social Influence in Opinion Dynamics: The role of Conformity. *Physica A* **414** (2014) (2014)

[102] Galam, S.: Stubbornness as an unfortunate key to win a public debate: an illustration from sociophysics *Mind and Society* **15-1** (2016)

[103] Battiston F, Cairoli A, Nicosia V, Baule A, Latora V.: Interplay between consensus and coherence in a model of interacting opinions. *Physica D* **323-324** 12–19 (2016)

[104] Galam, S.: Contrarian deterministic effects on opinion dynamics: 'the hung elections scenario'. *Physica A* **333** 453–460 (2004)

[105] Sznajd-Weron: Opinion Evolution in Closed Community. *Int. J. Mod.Phys. C* **11** 1157 (2000)

[106] Javarone, M.A., Antonioni, A., Caravelli, F.: Conformity-Driven Agents Support Ordered Phases in the Spatial Public Goods Game. *Europhysics Letters* **114** 38001 (2016)

[107] Crokidakis, N., Anteneodo, C.: Role of conviction in nonequilibrium models of opinion formation. *Physical Review E* **86** 061127 (2012)

[108] Crokidakis, N.: Effects of mass media on opinion spreading in the Sznajd sociophysics model. *Physica A* **391** 1729 (2012)

[109] Crokidakis, N.: Role of noise and agents' convictions on opinion spreading in a three-state voter-like model. *Journal of Statistical Mechanics: Theory and Experiment* P07008 (2013)

[110] Crokidakis, N., Blanco, V.H., Anteneodo, C.: Impact of contrarians and intransigents in a kinetic model of opinion dynamics. *Physical Review E* **89** 013310 (2014)

[111] Crokidakis, N., Castro de Oliveira, P.M.: Inflexibility and independence: Phase transitions in the majority-rule model. *Physical Review E* **92** 062122 (2015)

[112] Vieira, A.R., Anteneodo, C., Crokidakis, N.: Consequences of nonconformist behaviors in a continuous opinion model. *Journal of Statistical Mechanics: Theory and Experiment* P023204 (2016)

[113] Javarone, M.A.: Poker as a Skill Game: Rational versus Irrational Behaviors. *Journal of Statistical Mechanics: Theory and Experiment* P03018 (2015)

[114] Peña, J. et al.: Conformity hinders the evolution of cooperation on scale-free networks. *Physical Review E* **80** 016110 (2009)

[115] Javarone, M.A., et al.: Emergence of Cooperation in the Prisoners Dilemma Driven by Conformity. *LNCS - Springer* **9028** (2015) 155–163

[116] Floria, L.M., et al.: Social network reciprocity as a phase transition in evolutionary cooperation. *Physical Review E* **79** 026106 (2009)

[117] Javarone, M.A.: Solving Optimization Problems by the Public Goods Game. *arxiv:1604.02929* (2016)

[118] Holland, J.H. Adaptation in Natural and Artificial Systems. *The University of Michigan Press* (1975)

[119] Goldberg, D.E. Genetic algorithms in search, optimization, and machine learning. *Machine Learning* **2** (1989)

[120] Krentel, M.W.: The complexity of optimization problems. *Proceedings of the eighteenth annual ACM symposium on Theory of computing* 69–76 (1986)

[121] Dorigo, M., Blum, C.: Ant colony optimization theory: A survey. *Theoretical Computer Science* **344-2** 243–278 (2005)

[122] Kellerer, H., Pferschy, U., Pisinger, D.: Introduction to NP-Completeness of Knapsack Problems. *Springer* (2004)

[123] Dorigo, M., Caro, G., Gambardella, L.M.: Ant Algorithms for Discrete Optimization. *Artificial Life* 5–2 (1999)

[124] Baldassi, C., Braunstein, A., Ramezanpour, A., Zecchina, R.: Statistical Physics and Network Optimization Problems. *Mathematical Foundations of Complex Networked Information Systems* 27–49 (2015)

[125] Altarelli, F., Braunstein, A., Ramezanpour, A., Zecchina, R.: Stochastic optimization by message passing. *Journal of Statistical Mechanics: Theory and Experiment* **11** P11009 (2011)

[126] Zdeborova, L., Krzakala, F.: Statistical physics of inference: Thresholds and algorithms. *arxiv:1511.02476* (2015)

[127] Jorg, T., Krzakala, F., Semerjian, G., Zamponi, F.: First-order transitions and the performance of quantum algorithms in random optimization problems. *Physical Review Letters* **104-20** 207206 (2010)

[128] Amit, D.: Modeling Brain Function. *Cambridge University Press* (1989)

[129] Hopfield, J.J., Tank, D.W.: Neural Computation of Decisions in Optimization Problems. *Biological Cybernetics* **52** 141-152 (1985)

[130] Kirkpatrick, S.: Optimization by simulated annealing: Quantitative studies. *Journal of Statistical Physics* **34-5** 975-986 (1983)

[131] Vannimenus, J., Mezard, M.: On the statistical mechanics of optimization problems of the traveling salesman type. *J. Physique Lett.* **45-24** (1984)

[132] San Miguel, M., et al.: Challenges in complex systems science. *The European Physical Journal Special Topics* **214-1** 245–271 (2012)

[133] Dorigo, M., Gambardella, L.M.: Ant colony system: a cooperative learning approach to the traveling salesman problem. *IEEE, Evolutionary Computation* 53–66 (1997)

[134] Bellingeri, M., Agliari, A., Cassi, D.: Optimization strategies with resource scarcity: From immunization of networks to the traveling salesman problem. *Modern Physics Letters B* **29-29** (2015)

[135] Kochmanski, M., Paszkiewicz, T., and Wolski, S.: CurieWeiss magneta simple model of phase transition Statistical Mechanics. *European Journal of Physics* **34** 1555 (2013)

[136] Mezard, M., Parisi, G., Virasoro, M.A.: Spin glass theory and beyond. *World Scientific Publishing* (1990)

[137] Franz, S.,et al.: Quantitative field theory of the glass transition. *PNAS* **109-46** 18725–18730 (2012)

[138] E. Agliari, et al.: Hierarchical neural networks perform both serial and parallel processing. *Neural Networks* **66** 22–35 (2015)

[139] Javarone, M.A.: An Evolutionary Strategy based on Partial Imitation for Solving Optimization Problems. *Physica A: Statistical Mechanics and its Applications* **463** 262269 (2016)

[140] Fehr, E., Gachter, S.: Altruistic punishment in humans *Nature* **415** 137–140 (2002)

[141] Sood, V., and Redner, S.: Voter Model on Heterogeneous Graphs. *Physical Review Letters* **94** 178701 (2005)

[142] Wang, D., Zhang, Q.Y.: Research on Laser Marking Speed Optimization by Using Genetic Algorithm. *PLoS ONE* **10-5** e0126141 (2015)

[143] Javarone, M.A.: Modeling Poker Challenges by Evolutionary Game Theory. *Games* **7-4** 39 (2016)

[144] Bowling, M., Burch, N., Johanson, M., Tammelin, O.: Heads-up limit hold'em poker is solved. *Science* **347-6218** 145–149 (2015)

[145] Dahl, F.A.: A Reinforcement Learning Algorithm Applied to Simplified Two-Player Texas Hold'em Poker. *Machine Learning: ECML 2001 - LNCS* **2167** 85–96 (2001)

[146] Teofilo, L.F., Reis, L.P., Lopes Cardoso, H.: Computing card probabilities in Texas Hold'em. *Information Systems and Technologies (CISTI), 2013 8th Iberian Conference on* 1–6 (2013)

[147] Seale, D.A., Phelan, S.E.: Bluffing and betting behavior in a simplified poker game. *Journal of Behavioral Decision Making* **23-4** 335–352 (2010)

[148] Hannum, R.C., Cabot, A.N.: Toward Legalization of Poker: The Skill vs. Chance Debate *UNLV Gaming Research & Review Journal* **1-13** (2009)

[149] Kelly, J.M., Dhar, Z., Verbiest, T.: Poker and the Law: Is It a Game of Skill or Chance and Legally Does It Matter?. *Gaming Law Review* **3-11** (2007)

[150] Cabot, A., Hannum, R.: Poker: Public Policy, Law, Mathematics, and the Future of an American Tradition. *TM Cooley L. Rev.* **22-443** (2005)

[151] Moreno, Y., Vazquez, A.: Disease spreading in structured scale-free networks. *The European Physical Journal B* 31 **2** (2003)

[152] Javarone, M.A., Interdonato, R., Tagarelli, A.: Modeling Evolutionary Dynamics of Lurking in Social Networks. *Studies in Computational Intelligence* Springer-Verlag 39 (2016)

[153] Sklansky, D., and Malmuth, M.: Hold'em Poker for Advanced Players. *Two Plus Two Publications* (1999)

[154] Gomez-Gardenes, J., Campillo, M., Floria, L.M., and Moreno, Y.: Dynamical Organization of Cooperation in Complex Topologies. *Physical Review Letters* **98** 108103 (2007)

[155] Javarone, M.A., Marinazzo, D.: Evolutionary Dynamics of Group Formation. *arxiv:1612.03834* (2016)

[156] Curry, O., Dunbar, RIM: Do birds of a feather flock together?. *Human Nature* **24-3** 336–347 (2013)

[157] Kao, A.B. et al.: Collective learning and optimal consensus decisions in social animal groups *PLoS Comput Biol* **10-8** e1003762 (2014)

[158] Couzin, I.D.: Collective Minds. *Nature* **445-7129** 715–715 (2007)

[159] Sumpter, D. J.T.: The principles of collective animal behaviour. *Philosophical Transactions of the Royal Society B: Biological Sciences* **361-1465** 5–22 (2006)

[160] Lehmann, J., Dunbar, RIM: Network cohesion, group size and neocortex size in female-bonded Old World primates. *Proceedings of the Royal Society of London B: Biological Sciences* rspb20091409 (2009)

[161] Parrish, J.K., Edelstein-Keshet, L.: Complexity, Pattern, and Evolutionary Trade-Offs in Animal Aggregation. *Science* **284-5411** 99–101 (1999)

[162] Alcock, J.: Animal Behavior: an Evolutionary Approach. *Sinauer Associates* (2013)

[163] Dunbar, RIM: Group size, vocal grooming and the origins of language. *Psychonomic Bulletin & Review* 1–4 (2016)

[164] Dunbar, RIM: Coevolution of neocortical size, group size and language in humans. *Behavioral and Brain Sciences* **56-16** 681–735 (1993)

[165] Lee, J., Lee, K., Rho, S.: An evolutionary perspective on strategic group emergence: a genetic algorithm-based model. *Strategic Management Journal* **23-8** 727–746 (2002)

[166] Guillen, M.F.: Business groups in emerging economies: a resource-based view. *ACAD MANAGE J* **43-3** 362–380 (2000)

[167] Galam, S., Zucker, J.D.: From individual choice to group decision-making. *Physica A* **287-3** 644–659 (2000)

[168] Galam, S., Moscovici, S.: Towards a theory of collective phenomena: consensus and attitude changes in groups. *European Journal of Social Psychology* **21-1** 49–74 (1991)

[169] Michod, R.E.: The group covariance effect and fitness trade-offs during evolutionary transitions in individuality. *PNAS* **103-24** 9113–9117 (2006)

[170] Stewart, A.J., Parsons, T.L., Plotkin, J.B.: Evolutionary consequences of behavioral diversity. *PNAS* **113–45** E7003E7009 (2016)

[171] Korstjens, A., Verhoeckx, I.L.,, Dunbar, RIM: Time as a constraint on group size in spider monkeys. *Behavioral Ecology and Sociobiology* **60-5** 683-694 (2006)

[172] Hoare, D.J., Couzin, I.D., Godin, J.G.J., Krause, J.: Context-dependent group size choice in fish. *Animal Behaviour* **67-1** 155–164 (2004)

[173] HIoannou, C.C., Guttal, V., Couzin, I.D.: Predatory Fish Select for Coordinated Collective Motion in Virtual Prey. *Science* **337-6099** 1212–1215 (2012)

[174] Sueur, C., Deneubourg, J.-L., Petit, O., Couzin, I.D.: Group size, grooming and fission in primates: a modeling approach based on group structure. *Journal of Theoretical Biology* **273-1** 156–166 (2011)

[175] Hofmann, H.A. et al.: An evolutionary framework for studying mechanisms of social behavior. *Trends in ecology & evolution* **29-10** 581–589 (2014)

[176] Frewen, T.A., et al.: Coarse collective dynamics of animal groups. *Coping with complexity: Model reduction and data analysis* 299–239 (2011)

[177] Couzin, I.D., Krause, J., James, R., Ruxton, G.D.: Collective memory and spatial sorting in animal groups. *Journal of Theoretical Biology* **218** 1–11 (2002)

[178] Gerard, J.-F., Loisel, P.: Spontaneous Emergence of a Relationship between Habitat Openness and Mean Group Size and its Possible Evolutionary Consequences in Large Herbivores *Journal of Theoretical Biology* **176-4** 511–522 (1995)

[179] Johnsons, K.V-A, Dunbar, RIM: Pain tolerance predicts human social network size. *Scientific Reports* **6** (2016)

[180] Kao, A.B., Couzin, I.D.: Decision accuracy in complex environments is often maximized by small group sizes. *Proc. R. Soc. B* **281-1784** 20133305 (2014)

[181] Miller, N., Garnier, S., Hartnett, A.T., Couzin, I.D.: Both information and social cohesion determine collective decisions in animal groups. *Proceedings of the National Academy of Sciences* **110-13** 5263–5268 (2013)

[182] David-Barrett, T., Dunbar, RIM: Processing power limits social group size: computational evidence for the cognitive costs of sociality. *Proc. R. Soc. B* **280-1765** 20131151 (2013)

[183] Couzin, I.D.: Collective cognition in animal groups. *Trends in cognite sciences* **13-1** 36–43 (2009)

[184] Perc, M., Gomez-Gardenes, J., Szolnoki, A., Floria, L.M., and Moreno, Y.: Evolutionary dynamics of group interactions on structured populations: a review. *J. R. Soc. Interface* **10-80** 20120997 (2013)

[185] Johnson, S., Torres, J., Marro, J., Muñoz, M.A.: Entropic Origin of Disassortativity in Complex Networks. *Physical Review Letters* **104-10** 108702 (2010)

[186] Tehrani, J.J., Collard, M.: On the relationship between interindividual cultural transmission and population-level cultural diversity: a case study of weaving in Iranian tribal populations. *Evolution and Human Behavior* **30-4** 286–300 (2009)

[187] Meenakshi, J.V., Ray, R.: Impact of household size and family composition on poverty in rural India. *Journal of Policy Modeling* **24-6** 539–559 (2002)

[188] Dizard J.E., Gadlin, H.: The Minimal Family. *The University of Massachussets Press* (1990)

[189] Galam S.: Social paradoxes of majority rule voting and renormalization group. *Journal of Statistical Physics*, **61** (1990).

[190] Castellano C., Muoz M.A., Pastor-Satorras R.: Non-linear q-voter model. *Physical Review E*, **80** 041129 (2009).

[191] Timpanaro A.M., Prado P.C.: On the exit probability of the one dimensional q-voter model. Analytical results and simulations for large networks. *Physical Review E* **89** 052808 (2014).

[192] Timpanaro A.M., Galam S.: An analytical expression for the exit probability of the q-voter model in one dimension. *Physical Review E* **92** 012807 (2015).

[193] Nyczka P., Sznajd-Weron K., Cislo J.: Phase transitions in the q-voter model with two types of stochastic driving. *Physical Review E*, **86** 011105 (2012).

[194] Javarone M.A.: Social Influence in Opinion Dynamics: the Role of Conformity *Physica A*, **414** 19–30 (2014).

[195] Hisakado M., Mori S.: Two kinds of phase transitions in a voting model. *J. Phys. A*, **45** 345002, DOI:10.1088/1751-8113/45/34/345002 (2012).

[196] Vazquez F., Eguiluz V.M.: Analytical solution of the voter model on uncorrelated networks. *New Journal of Physics*, **10** 063011 (2008).

[197] Sood V., Redener S.: Voter models on heterogeneous networks. *Physical Review E*, **77** 041121 (2008).

[198] Moretti, P., Liu S., Castellano C., Pastor-Satorras R.: Mean-field analysis of the q-voter model on networks. *Journal of Statistical Physics* **151** (2014).